NTNU – Trondheim
Norwegian University of
Science and Technology

VMAT for small cell lung cancer

Vera Gjervan

Master of Science in Physics and Mathematics
Submission date: June 2015
Supervisor: Pål Erik Goa, IFY
Co-supervisor: Nina Levin, St. Olavs Hospital

Norwegian University of Science and Technology
Department of Physics

Abstract

Limited stage small cell lung cancer (SCLC-LS) is an aggressive cancer form affecting a relatively small group of patients. The prognosis for these patients is poor, and those who are treated with radiotherapy often develop serious side effects, indicating a potential room for improvement of the treatment given to these patients. The newest technique for delivering external photon beam radiotherapy, volumetric modulated arc therapy (VMAT), has not yet been used for this patient group at St. Olavs Hospital, and little research has been published on the topic. The purpose of this thesis is to explore the possibilities of using VMAT for SCLC-LS patients, with special consideration to the irradiated lung volume and possible tumor dose escalation.

VMAT plans were simulated using the CT images of 20 SCLC-LS patients previously treated using 3D conformal radiotherapy (3DCRT) at different hospitals in Norway. Dose-volume parameters for target volumes and organs at risk were evaluated and compared with those of the 3DCRT plans originally given to the patients. The probability for radiation pneumonitis was estimated using a normal tissue complication probability (NTCP) model. Tumor dose escalation within the recommended limits for dose to organs at risk was attempted.

Target coverage, conformity, and homogeneity were kept unchanged or slightly improved for all VMAT plans compared to 3DCRT. A significant reduction of all lung dose parameters was achieved, while dose to the esophagus and spinal cord were kept below given constraints. Mean lung dose was reduced from 16.3 Gy to 13.8 Gy, lung V_{20} from 33.6% to 27.7%, and lung V_5 from 59.1% to 52.4%. The average reduction in NTCP values was 34%. Dose escalation above 45 Gy was possible for 17 of the 20 patients studied, with a mean prescribed dose of 59.0 Gy. Lung doses were the main limiting factor for further escalation.

A new treatment planning system, RayStation 4.5 (RaySearch Laboratories) was recently installed and put into clinical use at the radiotherapy department at St. Olavs Hospital. The new VMAT plans were made in this system, while the 3DCRT plans used for comparison were made in a treatment planning system from Oncentra (Elekta). These systems use slightly different versions of the Collapsed Cone algorithm for dose calculation. A brief comparison was done of the resulting dose distributions when using these algorithms. The difference in dose-volume parameters between plans from the two systems were not likely to be clinically relevant.

This study showed that both low lung doses with acceptable tumor doses and high tumor doses with acceptable organ at risk doses are feasible with VMAT. There is always a trade-off between high tumor doses and acceptable organ at risk doses in radiotherapy, and VMAT may make it easier to control this trade-off. VMAT can be introduced either as a substitute for 3DCRT, or an alternative. The potential for decreased lung doses may be especially beneficial in cases where lung dose objectives are not fulfilled using 3DCRT, and it may be natural to start with these cases if VMAT is to be gradually introduced. However, accurate target volume delineation and sufficient compensation for target volume motion is particularly important with the increased target conformity of VMAT.

Sammendrag

Småcellet lungekreft, begrenset sykdom (SCLC-LS) er en aggressiv krefttype som rammer en relativt liten gruppe pasienter. Prognosen for disse pasientene er dårlig, og de som gis strålebehandling utvikler ofte seriøse bivirkninger. Dette tyder på at det er rom for forbedring av behandlingen som gis til disse pasientene. Den nyeste teknikken for levering av ekstern stråleterapi med fotoner, volumetrisk modulert stråleterapi (VMAT), har enda ikke blitt brukt for denne pasientgruppen på St. Olavs Hospital, og lite forskning har blitt publisert om VMAT for småcellet lungekreft. Hensikten med denne oppgaven er å utforske mulighetene med å bruke VMAT for pasienter med småcellet lungekreft, begrenset sykdom, spesielt med tanke på bestrålt lungevolum og muligheter for doseeskalering.

VMAT-planer ble simulert med utgangspunkt i CT-bilder fra 20 SCLC-pasienter tidligere behandlet med 3D-konform stråleterapi (3DCRT) ved ulike sykehus i Norge. Dose-/volumparametre for målvolumer og risikoorganer ble evaluert og sammenlignet med verdiene fra 3DCRT-planene opprinnelig brukt til behandling. Sannsynligheten for stråleindusert pneumonitt ble estimert ved å bruke en NTCP-modell (normal tissue complication probability). Doseeskalering til tumor innenfor anbefalte grenser for risikoorgandoser ble forsøkt.

Målvolumdekning, konformitet og homogenitet var forbedret eller uendret for VMAT sammenlignet med 3DCRT. En signifikant reduksjon av alle lungedoseparametre ble oppnådd, mens dose til øsofagus og ryggmarg ble holdt under gitte grenser. Middeldosen til friskt lungevev ble redusert fra 16,3 Gy til 13,8 Gy, V_{20} fra 33,6% til 27,7% og V_5 fra 59,1% til 52,4%. Gjennomsnittlig reduksjon i NTCP-verdier var 34%. Doseeskalering over 45 Gy var mulig for 17 av de 20 inkluderte pasientene, med en gjennomsnittlig foreskrevet dose på 59,0 Gy. Dose til friskt lungevev var den viktigste begrensende faktoren for videre doseeskalering.

Et nytt doseplanleggingssystem, RayStation 4.5 (RaySearch Laboratories), ble nylig installert og tatt i bruk ved stråleterapiavdelingen på St. Olavs Hospital. VMAT-planene i denne oppgaven ble laget i RayStation, mens 3DCRT-planene ble laget i et doseplanleggingssystem fra Oncentra (Elekta). Disse systemene bruker noe forskjellige versjoner av Collapsed Cone-algoritmen for doseberegning. Det ble utført en sammenligning av de resulterende dosefordelingene ved bruk av disse algoritmene. Forskjellen i dose-/volumparametre mellom planer beregnet i de to systemene var sannsynligvis av liten klinisk relevans.

Det ble vist at både lave lungedoser med akseptable tumordoser og høye tumordoser med akseptable risikoorgandoser var mulig å oppnå med VMAT. Det vil alltid være en avveining mellom høye tumordoser og akseptable risikoorgandoser i stråleterapi, og VMAT kan gjøre det enklere å kontrollere og styre dette kompromisset. VMAT kan introduseres enten som en erstatning eller et alternativ for 3DCRT. Potensialet for lungedosereduksjon kan være spesielt gunstig i tilfeller hvor lungedoseobjektivene ikke lar seg oppfylle ved bruk av 3DCRT, og det kan være naturlig å starte med disse tilfellene ved en gradvis innføring av VMAT. Presis målvoluminntegning og tilstrekkelig kompensering for målvolumbevegelse er spesielt viktig med den økte konformiteten VMAT medfører.

Preface

This thesis concludes the final work leading to my MSc degree in Biophysics and Medical Technology at the Norwegian University of Science and Technology (NTNU). The work was carried out at the Department of Radiotherapy at St. Olavs Hospital during the spring of 2015, under supervision of medical physicist Nina Levin. Associate professor Pål Erik Goa was my supervisor at the Department of Physics, NTNU.

I would like to thank Nina for her continuous encouragement and support during the entire process, and for always being available to provide help or discuss any ideas or concerns I might have. Thanks also to Pål Erik for his feedback on the final thesis draft. I am also grateful to Jomar Frengen, Sigrun Almberg, and other staff at the radiotherapy department for useful help and input.

Patient images and dose plans used in this study came from a concluded clinical trial, and I would like to thank the oncologists responsible for the trial, Bjørn Henning Grønberg and Tarje Halvorsen, for showing interest in the project and giving valuable input.

Thanks to Dr. Vesna Prokic of the University Medical Center Freiburg in Germany for providing extra details on her study on VMAT for SCLC patients.

This thesis is to a certain degree a continuation of my specialization project from the fall of 2014. Some parts of the background chapter are therefore based on, and translated from, the project report.

Vera Gjervan
Trondheim, June 2015

Contents

Acronyms

3DCRT	3-dimensional conformal radiation therapy
4D-CT	4-dimensional computed tomography
AAA	Analytical anisotropic algorithm
BED	Biologically effective dose
CC	Collapsed cone
CPE	Charged particle equilibrium
CT	(X-ray) computed tomography
CTV	Clinical target volume
DVH	Dose volume histogram
EQD_2	Equivalent dose in 2 Gy fractions
EUD	Equivalent uniform dose
GTV	Gross tumor volume
HU	Hounsfield unit(s)
ICRU	International Commission on Radiation Units and Measurements
IMRT	Intensity modulated radiation therapy
ITV	Internal target volume
KERMA	Kinetic energy released per unit mass
KVIST	Kvalitetssikring i stråleterapi
LKB	Lyman-Kutcher-Burman
MLC	Multi leaf collimator
MRI	Magnetic resonance imaging
MU	Monitor unit(s)
NRPA	Norwegian Radiation Protection Authority (Statens strålevern)
NSCLC	Non-small cell lung cancer
NTCP	Normal tissue complication probability
OAR	Organ at risk
PB	Pencil beam
PD	Prescribed dose

PET	Positron emission tomography
PRV	Planning organ at risk volume
PTV	Planning target volume
QUANTEC	Quantitative Analyses of Normal Tissue Effects in the Clinic
ROI	Region of interest
RVR	Remaining volume at risk
SCLC	Small cell lung cancer
SCLC-LD	Small cell lung cancer, limited disease
SCLC-LS	Small cell lung cancer, limited stage
TD	Tolerance dose
TERMA	Total energy released per unit mass
VMAT	Volumetric modulated arc therapy

1 Introduction

Lung cancer is the second most common cancer form in men and the third most common in women in Norway, and is the leading cause of cancer death among both sexes. Approximately 20% of cancer deaths in Norway in 2013 were associated with lung cancer [1]. Small cell lung cancer (SCLC), which is the most aggressive form of lung cancer, accounts for about 15-20% of all lung cancer cases [2]. SCLC cases are characterized as either limited or extensive stage/disease, and approximately 35% of SCLC cases fall under the limited stage definition (SCLC-LS/SCLC-LD). The recommended treatment for these patients is chemotherapy with concomitant thoracic radiotherapy, preferrably early in the treatment course [3, 4]. Patients may also receive prophylactic cranial irradiation, as SCLC can metastasize to the brain. The 5-year survival rate for patients with SCLC-LS is 10-15% [5].

SCLC-LS patients at St. Olavs Hospital are currently treated using 3D conformal radiotherapy (3DCRT). 3DCRT entails using a discrete number of static fields, shaped after the target volumes using a multi-leaf collimator (MLC). A newer, more advanced technique is volumetric modulated arc therapy (VMAT), in which radiation is delivered continuously as the head of the treatment machine rotates around the patient. The intensity and shape of the radiation field is modulated during treatment. It has been shown for other diagnoses that VMAT makes it possible to shape the high dose volumes to conform to the target volumes to a higher degree than 3DCRT. Steeper gradients to near-lying normal tissue are possible, which makes it possible to deliver higher target doses without increasing dose to healthy organs.

The potential of increased normal tissue sparing is of interest for all radiotherapy patients, as it may reduce the incidence of normal tissue complications. Two serious complications often developed in SCLC-LS patients are radiation esophagitis and radiation pneumonitis. Radiation esophagitis is an acute inflammation of the esophageal tissue, with symptoms including pain and discomfort while swallowing. Afflicted patients often require hospitalization and insertion of feeding tubes. Radiation pneumonitis is an inflammation of lung tissue. It can be a severe and possibly fatal complication. Symptoms include fever, coughing, shortness of breath, and respiratory failure [6]. 35% of the patients in a Norwegian study (HAST[1]) developed a severe grade of esophagitis, while 6% developed a severe grade of pneumonitis. 2 of the 159 patients died from pneumonitis [7].

[1] A randomized phase II study comparing two fractionation patterns for limited stage SCLC.

Due to high recurrence rates and low survival rates both for SCLC-LS and other types of lung cancers, there are ongoing studies trying to escalate the tumor dose within the limits of dose to healthy tissue. Results from dose escalation trials for patients with locally advanced NSCLC, which is similar in anatomy to SCLC-LS, indicate that increasing the dose to the tumor improves tumor control and survival [8–10].

The scope of this thesis was primarily to explore VMAT as a technique and assess whether it is an acceptable alternative or substitute for 3DCRT for delivering radiation therapy to patients with limited stage small-cell lung cancer. While esophagus complications are more frequent than lung complications, the latter can be more severe. It was investigated whether it was possible to reduce the dose to healthy lung tissue using VMAT, thus possibly reducing the risk of severe pneumonitis, and making it possible to escalate the tumor dose. Two main research questions were formulated, and looked at separately:

- To what degree can VMAT reduce lung doses to SCLC-LS patients, while maintaining or improving target coverage compared to 3DCRT?
- Using VMAT, to what degree is it possible to escalate the prescribed tumor dose while keeping the dose to organs at risk (lungs, esophagus, and spinal canal) within recommended limits?

2 Background

2.1 The linear accelerator

External photon beam radiation therapy is usually delivered using a linear accelerator, or *linac*, in which electrons are accelerated through interactions with a synchronized RF electromagnetic field. A magnet bending system directs the electron beam towards the patient in the case of electron treatments, or towards a target made of a material with a high atomic number in the case of photon irradiation. The electrons decelerate when they hit the target, and this energy loss is converted into bremsstrahlung photons [11].

The treatment head of the linear accelerator contains several components that scatter, filter, or shape the radiation beam. The schematic structure of the treatment head of an Elekta linac is shown in Fig. 2.1. Radiation fields from photon beams are shaped by a collimator system, where the main components are primary and secondary collimators, wedges, and the multi-leaf collimator (MLC). A multi-leaf collimator consists of several pairs of metal "leaves" placed in opposing leaf banks, where each leaf can move almost independently of the others.

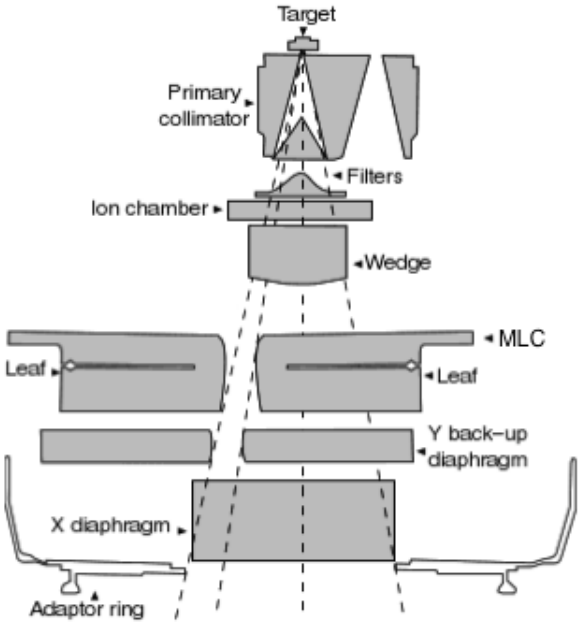

Figure 2.1: Diagram of an Elekta treatment head (from [11]). Elekta's newest MLC, Agility, does not have backup diaphragms.

The treatment head is mounted on a gantry which is able to rotate 360° around the horizontal axis. The gantry angle is zero when the gantry is in the top position, i.e. directly above the patient with the radiation beam pointing vertically down, and the gantry angle increases as the gantry rotates clockwise. The collimator system can rotate 360° around the central axis of the photon beam, and the treatment couch can move in all three directions, in addition to rotation around the vertical axis. The isocenter of the linac is defined as the cross section between the photon beam's central axis and the gantry's rotational axis. A set of laser beams mark the position of the isocenter, and are used to position the patient correctly before treatment.

The output from a linear accelerator is measured in monitor units (MU). The linear accelerators at St. Olavs Hospital are calibrated to deliver 100 MU when an absorbed dose of 1 Gy is delivered to a point at a certain depth (10 cm for photons, the depth of maximum dose for electrons) in a water phantom, with a source-to-surface distance of 90 cm and a field size 10x10 cm^2 at the isocenter distance.

A clinical photon beam consists of a spectrum of energies, where the maximum energy equals the energy of the accelerated electrons, and the mean energy equals approximately 1/3 of the maximum energy. The photon beam energy is given as the nominal accelerating potential, which means that electrons accelerated to e.g. 6 MeV will produce a photon beam with energy called 6 MV.

2.2 Dosimetry

The intensity $I(x)$ of a narrow monoenergetic photon beam that has been attenuated by passing through a material of thickness x is given by

$$I(x) = I(0)e^{-\mu x}, \tag{2.1}$$

where $I(0)$ is the original intensity of the unattenuated beam and μ is the linear attenuation coefficient, which depends both on the photon energy and the atomic number of the material. Multiple processes contribute to this attenuation, and the total linear attenuation coefficient can be given as the sum of atomic attenuation coefficients for these processes.

Photons transfer energy to matter in a two step process. In the first step, energy is transferred to secondary charged particles. Compton scattering is the

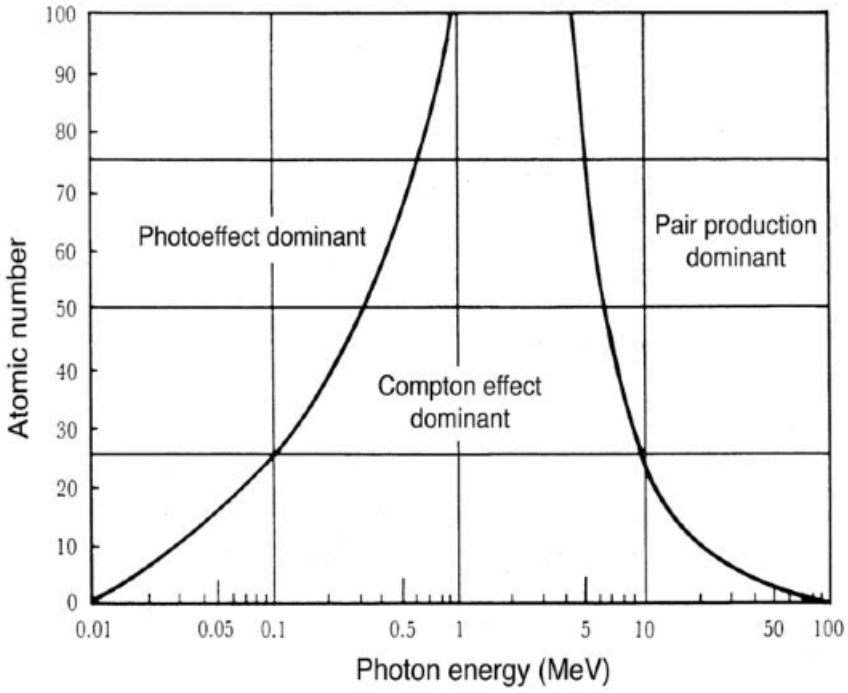

Figure 2.2: Regions of relative predominance for the three main forms of photon interactions with matter for different atomic numbers Z and photon energies. The left curve shows the situations in which the atomic coefficients for the photoelectric effect and the Compton effect are equal, while the right curve shows where the atomic coefficients for the Compton effect and pair production are equal. From [12].

predominating interaction through which energy is transferred from photons to charged particles in soft tissue (low atomic numbers) at energies used for radiation therapy, as shown in Fig. 2.2. The atomic attenuation coefficient for Compton scattering is proportional to the atomic number Z and decreases with energy [12].

The secondary charged particles, electrons in the case of Compton scattering, later transfer some of their energy to matter via atomic excitations or ionizations. The energy transferred in the first step of this process is quantified as KERMA (kinetic energy released per mass unit), defined as the kinetic energy transferred from indirectly ionizing radiation to charged particles per unit mass, while the second step results in absorbed dose D, defined as the mean energy imparted by ionizing radiation per unit mass [11, 12].

2.2.1 Stopping powers, KERMA, and absorbed dose

Stopping powers describe the energy loss of charged particles. Linear stopping power is defined as the expectation value of the rate of energy loss per unit path length of the charged particle, and is typically given in units of MeV/cm. Dividing the linear stopping power by the mass density ρ of the medium results in mass stopping power, with typical units MeV·cm^2/g [12]. There are two types of stopping powers for electrons, as energy transfer from electrons to matter can happen in two ways. These are collision and radiative stopping powers, S_{col} and S_{rad}, where the former results from the charged particles interacting with atomic orbital electrons, i.e. collisions leading to ionization or excitation, and the latter results from interactions with atomic nuclei, i.e. bremsstrahlung. The total mass stopping power is the sum of the collision and radiative mass stopping power,

$$\frac{S_{\text{tot}}}{\rho} = \frac{S_{\text{col}}}{\rho} + \frac{S_{\text{rad}}}{\rho}. \tag{2.2}$$

KERMA is also divided into collision and radiative KERMA, K_{col} and K_{rad}. Absorbed dose is related to collision KERMA, and the relationship between the two is given by the parameter β,

$$\beta = \frac{D}{K_{\text{col}}}. \tag{2.3}$$

The energy absorption in the medium will not happen at the same location as the first photon interactions due to the secondary charged particles travelling in the medium and depositing energy along their tracks. This causes a build-up effect when a photon beam enters a medium, as shown in Fig. 2.3.

Absorbed dose increases until charged particle equilibrium (CPE) is reached at the depth of dose maximum z_{max}, which corresponds approximately to the range of the secondary charged particles. CPE is present in a volume element when the same number of charged particles with the same energy distribution enter and exit the volume element. Due to photon attenuation and scattering, absorbed dose will decrease after the build-up region, and CPE will not be present, $\beta \neq 1$. However, a transient charged particle equilibrium (TCPE) will be present, with $\beta =$ constant [11, 12].

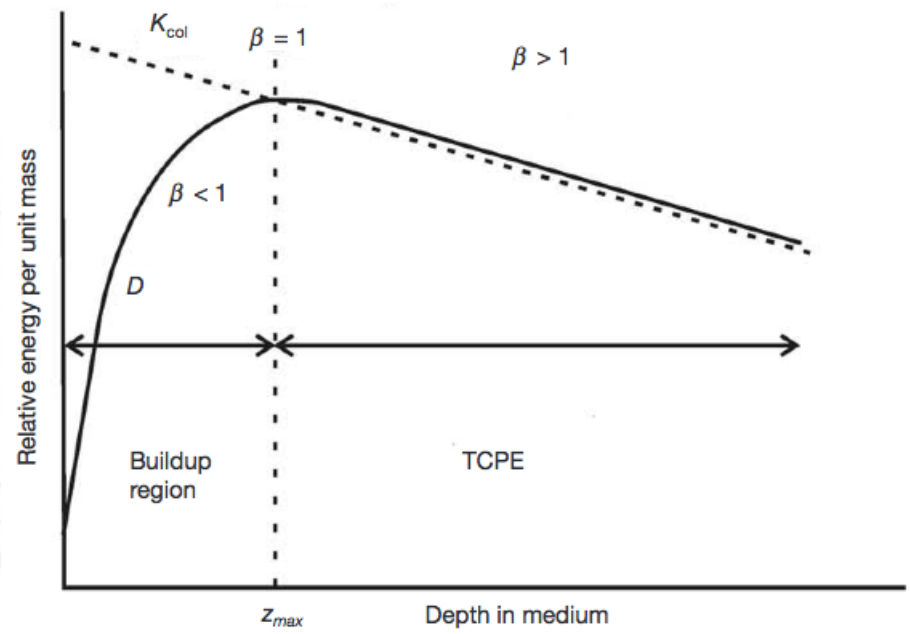

Figure 2.3: Variation of absorbed dose D, collision KERMA K_{col} and the ratio $\beta = D/K_{\text{col}}$ at different depths in a material. z_{max} is the depth of maximum absorbed dose. TCPE, transient charged particle equilibrium, is present at depths deeper than z_{max}. From [12].

2.2.2 Photon beam description

Depth dose curves for photon beams of different energies are shown in Fig. 2.4. Increasing photon energy leads to more energetic secondary electrons and thus a longer electron range, which again leads to a longer build-up region and z_{max} deeper in the medium. The linear attenuation coefficient decreases with increasing photon energy, which means that photon beams of higher energy will be more penetrating and the fall-off region of the depth dose curve will be less steep.

At the lateral edges of a photon beam, the dose falls off rapidly. The width of this region is described as the beam's penumbra, which for flattened beams is typically defined as the distance between the 80% and 20% dose levels, or between 90% and 10% (of the maximum dose). Factors affecting the penumbra include the size of the source/target, the photon energy, the collimating system, the depth at which the beam profile is measured, source-surface distance, and whether electronic equilibrium is present or not [12].

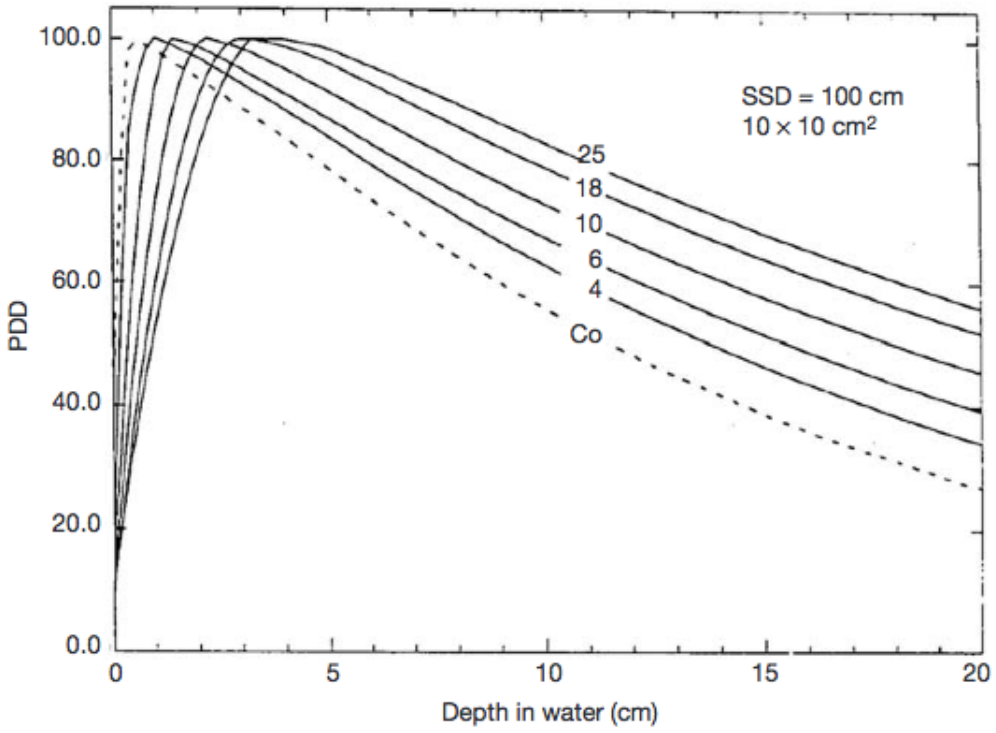

Figure 2.4: Percentage depth dose curves in water for a 10 x 10 cm^2 field at source-to-surface distance 100 cm for photon beams of energies from 4 MV to 25 MV and ^{60}Co γ-rays. From [12].

2.2.3 Tissue inhomogeneities

Most of the body is water-like, with mass density around 1 g/cm^3. The main exceptions are bone, which has a higher density, and lung tissue, where the density is lower.

There will be a lack of electronic equilibrium at interfaces between materials of different density or atomic number Z, for example between lung tissue and soft tissue/tumor tissue. This loss of equilibrium will cause a build-up region in the tumor when photons enter tumor tissue from lung. The extent of this build-up region increases with increasing photon beam energy. In addition, the range of the secondary electrons is inversely proportional to the density. There will be a broadening of the beam penumbra in lung tissue due to the increased electron range. This effect will be more pronounced for lower densities, higher beam energies, and smaller fields [13–16].

2.3 Volume delineation

The design of a treatment plan begins with the identification and delineation of certain regions of interest (ROIs) in the patient's images. These ROIs can be divided into target and risk volumes. A precise definition of these volumes is essential for plan design and evaluation, treatment documentation and follow-up. The volumes and margins mentioned here are defined in guidelines from the KVIST group[1] at the NRPA[2], which again are based on international recommendations from the ICRU[3] [17, 18].

2.3.1 Target volumes

The target volumes recommended in ICRU Report 83 [17, 18] are listed below and illustrated in Fig. 2.5.

The **gross tumor volume** (GTV) is the palpable or visible extent of malignant growth, i.e. the primary tumor, lymph nodes and/or metastases. It is delineated using data from physical examinations, anatomical imaging modalities such as CT and MRI, and functional imaging modalities like PET and functional MRI. A patient can have several GTVs.

The **clinical target volume** (CTV) contains a GTV and/or areas where the probability of malignant growth is high. This could be areas near the boundaries of the primary tumor GTV, lymph nodes, or other organs where tumor infiltration or metastasis is likely. One CTV can cover multiple GTVs, and all GTVs must be included in a CTV.

The **internal target volume** (ITV) is generated by adding an internal margin to the CTV. This margin accounts for uncertainties in the CTV's size, shape, and/or position. For lung cancer patients, tumor movements due to breathing is the most important factor affecting the internal margin. The ITV was defined in ICRU Report 62 in 1999. In a later report, ICRU Report 83 from 2010, the ITV is considered as an optional tool in helping to delineate the PTV. It may be of use in situations where the uncertainty in the CTV location dominates over setup uncertainties, or when they are independent.

The **planning target volume** (PTV) is generated by adding a setup margin

[1] Kvalitetssikring i stråleterapi (Quality Assurance in Radiotherapy)
[2] Norwegian Radiation Protection Authority
[3] International Commission on Radiation Units and Measurements

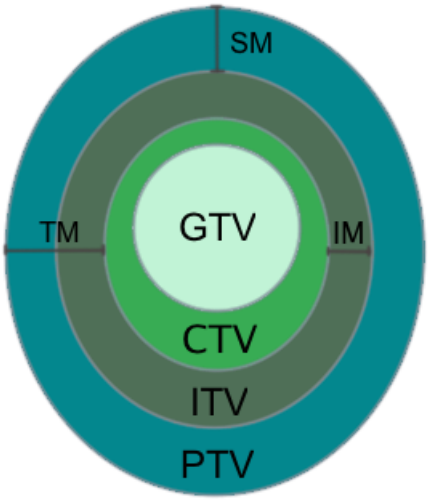

Figure 2.5: The target volumes and margins listed in ICRU Report 83. IM is the internal margin, SM is the setup margin, and TM is the total margin [17, 18].

to the ITV. This margin accounts for uncertainties in patient positioning, equipment uncertainties, image-transfer errors, dosimetric uncertainties, and other factors from fraction to fraction. When an ITV is not defined, the PTV is expanded directly from the CTV. In this case, a total margin combining the internal and setup margin is added.

The margins can be uniform over the whole volume or vary in different directions.

GTV and CTV are anatomical volumes in the patient, while ITV and PTV are geometrical volumes, independent of the patient geometry.

2.3.2 Organs at risk

All healthy tissue is at risk of damage when exposed to radiation. During treatment planning, certain normal tissues classified as **organs at risk** (OARs) are delineated. These are normal tissues whose radiation sensitivity may influence the treatment planning and/or the dose prescription. Limitations are set on the dose to these organs. All non-target tissues could in principle be regarded as OARs, however, which normal tissues are considered OARs in a given patient case depend on the tumor location and/or the prescribed dose level [18].

By adding a total margin accounting for both internal and setup variations, a

planning organ at risk volume (PRV) is generated. While the OAR itself is analogous to CTV for target volumes, the PRV is analogous to the PTV.

A concept that is useful for modelling the radiation response of normal tissues, and thus which type of dose limitations need to be set, is that of functional sub-units [19]. All organs can be considered as built up of these. The arrangement of the functional sub-units can be classified as serial, parallel, or a combination.

The maximum dose, or dose to a small volume, is the most important parameter to monitor for organs with a serial structure, as an excessive dose to a small region (only one or a few sub-units) may lead to loss of function for the entire organ. Examples of such organs are the spinal cord (medulla spinalis), esophagus, and trachea. High maximum doses to the spinal cord may result in paralysis.

Adding a margin around an OAR to generate a PRV is more relevant for organs with a serial structure than organs with a parallel structure. In the case of the spinal cord, the spinal canal is often used as a PRV.

For organs with parallel structures, such as the lungs, liver, or kidney, one should instead consider the average dose and/or how much of the organ receives dose above a certain level. The lungs and kidney are among the most radiosensitive organs when irradiating the entire volume, while a much higher dose is tolerable if only parts of the volume is irradiated. This volume effect is caused by the ability of the unaffected parts of the organ to reassume the function of the damaged parts [11, 17].

Another volume of interest is the **remaining volume at risk** (RVR), which is defined in ICRU Report 83 as the imaged volume within the external contour with the CTV(s) and any delineated organs at risk subtracted. Evaluating the dose to the RVR can help detect high dose regions outside of target volumes and organs at risk, and it might be useful in estimating the risk of late effects or secondary cancers [18].

2.4 Treatment techniques

The main objective of radiotherapy is delivering the desired dose to tumor volumes while simultaneously keeping the dose to adjacent healthy tissue at acceptable levels. To achieve this, the radiation field needs to be shaped after the tumor volume, and gradients to adjacent normal tissue or organs at risk must be sufficiently steep. The main treatment techniques used in external photon beam

radiotherapy today are 3DCRT, IMRT, and VMAT. All these techniques use information from modern imaging modalities such as CT and MRI to precisely locate tumors and surrounding healthy organs.

2.4.1 3DCRT

Conventional three-dimensional conformal radiation therapy (3DCRT) entails using static fields from different gantry angles. The treatment fields are shaped to conform to the tumor volume by using collimators, most importantly MLC's. The delivered dose varies from field to field, and the fluence intensity within a field can be given a linear gradient by the use of wedges. A disadvantage of using 3DCRT is that the shaping of concave high dose volumes is very complicated and time-demanding.

2.4.2 IMRT

Intensity modulated radiation therapy (IMRT) also consists of a discrete number of beams from different gantry angles. The intensity of each radiation field is modulated through the use of collimators, mainly the multi-leaf collimator (MLC). This leads to a larger degree of freedom in the shaping of high dose volumes, and makes it possible to conform the treatment fields to the target volumes to a larger degree than with 3DCRT.

2.4.3 VMAT

A further development of IMRT is volumetric modulated arc therapy (VMAT), with which radiation is delivered as the gantry rotates around the patient. There is a continuous modulation of the rotation speed of the gantry, the MLC field shape and the delivered dose rate [20, 21]. The treatment is given as one or more arcs, where each arc can cover up to 360° and go either clockwise or counter-clockwise. The term *dual arc* denotes the delivery of two oppositely oriented arcs covering the same gantry angles, where the optimization seeks to minimize the leaf travel.

2.5 The dose planning procedure

The most important difference between 3DCRT and IMRT/VMAT is how the plans are made. 3DCRT plans are made using forward planning, while inverse planning (also known as optimized planning) is used to create IMRT and VMAT plans.

Forward planning is a trial-and-error process in which the user decides parameters such as the number of beams, their angle of incidence, the intensity of each beam, whether and how wedges are used, and the collimator configuration. These are then used as a basis for calculations in the dose planning system. The parameters are changed until the desired dose distribution is achieved.

When doing inverse planning, a set of objectives and constraints for the dose to target volumes and organs at risk are selected by the user. The dose planning system then seeks to find the optimal dose distribution fulfilling these requirements by running an optimization algorithm. Constraints will always be satisfied if feasible points exist, while the objectives are improved as much as possible without violating the constraints [11].

In the optimization algorithm, voxels where objectives are not fulfilled are penalized. The optimization function for each objective is the sum of these penalties. The total optimization function is the weighted sum of all optimization functions, where the relative weight of each objective is user selected. This is the function which is to be minimized in the optimization process [22].

The optimization process is ended when the difference in optimization function values between the results from two subsequent iterations is below a given level (the optimization tolerance), or when the user-selected maximum number of iterations is reached.

2.5.1 Dose-volume parameters

A dose-volume histogram (DVH) shows the distribution of absorbed dose in a volume of interest. Differential DVHs show the volume receiving dose in a specified dose interval, while cumulative DVHs show the volume receiving dose equal to or higher than a certain level. DVHs are a useful way of representing information about a non-uniform dose distribution. However, they do not contain spatial information, e.g. about the location of low- or high-dose regions.

Parameters from DVHs are used for prescribing and reporting doses in radiotherapy. Dose parameters are given as D_V, which is the minimum dose to a volume V. Correspondingly, volume parameters are given as V_D, which is the volume receiving a dose D or higher. Both volume and dose can be given in either absolute values or relative to a reference value [17].

$D_{2\%}$ and $D_{98\%}$ are considered more clinically relevant alternatives for $D_{\max}$ and

D_{min}, which are the highest and lowest doses, respectively, to a point within the volume of interest [17]. However, for very small or very large volumes, 2% of the volume may be either too small or too large to be clinically relevant, and it may be better to report the dose to an absolute volume, e.g. 1 cm^3. The same may apply when there are variations in how a volume is defined or delineated, e.g. where the start and end points are set in the delineation of serial organs such as the spinal cord.

Examples of cumulative DVHs with selected dose- and volume parameters are shown in Fig. 2.6. The blue line shows information for an organ at risk, while the red line shows information for a target volume. V_5, V_{30}, median dose $D_{50\%}$, and mean dose D_{mean} are indicated for the organ at risk, while $D_{98\%}$, $D_{2\%}$, median dose D_{50}, and mean dose D_{mean} are indicated for the target volume. The DVH curve for the target volume is steeper, which indicates a more homogeneous dose distribution within the volume. This is also illustrated by the fact that $D_{50\%}$ and D_{mean} are closer for this volume than for the organ at risk.

The conformity of a dose distribution within a volume of interest can be assessed by using the conformity index C,

$$C = \frac{V_{TV}}{V_{PTV}}, \tag{2.4}$$

where V_{TV} is the treated volume within a relevant isodose surface (typically 90% or 95% of the prescribed dose) and V_{PTV} is the volume of the PTV (other target volumes may also be relevant). This parameter is only suitable if the treated volume completely encloses the PTV. If this is not the case, other indices such as the Jaccard index J may be more suited,

$$J = \frac{V_{PTV} \cap V_{TV}}{V_{PTV} \cup V_{TV}}, \tag{2.5}$$

where $0 < J < 1$ and a higher value indicates higher conformity [17]. Likewise, the homogeneity of a dose distribution can be quantified using the homogeneity index H,

$$H = \frac{D_{2\%} - D_{98\%}}{D_{50\%}}, \tag{2.6}$$

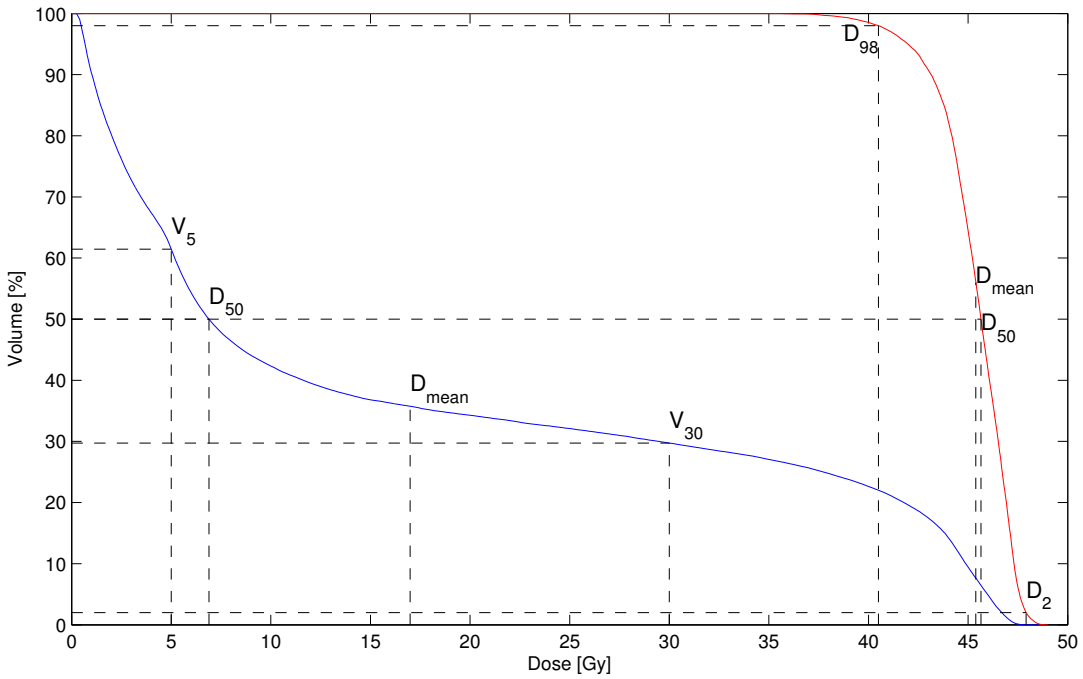

Figure 2.6: Examples of cumulative dose-volume histograms with selected dose- and volume parameters for an organ at risk (blue curve) and a target volume (red curve). V_5 and V_{30} are indicated for the organ at risk, and illustrate how to find the fractional volume receiving ≥5 Gy or ≥30 Gy, respectively. $D_{50\%}$ and D_{mean} are marked for both the organ at risk and the target volume, and show the median dose (50% of the volume receives this dose or higher) and mean dose, respectively. D_{98} and D_2 are indicated for the target volume. 98% of the target volume receives dose $\geq D_{98\%}$, and 2% of the target volume receives dose $\geq D_{2\%}$.

where a value closer to zero indicates a more homogeneous distribution [18].

2.5.2 VMAT parameters

Parameters that must be chosen by the user before VMAT optimization can start include the number of arcs and their lengths and directions, maximum allowed delivery time, the number of control points and the angle between them, limits on MLC leaf motion, maximum number of iterations, optimization constraints and/or objectives with corresponding weight, and optimization tolerance.

Multiple types of optimization functions can be used. The available optimization functions in RayStation 4.5 include Max/Min/Uniform Dose, Max/Min DVH,

Max/Min/Target EUD, and the Dose Fall-Off function [22]. These can be used either as constraints, or as objectives with a given weight.

The Max Dose and Min Dose functions penalize voxels where the dose is above or below the given level, while the Uniform Dose function will penalize voxels where the dose deviates from the selected level.

The Max DVH and Min DVH functions take two parameters; dose and volume, where the volume can be relative or absolute (in cm^3). These functions will penalize dose above or below the specified dose level everywhere in the organ except in the volume specified. It is not specified where in the organ the high or low dose areas should be.

The EUD functions calculate the equivalent uniform dose (EUD) according to Niemierko's generalized formulation, given in Eq. 2.22. These functions take two parameters; a dose level and a volume-specific parameter a, as described in Section 2.7.2. If a is set to one, the EUD will be equal to the mean dose [23, 24]. The Max EUD and Min EUD functions penalize dose levels above and below the specified EUD levels, while the Target EUD functions penalizes dose levels both above and below the given EUD.

The Dose Fall-Off function describes how the dose should decrease outside the target volumes, and takes three parameters: a high dose level, low dose level, and low dose distance. It behaves like a Max Dose function, but with different dose levels in different voxels, depending on the voxel's distance from the target contour. The dose level should decrease linearly from the high dose level just outside the target, to the low dose level in voxels where the distance from the target border equals the low dose distance [22].

2.5.3 Organ at risk dose limits in lung cancer treatments

Healthy lung tissue, the spinal cord, and the esophagus are the most important dose-limiting organs in the treatment of lung cancer patients [4]. The esophagus[4] is the tube connecting the throat and the stomach. It travels behind the airways and heart, and will often pass through the radiation field in lung cancer treatments.

The dose limits used in the VMAT optimization and plan evaluation in this study were based on national recommendations from the Norwegian Lung Cancer

[4] *Spiserør* in Norwegian.

Group and the KVIST group [4]. These guidelines are mainly based on QUANTEC[5] data.

Lungs

A QUANTEC review recommends keeping the mean lung dose below 20-23 Gy and the volume receiving 20 Gy or more (V_{20}) below 30-35% to keep the risk of symptomatic radiation pneumonitis below 20% in treatment of non small cell lung cancer (NSCLC) patients [25]. The same recommendations are given for SCLC patients in the KVIST recommendations, where it is also recommended to keep V_5 below 65% [4].

Esophagus

QUANTEC reviews and other studies have found that several dosimetric parameters are significantly related to the incidence of acute esophagitis [26, 27]. KVIST recommends keeping the mean esophageal dose below 34 Gy for SCLC patients. This is based on data from several studies, among these one by Singh et al., who evaluated predictors of radiation-induced esophageal toxicity in patients with NSCLC treated with 3DCRT and found that a mean esophageal dose >34 Gy was significantly associated with the incidence of Grade ≥3 esophageal toxicity [4, 28].

Bradley et al. found the volume receiving 60 Gy or more, V_{60}, to be one of the significant parameters for predicting acute esophagitis. $V_{60} = 10$ cm^3 was associated with a ∼50% probability of acute esophagitis when radiotherapy is given with concurrent chemotherapy. Reducing V_{60} to 5 cm^3 lowered the probability to ∼40%. These values were approximately halved when considering radiotherapy given alone [27].

Spinal canal

Kirkpatrick et al. (QUANTEC) found that when using conventional fractionation of 1.8-2 Gy per fraction to the full thickness spinal cord, the estimated risk of myelopathy is <1% and <10% at 54 Gy and 61 Gy, respectively. Total doses of 50 Gy, 60 Gy, and ∼69 Gy were associated with myelopathy rates of 0.2%, 6%, and 50%, respectively [29]. In addition, an analysis by Schultheiss et al. estimated the probability of myelopathy to be 0.03% and 0.2% at 45 Gy and 50 Gy, respectively [30].

[5]Quantitative Analyses of Normal Tissue Effects in the Clinic

Based on these data, KVIST recommends a maximum dose 50 Gy in 2 Gy fractions (EQD_2, to be explained further in Section 2.7.1) for SCLC patients when ordinary fractionation or mild hypofractionation (e.g. the 2.8 Gy x 15 arm in the HAST study) is used [4].

Ang et al. demonstrated an increased incidence of myelopathy compared to conventional fractionation when using hyperfractionation with less than six hours between fractions. Two fractions daily separated by a six hour interval lead to a 16.5% decrease in tolerance dose compared to one fraction per day. KVIST therefore recommends a minimum of six hours between fractions [4, 31].

2.6 Dose calculation algorithms

Dose calculation algorithms in use today use electron density information from CT images to predict the dose distribution within the patient or phantom. There is a trade-off between the accuracy and speed of different dose calculation algorithms. Monte Carlo dose calculations simulate the paths of millions of particles, using interaction probabilities to determine the fate of each particle. This produces the most accurate results, but it is very time demanding and requires large processing capacities. The most common dose calculation algorithms in clinical use today and in recent years are Pencil Beam (PB), Collapsed Cone (CC) and Analytical Anisotropic Algorithm (AAA). These are faster than Monte Carlo simulations, but also less accurate.

These algorithms calculate the dose by combining the total energy released per unit mass (TERMA) with energy deposition kernels. Energy deposition kernels describe the dose distribution around a primary photon interaction point or along a ray line in a homogeneous medium, and are precalculated using Monte Carlo simulations. Several types of energy deposition kernels exist. The two algorithms discussed here, Collapsed Cone and Pencil Beam, are based on point kernels and pencil beam kernels, respectively.

2.6.1 Collapsed Cone

In this algorithm the primary photon beam is ray traced through the patient, and the distribution of total energy released per mass unit (TERMA) is calculated, taking inhomogeneities into account by calculating effective radiological depth. This distribution is convolved with polyenergetic point kernels in each voxel.

Polyenergetic energy deposition kernels are calculated as a weighted sum of mo-

noenergetic kernels, where the weight of each kernel is determined according to the energy spectrum of the beam [32]. The energy deposition kernels are also scaled to account for inhomogeneities. Inhomogeneities are thus taken into account both laterally and along the primary fluence direction in the Collapsed Cone algorithm.

The convolution of TERMA with the polyenergetic kernels is facilitated by a collapsed cone approximation, which entails discretization and parametrization of the kernel data into coaxial cones [32]. The energy in one such cone is assumed to be transported, attenuated, and deposited along the cone axis.

Treatment planning systems may use different versions of Collapsed Cone, e.g. with respect to approximations used at various stages of the calculation. Systems from two vendors, Oncentra (External Beam or MasterPlan) and RaySearch (RayStation), are used in this study. One of the differences between these systems is that RayStation uses a no-tilt kernel approximation, which means that all kernels are aligned with the central beam axis. This is done to save computation time. This approximation gives acceptable results in most cases, but for large fields and/or small source-surface distances it may lead to an overestimation on the central axis, or an underestimation outside of the field. This is partly corrected for by inverse square law de-scaling of TERMA and rescaling of dose [11, 33]. Mzenda et al. found that the calculated dose did not always agree with measurements in out-of-field regions, especially for large fields, and the no-tilt approximation may be one possible explanation for this [34, 35].

Analytical Anisotropic Algorithm (AAA) is a dose calculation algorithm implemented in Varian's treatment planning systems. It is similar to Collapsed Cone in terms of how well it corrects for inhomogeneities [36].

2.6.2 Pencil Beam

The Pencil Beam algorithm calculates the dose distribution as a convolution of polyenergetic pencil beam kernels with a planar photon fluence distribution. Polyenergetic pencil beam kernels are generated as a superposition of monoenergetic pencil beam kernels weighted according to the photon beam energy spectrum, where the pencil beam kernels are obtained by integrating all point kernels along an infinite ray of photons [37, 38].

Inhomogeneities are corrected for by scaling of the kernels in the depth dimension using the equivalent path length method. Lateral scatter is not accounted for,

which reduces the precision of the Pencil Beam algorithm in tissues with low density, such as lungs. KVIST recommends using Collapsed Cone or AAA instead of Pencil Beam for calculating lung dose plans [4].

Several studies have been published comparing the accuracy of dose calculation algorithms in lung tissues, and the conclusion is generally that a CC algorithm is preferable to PB when inhomogeneous media, such as lungs, is present. Aarup et al. found that PB algorithms overestimated the dose to lung tissue and solid tumors in the lung, and that this overestimation increased with decreasing lung density and increased photon energy. Both Eclipse's AAA and Oncentra's CC algorithm showed good agreement with Monte Carlo simulations in lung densities ≥ 0.2 g/cm^3, however, for densities as low as 0.1 g/cm^3, there was a difference compared to Monte Carlo simulations that may be of clinical relevance [36]. Polednik et al. found that Oncentra's PB algorithm overestimated the dose in lung by up to 23%, and that CC underestimated the lung dose by up to 6% [39].

2.6.3 Dose to water vs. dose to medium

Monte Carlo simulations report dose to medium, and many Collapsed Cone algorithms, including the one used in Oncentra's treatment planning system, traditionally calculate dose to medium as well. The alternative is reporting dose to water, which essentially means that all materials are treated as water-like, but with different density. It is still debated which of the two methods is optimal [40, 41]. RayStation 4.5 computes the dose to medium D_{med} and converts it to dose to water D_w through the process described below [34].

CT images provide information about the patient density in CT numbers or Hounsfield units (HU), which are proportional to the linear attenuation coefficient μ at the energies of the CT scanner,

$$\text{HU} = 1000 \cdot \frac{\mu - \mu_{H_2O}}{\mu_{H_2O}}, \tag{2.7}$$

where HU = -1000 for air and HU = 0 for water. The mass density in each voxel is then determined from the CT number by interpolating in a HU-density table.

For photon energies between 0.1 MeV and 10 MeV, Compton scattering is the predominant attenuation process. The cross section for Compton scattering, and thus the linear mass attenuation coefficient, is proportional to the electron den-

sity of the medium in this energy range. However, for energies above 10 MeV pair-production becomes important (see Fig. 2.2), and the linear mass attenuation coefficient increases with energy and atomic number. To account for this, mass density is converted to effective density. For a monoenergetic photon beam with energy E, RayStation approximates the ratio of effective densities in medium and water by [34]

$$\frac{\rho_{eff,med}}{\rho_{eff,w}} = \frac{\rho_{m,med}}{\rho_{m,w}} \frac{\langle Z/A \rangle_{med}}{\langle Z/A \rangle_w} \frac{1 + \alpha \cdot (1 + \langle Z \rangle_{med}) \cdot \ln E \cdot E}{1 + \alpha \cdot (1 + \langle Z \rangle_w) \cdot \ln E \cdot E}, \tag{2.8}$$

where ρ_m is mass density, the parameter α equals $1.775 \cdot 10^{-3}$, E is the photon energy given in MeV, $\langle Z/A \rangle$ is the weighted mean nuclear Z/A ratio, and $\langle Z \rangle$ is the weighted mean nuclear Z,

$$\langle Z/A \rangle = \sum_i w_i \frac{Z_i}{A_i}, \tag{2.9}$$

$$\langle Z \rangle = \frac{\sum_i w_i (Z^2/A)_i}{\langle Z/A \rangle}, \tag{2.10}$$

where w_i, Z_i and A_i are the fraction by weight, atomic number, and atomic mass of atomic element i in the material in question.

Mass density is first determined from a HU-to-density table. A material is assigned to each voxel according to mass density, in order to calculate $\langle Z \rangle$ and $\langle Z/A \rangle$. A table relating effective density to mass density is created by summing Eq. 2.8 over the beam energy spectrum at isocenter in air. The mass density in each voxel is then converted to effective density using linear interpolation in this table. Finally, dose to medium D_{med} is converted to dose to water D_w through the relationship

$$D_w = D_{med} \frac{\rho_{eff,w}}{\rho_{eff,med}} \frac{\rho_{m,med}}{\rho_{m,w}}. \tag{2.11}$$

RayStation's method assumes the ratio of stopping powers between body tissues and water to be energy independent [34, 40]. Another common approach for

calculating the ratio between dose to medium and dose to water involves scaling by the ratio of the mass collision stopping powers,

$$\frac{D_{med}}{D_w} = \frac{\int_0^{E_{\max}} \Phi_{E,med}^{prim} \left(S_{\mathrm{col}}(E)/\rho\right)_{med} \mathrm{d}E}{\int_0^{E_{\max}} \Phi_{E,w}^{prim} \left(S_{\mathrm{col}}(E)/\rho\right)_{w} \mathrm{d}E} \tag{2.12}$$

where Φ^{prim} is the primary electron fluence. The assumption of charged particle equilibrium is made. This approach is used to convert D_{med} from Monte Carlo calculations to D_w. A possible simplification is to assume $\Phi_{E,med}^{prim} = \Phi_{E,w}^{prim}$, which leads to the Bragg-Gray stopping power ratio [40].

2.7 Radiobiology

Cell survival curves plot the surviving fraction of cells against dose. Several mathematical models have been developed to explain the dose-survival relationship. The most commonly used model today is the linear quadratic model, which states that the surviving fraction S of cells irradiated with a dose D in a single fraction is given by

$$S = p(\text{survival}) = e^{-\alpha D - \beta D^2}, \tag{2.13}$$

where α describes the linear component of the cell survival curve, and β describes the quadratic component. The ratio α/β is the dose where the linear contribution to the damage equals the quadratic contribution, and is commonly used to quantify the radiation response of normal tissues and tumors [42].

Normal tissues can be classified as early- or late-responding. Early-responding tissues start showing effects of radiation damage within a few weeks after the start of radiation, while late-responding tissues might not show effects until months or years have passed. Skin, mucosa, bone marrow, and the intestinal epithelium are examples of early-responding tissues, while lungs, kidney, and spinal cord are examples of late-responding tissues. α/β tends to be high for early-responding tissues and low for late-responding. Most tumors have a high α/β ratio. Standard values typically used are $\alpha/\beta = 3$ Gy for late-responding tissues and 10 Gy for early-responding tissues and tumors [42, 43].

2.7.1 Fractionation

The effect E of n fractions where the dose per fraction is d, and the total dose $D = nd$, is expressed as

$$E = -\ln S^n = n(\alpha d + \beta d^2) = \alpha D + \beta d D. \tag{2.14}$$

The relationship between the effects E_1 and E_2 of two fractionation schemes $d_1 \times n_1 = D_1$ and $d_2 \times n_2 = D_2$ is

$$\frac{E_2}{E_1} = \frac{\alpha D_1 + \beta d_1 D_1}{\alpha D_2 + \beta d_2 D_2} = \frac{D_1(d_1 + \alpha/\beta)}{D_2(d_2 + \alpha/\beta)}, \tag{2.15}$$

and the relationship between the total dose D_1 and D_2 in two isoeffective fractionation schemes ($E_1 = E_2$) is thus

$$\frac{D_2}{D_1} = \frac{d_1 + \alpha/\beta}{d_2 + \alpha/\beta}. \tag{2.16}$$

This can be used to calculate the biologically effective dose (BED) of a fractionation regimen,

$$\mathrm{BED} = \frac{E}{\alpha} = D\left(1 + \frac{d}{\alpha/\beta}\right), \tag{2.17}$$

or to convert a fractionation scheme $d \times n = D$ to the equivalent total dose when the radiation is given in 2 Gy fractions, EQD_2,

$$\mathrm{EQD}_2 = D\ \frac{d + \alpha/\beta}{2\ \mathrm{Gy} + \alpha/\beta}. \tag{2.18}$$

BED and EQD_2 are commonly used to compare fractionation schemes [42, 43]. As can be seen from Eq. 2.18, late-responding normal tissues (low α/β) show greater changes in sensitivity in response to fractionation changes than do early-responding tissues and tumors. Hypo- and hyperfractionation means delivering

higher and lower fraction doses, respectively, than the conventional fraction dose of 1.8-2 Gy. Hyperfractionation is useful for sparing late-responding normal tissues [11].

The expression for EQD_2 in Eq. 2.18 can be expanded to account for incomplete repair of sublethal damage between fractions:

$$\mathrm{EQD}_2 = \frac{\sum_{k=1}^{n}\left\{d_k\left(d_k + \frac{\alpha}{\beta} + 2(1-l)\sum_{p=1}^{k-1}\left(d_p\prod_{q=p}^{k-1}\theta_{s,q}\right) + 2l\sum_{p=1}^{k-1}\left(d_p\prod_{q=p}^{k-1}\theta_{l,q}\right)\right)\right\}}{2\ \mathrm{Gy} + \frac{\alpha}{\beta}}, \tag{2.19}$$

where d_k is fraction dose no. k, n is the total number of fractions, l is the fraction of the total repair that is due to long repair times, and

$$\theta_{s,q} = \exp\left(-\frac{\ln 2}{T_{(1/2),s}}\ \Delta t_q\right) \tag{2.20}$$

$$\theta_{l,q} = \exp\left(-\frac{\ln 2}{T_{(1/2),l}}\ \Delta t_q\right), \tag{2.21}$$

where $T_{(1/2),s}$ and $T_{(1/2),l}$ are the repair half-times for short and long repair, respectively, and Δt_q is the time between fraction q and fraction $q+1$ [34, 44]. This equation can be used both for tissues with biexponential repair (with both a short and long repair component) or monoexponential repair (by setting l=1).

2.7.2 NTCP models

The therapeutic index, or ratio, of a treatment is the ratio between the probability of tumor control and the probability of normal tissue damage [43]. Increasing this ratio is one of the main motivational factors in the development of new radiotherapy techniques. Both tumor control probability (TCP) and normal tissue complication probability (NTCP) vary with dose according to a sigmoid relationship, as shown in Fig. 2.7. Several mathematical models for TCP and NTCP have been developed, and can be used to estimate the probability of tumor control or normal tissue damage at a given dose level. One of the models used for describing NTCP curves is the Lyman-Kutcher-Burman (LKB) model.

Lyman's original model from 1985 described complication probabilities for whole or partial volumes receiving uniform irradiation. Uniform irradiation is rarely the case anymore, and several DVH reduction algorithms have been developed to account for non-uniform irradiation. One such method is the effective volume method developed by Kutcher and Burman in 1989, in which a non-uniform DVH is reduced to a uniform one where an effective volume receives a dose equal to the maximum dose. The combination of Lyman's model with Kutcher and Burman's expansion is referred to as the Lyman-Kutcher-Burman (LKB) model [45].

The equivalent uniform dose (EUD) was introduced by Niemierko in 1997, and can be used for reporting non-uniform dose distributions. EUD is defined as the uniform dose that results in the same radiobiological effect (e.g. cell survival) as the non-uniform dose distribution of interest. The generalized EUD is valid for both tumors and normal tissues, and is given by

$$\mathrm{EUD} = \sum_i \left(D_i{}^a v_i\right)^{1/a}, \tag{2.22}$$

where D_i is the dose to voxel no. i, and v_i is the voxel's relative volume. The tissue-specific parameter a is negative for tumors and positive for normal tissues,

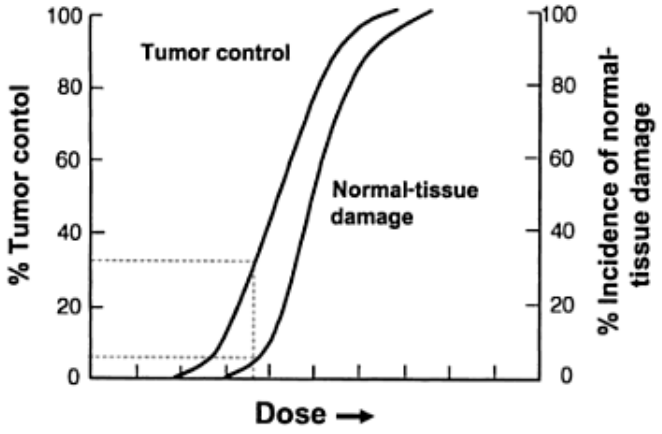

Figure 2.7: The probability of tumor control and normal tissue damage in a treatment as a function of dose. In this example, about 30% tumor control can be achieved if a 5% probability of normal tissue damage is accepted. From [43].

and tends to be large for serial organs and close to 1 for parallel organs. EUD is equal to mean dose when $a = 1$ [23, 24].

In the LKB model, the sigmoid shape of the NTCP curve is represented by the integral of the normal distribution,

$$\text{NTCP} = \frac{1}{\sqrt{2\pi}} \int_{-\infty}^{t} e^{-\tau^2/2} \, d\tau, \tag{2.23}$$

where

$$t = \frac{D_{\text{eff}} - TD_{50}}{m \cdot TD_{50}}. \tag{2.24}$$

This mathematical formulation of the NTCP curve was first proposed by Mohan et al. [46]. TD_{50} is the dose corresponding with a complication rate of 50%, m is a parameter describing the steepness of the curve, and the effective dose D_{eff} is given by

$$D_{\text{eff}} = \sum_i \left(D_i^{1/n} v_i \right)^n. \tag{2.25}$$

D_{eff} is identical to EUD with parameter $a = 1/n$. To summarize, the three parameters needed for this NTCP model are TD_{50}, m, and n.

To correct for fraction doses other than 2 Gy, D_i in Eq. 2.25 is converted to $\text{EQD}_{2,i}$ through the relation in Eq. 2.18.

When calculating NTCP values, the following relation between the integral of the standard normal distribution and the error function erf(x) can be useful [47],

$$\frac{1}{\sqrt{2\pi}} \int_{-\infty}^{t} e^{-\tau^2/2} \, d\tau = \frac{1}{2} + \frac{1}{2} \, \text{erf}\left(\frac{t}{\sqrt{2}} \right). \tag{2.26}$$

3 Material and methods

3.1 Original data

The recently concluded Norwegian study HAST was a randomized phase II study comparing two fractionation patterns for patients with limited stage SCLC [7]. CT images from 20 patients included in the HAST study, with delineated target volumes and organs at risk, were used as a basis for simulation of VMAT plans. The patients were treated between 2006 and 2010 at different hospitals in Norway. 15 of the 20 patients included here received their treatment at St. Olavs Hospital.

A description of this project was assessed by the leader of the Regional Ethics Committee (REK), who concluded that advance approval was not necessary.

3.1.1 Patient selection

The criteria for choosing patients were that the volumes delineated were as recommended in the HAST protocol (see Section 3.1.3), and that the original 3DCRT plan was calculated using the Collapsed Cone algorithm. Patients where the original plan had been calculated using Pencil Beam, but later recalculated using Collapsed Cone, were also eligible. This was the case for some HAST patients treated at St. Olavs Hospital in the earlier years of the study. Recalculation was not possible for patients from other centers as the models for the treatment machines used were not available.

The 3DCRT plans for all the selected patients were originally made in one of the versions of Oncentra's treatment planning system (Elekta AB, Stockholm, Sweden).

3.1.2 Imported 3DCRT plans

Photon beams with energies both 6 and 15 MV were used in the original 3DCRT plans. Four plans used only 6 MV beams, nine plans used only 15 MV, while the remaining seven plans used a combination of both energies. The basis for all plans was two opposing fields, with additional fields or segments for 17 of the 20 plans.

The HAST study compared two fractionation regimes, 2.8 Gy x 15 delivered once daily vs. 1.5 Gy x 30 delivered twice daily. The chosen scheme for the simulated VMAT plans was 1.5 Gy x 30 delivered twice daily, as recommended by

the Norwegian Directorate of Health and the KVIST group [3, 4]. However, patients from both arms of the HAST study were included. All original treatments plans were therefore rescaled to give a mean dose of 45 Gy to the union of all delineated CTVs to allow for easier plan comparisons. This scaling was deemed unproblematic as the same field setup would likely have been used regardless of fractionation.

The 3DCRT plans were imported to the treatment planning system RayStation 4.5 (RaySearch Laboratories AB, Stockholm, Sweden), in which the new VMAT plans were made. The comparison between the 3DCRT and VMAT plans was done based on DVHs and dose parameters from RayStation.

3.1.3 Volume delineation

The HAST study protocol had the following guidelines for target volume definitions: the primary tumor, the mediastinum, and affected lymph nodes were defined as GTVs. A margin of 1 cm was added to the tumor GTV to generate the tumor CTV, but no margin was added to the GTV of the mediastinum or lymph nodes. The ITV was generated from the union of all CTVs by adding a margin between 0.5 and 1 cm in the transversal plane and a margin between 1 and 1.5 cm in the axial plane. The PTV was expanded from the ITV according to each hospital's routines [48].

There was a varying degree of consistency in the target volume delineation in the original patient cases, and some changes were needed before the simulation of the VMAT plans could begin. The radiation fields were not always consistent with the volumes, i.e. the margins from the target volume to the field borders varied, and some volumes were missing. New PTVs were created in the patients where this was missing. This was done by adding a margin to the existing ITV volumes, or to the CTV for one patient who lacked an ITV. It was decided that the border of a patient's PTV was to be at least 5 mm from the borders of the main fields used in the conventional plan. This was done to ensure that the comparison of the 3DCRT and VMAT plans was as fair as possible.

The resulting PTVs had volumes ranging from 341 cm^3 to 2042 cm^3 (median 887 cm^3, mean 913 cm^3).

The union of all CTVs and the PTV were chosen for plan optimization and evaluation, and the CTV was chosen for plan normalization. While almost all the HAST patients had an ITV originally, very few had a PTV. However, the

PTV is used more than ITV nowadays. This is in compliance with ICRU Report 83, as mentioned in Section 2.3.1. The CTV mediastinum and GTV mediastinum were identical, and it was not necessary to delineate both. Most patients in this study only had a CTV mediastinum. Choosing the CTV instead of GTV for optimization and evaluation ensured that all volumes were accounted for.

The organs at risk contoured were the spinal canal (as a PRV for the spinal cord), both lungs minus GTV, and the esophagus according to KVIST guidelines [4]. The delineation of organs at risk was done by different radiation oncologists at different hospitals, and thus some degree of interobserver variation was expected. To limit these variations, the delineation of the lung and esophagus volumes of all patients were reviewed – and altered if necessary – by a radiation oncologist at St. Olavs Hospital.

3.2 Dose planning

The VMAT plans were made in RayStation 4.5. This program was installed and put into clinical use in the radiotherapy department during the work with this thesis, and thus some time was spent exploring and testing the program before the final work could start.

3.2.1 VMAT parameters

All VMAT plans were made using photon energy 6 MV. The plans were made to be delivered on an Elekta Versa HD linac with an Agility MLC treatment head (Elekta AB, Stockholm, Sweden). Agility has 160 MLC leaves with projected width 5 mm in the isocenter. The collimator angle was set to 45° for all arcs, and the maximum delivery time was set to 90 seconds per arc. The optimization tolerance was set to 10^{-5}. The gantry angle between subsequent control points was set to 4°. A constraint of maximum 0.5 cm movement per degree was set on the MLC leaf motion. The isocenter for all arcs was set to the center of PTV union. These settings were chosen based on earlier experience in the clinic.

Two or three VMAT plans for each patient were included in the dosimetric analysis. Two plans with prescribed dose 45 Gy were included for each patient, in addition to a plan with dose higher than 45 Gy for 17 of 20 patients. This is explained further in Section 3.3.

The first 45 Gy plan consisted of two full dual arcs, covering the angles between 178° and 182°. Dual implies that the two arcs are treated as one during the

optimization process. The second plan, called the partial-arc plan, consisted of between one and four shorter arc segments (all dual, i.e. a total of between two and eight segments). The angles used in these segments were chosen based on the full-arc plans. Angles indicating a direction not optimal for dose delivery, i.e. angles where the delivered dose per segment per fraction was 1 MU or slightly higher, were excluded. 1 MU per segment per fraction is the lowest deliverable dose due to machine restrictions.

The plans were scaled, i.e. the number of delivered MUs was adjusted, so the mean dose to the CTV union was exactly 45 Gy.

Dose calculation for the VMAT plans was done using the Collapsed Cone algorithm in RayStation 4.5, while the 3DCRT plans were calculated (or recalculated, as mentioned in Section 3.1.1) using the Collapsed Cone algorithm in Oncentra's treatment planning system.

During the optimization of VMAT plans in RayStation 4.5 a Singular Value Decomposition (SVD) dose engine is used. This simplified dose engine is faster than Collapsed Cone, but has lower accuracy and must not be used for clinical decisions. The resulting dose distribution after the final dose calculation will therefore differ from the approximate distribution shown during the optimization, and it will often be necessary to run the optimization process one more time. In this case, the optimization was run twice with a final dose calculation after each run ("warm start" after the first final dose calculation). The optimization process ran for a maximum of 200 iterations, or until the optimal solution was found.

3.2.2 Organ at risk dose limits

The dose limits for organs at risk were chosen based on national recommendations from the Norwegian Lung Cancer Group and the KVIST group, as summarized in Section 2.5.3.

The dose-volume constraints chosen for the lungs were $V_{20} < 35\%$, $V_5 < 65\%$, and mean dose < 20 Gy. These constraints were set on the total volume of both lungs with the GTV subtracted. The same constraints were used in the 45 Gy plans and the escalated plans.

Mean esophageal dose < 34 Gy was used for both the 45 Gy plans and the escalated plans. For the escalated plans, the volume receiving 100% or more of

Table 3.1: Objectives used in the first run of the plan optimization of the 45 Gy VMAT plans. Parameters listed in **bold text** were adjusted in the following plans. EUD with $a = 1$ is equivalent to mean dose.

ROI	Objective	Weight
PTV union	Min 42.75 Gy	3000
CTV (all volumes)	Uniform dose 45 Gy	**800**
External / PTV union	Max 47.25 Gy	**500**
External / lungs	Dose fall-off 45 Gy to **20 Gy** in 2 cm	**100**
Total lung minus GTV	Max 20 Gy to **35**% volume	1000
Total lung minus GTV	Max 5 Gy to **65**% volume	800
Total lung minus GTV	Max EUD **20 Gy**, $a = 1$	1000
Spinal canal	Max **45 Gy**	500

the prescribed dose $V_{100\%} < 2\%$ was used in the optimization. V_{60} was evaluated for the escalated plans, but not used in the optimization process.

A maximum dose of 45 Gy to the spinal cord in 1.5 Gy fractions twice daily was used. The same limit was used for both the 45 Gy plans and the escalated plans.

3.2.3 Objectives and constraints

Several VMAT plans were created for each patient before the final plan was chosen. The first plan for each patient used the objectives listed in Tab. 3.1. In the subsequent plans, the planning objectives were adjusted to try to get the lung dose as low as possible without compromising the PTV coverage and exceeding the recommended maximum dose to the spinal cord.

When lung radiotherapy plans are made in the clinic, the aim is for the PTV to be covered by the 90% isodose in lung tissue and the 95% isodose in soft tissue (e.g. the mediastinum). An objective of Min 40.5 Gy (90%) to PTV union was tried in the first test runs. This did not result in an acceptable PTV coverage, and the objective was instead set to Min 42.75 Gy (95%).

The objective of Max 47.25 Gy was set to the PTV, or to the entire volume imaged in the CT scans (within the external contour, denoted as "External" in tables and figures to follow) for patients where the first few iterations showed a tendency to deposit high doses outside the PTV. The weighting of this objective was increased if the resulting maximum dose was much higher than in the original

3DCRT plan.

The dose fall-off objective, described in Section 2.5.2, is usually set to the volume within the external contour. For some cases, a fall-off objective was tried for the residual lung volume, either in addition to or replacing the objective to the external contour. The lung fall-off objective had higher weight than the external fall-off objective. This was done to stear the deposition of dose outside the target volumes away from the lungs.

The objectives for lung doses were set to the union of both lungs with the GTVs subtracted. The first plans used objectives based on recommendations mentioned in Section 2.5.3.

Setting the maximum allowed spinal cord dose to 45 Gy during optimization resulted in a maximum dose slightly above 45 Gy after optimization and final dose calculation. This objective was lowered to 43 Gy for all patients in subsequent plans, and this ensured that the final maximum dose stayed below 45 Gy.

It was necessary to add an objective for esophagus dose for two patients. This objective was mean dose < 34 Gy (Max EUD 34 Gy with parameter $a = 1$) with weight 500.

The same objectives were used in each patient's final full-arc plan and partial-arc plan.

3.3 Dose escalation

A plan with optimization dose (OD) 60 Gy was made for each patient. These plans were scaled so the mean CTV dose was exactly 60 Gy. For patients where the lung, spinal cord, and esophagus doses in this plan were acceptable (below the given limits), further dose escalation was done. The OD was increased by one fraction (1.5 Gy) at the time until one of the given objectives no longer was fulfilled. The opposite was done for patients where the doses were above the limits in the 60 Gy. The de-escalation was done 1.5 Gy at the time. The objectives used in the escalated plans, including the first 60 Gy plan, are shown in Tab. 3.2.

The escalated plans were not scaled, so the optimization dose (OD) was not equal to the resulting prescribed dose (PD), which was defined as the mean CTV dose.

Table 3.2: Objectives used for the escalated VMAT plans. The optimization dose OD is a multiple of 1.5 Gy.

ROI	Objective	Weight
PTV union	Min 95% of OD	3000
CTV (all volumes)	Uniform dose 100% of OD	300
External	Max 105% of OD	1000
External	Dose fall-off 100% to ∼75% of OD in 2 cm	100
Total lung minus GTV	Max 20 Gy to 35% volume	1000
Total lung minus GTV	Max 5 Gy to 65% volume	800
Total lung minus GTV	Max EUD 20 Gy, $a = 1$	1000
Spinal canal	Max 43 Gy	500
Esophagus	Max EUD 34 Gy, $a = 1$	500
Esophagus (OD $\geq$ 60 Gy)	Max OD to 2% volume	300
Esophagus (OD $<$ 60 Gy)	Max 60 Gy to 2% volume	300

3.4 Plan evaluation

Dose-volume histograms for all plans were exported from RayStation 4.5 and imported to MATLAB. Dose-volume parameters and NTCP were calculated using the MATLAB scripts listed in Appendix A. It is possible to calculate NTCP in RayStation, but the necessary module was not available at the time of this study. However, a research version was available, and this was used to check that the MATLAB script gave the same results as the NTCP function in RayStation when the same parameters were used.

The doses mentioned are physical doses delivered in 1.5 Gy fractions twice daily, not recalculated as 2 Gy fractions unless specifically stated otherwise.

3.4.1 Dose-volume parameters

The PTV union and CTV union were the target volumes used for evaluation. The fractional volume receiving more than 90% of the prescribed dose ($V_{90\%}$), the near-minimum ($D_{98\%}$) and near-maximum doses ($D_{2\%}$) were evaluated for the PTV union. For the CTV union, $V_{95\%}$ and the near-minimum dose $D_{98\%}$ were evaluated. The conformity between the 95% isodose and the CTV volume was evaluated by calculating the Jaccard index given in Eq. 2.5. In addition, homogeneity within the CTV volume was assessed using Eq. 2.6.

The lung dose parameters evaluated were V_{20} and V_5 (the lung volumes receiving more than 20 Gy and 5 Gy, respectively), mean dose, and NTCP for radiation pneumonitis. For the esophagus the mean dose and NTCP for esophagitis were considered, in addition to V_{60} for the escalated plans. The dose delivered to the hottest 0.1 cm^3 of the spinal cord ($D_{0.1\text{cm}^3}$) was also evaluated.

For the entire volume within the external contour, the dose to the hottest 2% ($D_{2\%}$) and the volume receiving 90% of the prescribed dose or more ($V_{90\%}$) were considered.

The remaining volume at risk (RVR) was defined as the volume within the external contour with the CTV, spinal canal, lungs, and esophagus subtracted. For this volume, $V_{90\%}$ was evaluated.

3.4.2 NTCP

The NTCP for radiation-induced pneumonitis was assessed using the LKB model with parameters $TD_{50} = 28.4$ Gy, $m = 0.374$ and $n = 0.99$. These numbers are taken from the work of Hedin and Bäck, who adjusted the parameters found by Seppenwoolde et al. to make them valid for different cancer treatments and dose calculation algorithms [49], in this case lung cancer treatments using Oncentra's Collapsed Cone. Seppenwoolde et al. used data from 382 patients with inoperable NSCLC, breast cancer, or malignant lymphoma. The end point was Grade $\geq$2 radiation pneumonitis[1], and the parameters giving the best fit were $TD_{50} =$ 30.8 Gy, $m = 0.37$, and $n = 0.99$ [50].

The lung DVHs were corrected for fractionation and incomplete repair using Eq. 2.19. $\alpha/\beta = 3$ Gy was used. For correction for incomplete repair between fractions, biexponential repair with half times $T_{(1/2),s} = 0.3$ h and $T_{(1/2),l} = 4$ h was assumed, with the short and long component having equal weight ($l = 0.5$ in Eq. 2.19). These values were taken from the biological module in the RayStation research version 4.4.100.

The fractionation schedule used was 2 fractions per day with 6 hours between, delivered 5 days a week, i.e. the time between fraction q and $q + 1$ was

[1]Scored using the Southwest Oncology Group (SWOG) toxicity criteria

$$\Delta t_q = \begin{cases} 6 \text{ hours} & \text{for } q = 1, 3, 5, ... \\ 66 \text{ hours} & \text{for } q = 10, 20, 30, ... \\ 18 \text{ hours} & \text{otherwise.} \end{cases} \tag{3.1}$$

The NTCP for radiation esophagitis was calculated using the LKB model with parameters found by Chapet et al.; $TD_{50} = 51$ Gy, $n = 0.44$, and $m = 0.32$ [51]. These numbers are based on DVH data from 101 patients with NSCLC treated with 3DCRT, where Grade 2-3 esophagitis[2] counted as events. The rates of esophagitis were 2.5, 7, 9 and 13.4%, respectively, when the NTCP values were <10%, <15%, <20% and <25%. The esophagus was contoured from the first rib superiorly to the gastro-esophageal junction inferiorly. $\alpha/\beta = 10$ Gy was used, as esophagitis is an early effect. Correction for incomplete repair was not done due to lack of reliable $T_{1/2}$ values; that is, Eq. 2.18 was used instead of Eq. 2.19. It was not necessary to correct for PB/CC differences, as the two algorithms give similar results in soft tissue.

To avoid numerical integration, the relation in Eq. 2.26 was used. The error function erf(x) can be calculated using a built-in function in MATLAB.

3.4.3 Statistical analysis

Comparison of dosimetric parameters was done using the paired, two-sided Student's t-test with significance level 0.05. The MATLAB function *ttest(x,y)*, which takes two vectors x and y as arguments and returns a test decision and a p-value for the null hypothesis that the data in the vector $x - y$ comes from a normal distribution with mean equal to zero and unknown variance, was used.

3.5 Dose calculated in RayStation vs. Oncentra

Two different treatment planning systems are available at St. Olavs Hospital today: RayStation 4.5 and Oncentra External Beam v4.3 (referred to as Oncentra from here on). The VMAT plans in this study were made in RayStation 4.5, while the 3DCRT plans were made in different versions of Oncentra's treatment planning system. Recalculation of the 3DCRT plans was not possible, as mentioned earlier in Section 3.1.1. A brief comparison of the dose distributions resulting

[2]Scored using the Radiation Therapy Oncology Group (RTOG) toxicity criteria

from calculations in RayStation and Oncentra was done to see if there were differences between the systems, and if so, where and how large the differences were.

A new 3DCRT plan was made in Oncentra for one of the HAST patients. The field arrangement in this plan was similar to that of the plan originally delivered to the patient. Photon energy 6 MV was used exclusively. No wedges were used in this plan. Dose was first calculated using the Collapsed Cone engine in Oncentra. The plan, including the original dose, was then exported to RayStation. A copy of the plan was then made, and dose was recalculated using RayStation's Collapsed Cone engine. The plans were then compared in RayStation, first without normalization (i.e. the number of MUs delivered was not changed), then after the plans were normalized so the mean CTV dose was 45 Gy.

The parameters compared were the mean lung dose, V_{20} and V_5 to the union of both lungs with the GTV subtracted, NTCP for radiation pneumonitis (using the parameters in 3.4.2), mean dose to the volume within the external contour, mean dose to the PTV union, mean dose to the CTV union, and $D_{98\%}$ to the CTV union.

In addition, the same plan was calculated for a virtual phantom (a 40x40x40 cm^3 box with CT number 0 HU, density 1 g/cm^3), first in Oncentra and then in RayStation.

4 Results

Parameters for all plans are summarized in Tab. 4.1 on page 40. As stated earlier, all doses mentioned are in 1.5 Gy fractions delivered twice daily, and not recalculated as 2 Gy fractions unless specified.

4.1 VMAT vs. 3DCRT: 45 Gy

Dose distributions and DVHs for the full-arc VMAT plan and 3DCRT plan of four selected patients are shown in Appendix D.

4.1.1 Partial arcs

The total arc lengths of the partial arc plans ranged from 92° to 264°, and the average value was 163°. The arc segments used for each patients are listed in Appendix B. The resulting field arrangements tended to be similar to two opposing fields.

The significant differences found when comparing the partial-arc plans to the full-arc plans were a decrease in $V_{90\%,\mathrm{PTV}}$ and $D_{98\%,\mathrm{PTV}}$, a higher (worse) CTV homogeneity index, higher V_{20} to the residual lung volume, higher mean esophagus dose, and a higher NTCP for radiation esophagitis ($p < 0.05$ for all parameters listed). These differences are all in favor of the full-arc plans.

It should be noted that all the differences listed above are small, as summarized in Tab. 4.1. For the remainder of the analysis, only the full-arc plan will be considered.

4.1.2 Target coverage

The target coverage was better for VMAT than 3DCRT. $V_{90\%,\mathrm{PTV}}$, $D_{98\%,\mathrm{PTV}}$, and $V_{95\%,\mathrm{CTV}}$ were all significantly improved when changing from 3DCRT to VMAT ($p < 0.05$); as were $D_{98\%,\mathrm{CTV}}$, conformity between the CTV volume and the 95% isodose, and CTV homogeneity ($p < 10^{-4}$). The mean values for these parameters are listed in Tab. 4.1.

$V_{90\%,\mathrm{PTV}}$ was higher than 95% for all VMAT plans, while there was a larger spread in the values for the 3DCRT plans, as illustrated in Fig. 4.1. The lowest value observed for the 3DCRT plans was 90.0%.

The near-minimum dose to the PTV, $D_{98\%,\mathrm{PTV}}$, was increased from on average 39.6 Gy for the 3DCRT plans to 40.8 Gy for the VMAT plans ($p < 0.05$). The near-maximum dose, $D_{2\%,\mathrm{PTV}}$, was unchanged between the plans.

The near-minimum dose to the CTV, $D_{98\%,\mathrm{CTV}}$, was higher than 95% of the prescribed dose for all VMAT plans, while there was a larger variation for the 3DCRT plans, as can be seen in Fig. 4.1. The 95% isodose covered $\geq 99\%$ of the CTV volume in all full-arc VMAT plans.

The mean conformity between the CTV volume and the 95% isodose was improved from 0.27 for the 3DCRT plans to 0.38 for the VMAT plans ($p < 10^{-4}$). Homogeneity improved from 0.114 to 0.058 ($p < 10^{-4}$).

It was observed that as the lung dose was reduced, high dose areas appeared outside the PTV to a larger degree, especially in the patient's anterior-posterior direction.

4.1.3 Organs at risk

Graphs showing the values of the selected dosimetric parameters for all patients are in Appendix C.

Lungs

V_{20}, mean lung dose, and NTCP for radiation pneumonitis were reduced in the VMAT plans compared to 3DCRT for all patients, as shown in Fig. C.1, C.2 and C.3. In the 3DCRT plans, the mean V_{20} for all patients was 33.6%. This was reduced to 27.7% for VMAT ($p < 10^{-7}$). The mean lung dose was reduced from 16.3 Gy on average for the 3DCRT plans to 13.8 Gy for VMAT ($p < 10^{-7}$). NTCP for radiation pneumonitis was reduced from 10.1% for 3DCRT to 6.3% for VMAT ($p < 10^{-4}$). V_{20} was above 35% in three VMAT plans and mean lung dose was below 20 Gy in all VMAT plans.

V_5 was also significantly reduced for VMAT compared to 3DCRT ($p < 0.05$), although the values were higher for VMAT for three patients, as shown in Fig. C.4. The mean value for all patients was 59.1% for 3DCRT and 52.4% for VMAT. V_5 was above 65% in two VMAT plans, and the highest observed value in the VMAT plans was 65.3%.

The mean reduction from 3DCRT to VMAT was 18% for V_{20}, 15% for mean lung dose, 10% for V_5, and 34% for NTCP, and the lowest observed parameters

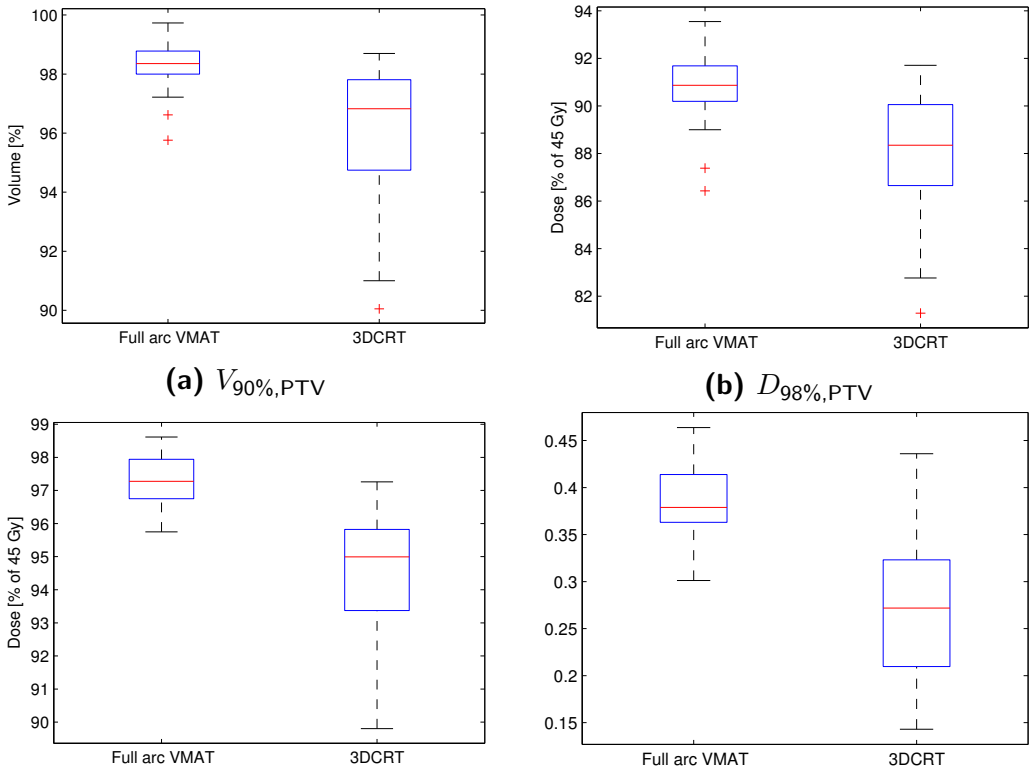

(a) $V_{90\%,\text{PTV}}$ **(b)** $D_{98\%,\text{PTV}}$

(c) $D_{98\%,\text{CTV}}$ **(d)** Conformity CTV

Figure 4.1: Box plots illustrating the distribution of $V_{90\%,\text{PTV}}$, $D_{98\%,\text{PTV}}$, $D_{98\%,\text{CTV}}$, and the conformity between the 95% isodose and the CTV volume for the 45 Gy full-arc VMAT plans and 3DCRT plans. The red lines indicate the median value, the edges of the blue boxes mark the 25th and 75th percentiles, and the whiskers extend to the most extreme data points not considered outliers. Outliers are marked as red crosses. The box plots were made in MATLAB, in which data points larger than $q_3 + w(q_3 - q_1$ or smaller than $q_1 - w(q_3 - q_1)$ are drawn as outliers. q_1 and q_3 are the 25th and 75th percentile, and w is a parameter determining the maximum whisker length, set to 1.5 as default [52].

Table 4.1: Average dose parameters for all plans. Conformity is calculated as the Jaccard index between 95% isodose and CTV union. Homogeneity is defined as $(D_{2\%} - D_{98\%})/D_{50\%}$. The GTVs were subtracted from the total lung volume. RP = radiation pneumonitis, RE = radiation esophagitis, PD = prescribed dose (mean CTV dose), RVR = remaining volume at risk.

ROI	Parameter	3DCRT 45 Gy	VMAT 45 Gy full arcs	VMAT 45 Gy partial arcs	VMAT Escalated full arcs
PTV union	$V_{90\%}$ (%)	96.0	98.2	97.6	99.1
	$D_{98\%}$ (% of PD)	87.9	90.7	89.6	92.5
	$D_{2\%}$ (% of PD)	105.7	105.3	105.3	105.5
CTV union	$V_{95\%}$ (%)	96.2	99.9	99.8	99.7
	$D_{98\%}$ (% of PD)	94.2	97.3	97.0	97.3
	Conformity	0.27	0.38	0.38	0.39
	Homogeneity	0.114	0.058	0.069	0.057
Lungs	V_{20} (%)	33.6	27.7	28.3	34.3
	V_5 (%)	59.1	52.4	51.8	63.2
	Mean dose (Gy)	16.3	13.8	13.8	18.8
	NTCP for RP (%)	10.1	6.3	6.4	12.0
Esophagus	Mean dose (Gy)	25.5	24.9	25.2	30.6
	V_{60} (cm^3)	0	0	0	3.9
	NTCP for RE (%)	12.0	11.7	12.0	24.3
Spinal canal	$D_{0.1cm^3}$ (Gy)	44.3	43.5	43.6	44.1
External	$V_{90\%}$ (cm^3)	2091	1469	1472	1316
	$D_{2\%}$ (% of PD)	102.4	99.8	100.0	99.6
RVR	$V_{90\%}$ (cm^3)	1089	667	667	519

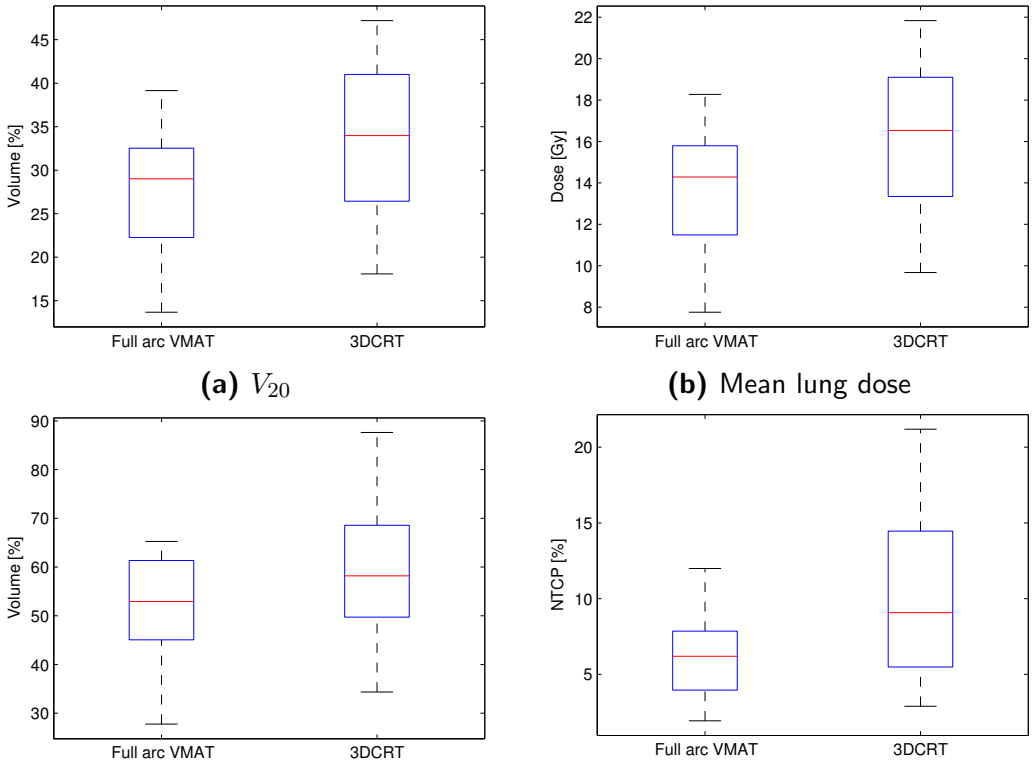

(a) V_{20} **(b)** Mean lung dose

(c) V_5 **(d)** NTCP for RP

Figure 4.2: Box plots illustrating the distribution of lung V_{20}, mean dose, V_5, and NTCP for radiation pneumonitis for the 45 Gy full-arc VMAT plans and 3DCRT plans.

in the VMAT plans were $V_{20} = 13.7\%$, mean lung dose = 7.8 Gy, $V_5 = 27.8\%$, and NTCP = 1.9%.

The distributions of the mentioned parameters are shown in Fig. 4.2.

Esophagus

There was no significant difference in mean esophagus dose ($p = 0.15$) nor NTCP for radiation esophagitis ($p = 0.56$) between the 3DCRT and full-arc VMAT plans. The mean esophagus dose was below 34 Gy as desired for all VMAT plans, and for 18 of the 20 3DCRT plans. The highest mean esophagus dose observed in the 3DCRT plans was 37.9 Gy.

Spinal canal

$D_{0.1\text{cm}^3}$ was below 45 Gy (in 1.5 Gy fractions twice daily) for all the full-arc VMAT plans, as desired in the making of the plans. It was higher than 45 Gy for 13 of 20 3DCRT plans, and the highest observed value was 49.8 Gy. There were no significant differences between the plan sets ($p = 0.33$).

There was a tendency for $D_{0.1\text{cm}^3}$ to be lower for VMAT than 3DCRT for those patients where $D_{0.1\text{cm}^3}$ was higher than 45 Gy in the 3DCRT plans, and the opposite for patients where $D_{0.1\text{cm}^3}$ was very low (below ∼40 Gy), as shown in Fig. C.5.

External/RVR

There was a significant reduction in the volume receiving more than 40.5 Gy (90% of the prescribed dose) within the external contour when changing from 3DCRT to full-arc VMAT, from 2091 cm^3 to 1469 cm^3 ($p < 10^{-4}$). $V_{90\%}$ was also significantly lowered for the remaining volume at risk (RVR), from 1089 cm^3 for 3DCRT to 667 cm^3 for full-arc VMAT ($p < 10^{-3}$).

$D_{2\%}$ was significantly higher for 3DCRT than VMAT (102.4% of 45 Gy vs. 99.8% of 45 Gy, $p < 10^{-3}$).

The DVHs for the RVR averaged for all patients for the VMAT plans and 3DCRT plans are shown in Fig. 4.3. It can be observed that a larger volume receives doses below approximately 10 Gy for VMAT.

4.2 Dose escalation

Dose escalation above 45 Gy (mean dose to CTV) was possible for 17 of 20 patients, while escalation above 60 Gy was possible for 7 of these 17. For the final three patients, escalation above 45 Gy was not possible as some dose limits were already exceeded at 45 Gy.

Dose escalation was not possible for three patients. One of these was the patient with the largest PTV volume of all the patients (2042 cm^3, the median value was 887 cm^3). The other two had satellite tumors in the lung, resulting in areas of high dose in the lung between the satellite and the rest of the tumor volume. Dose distributions for the 45 Gy VMAT and 3DCRT plans for one of these patients are shown in Fig. D.4 in Appendix D.

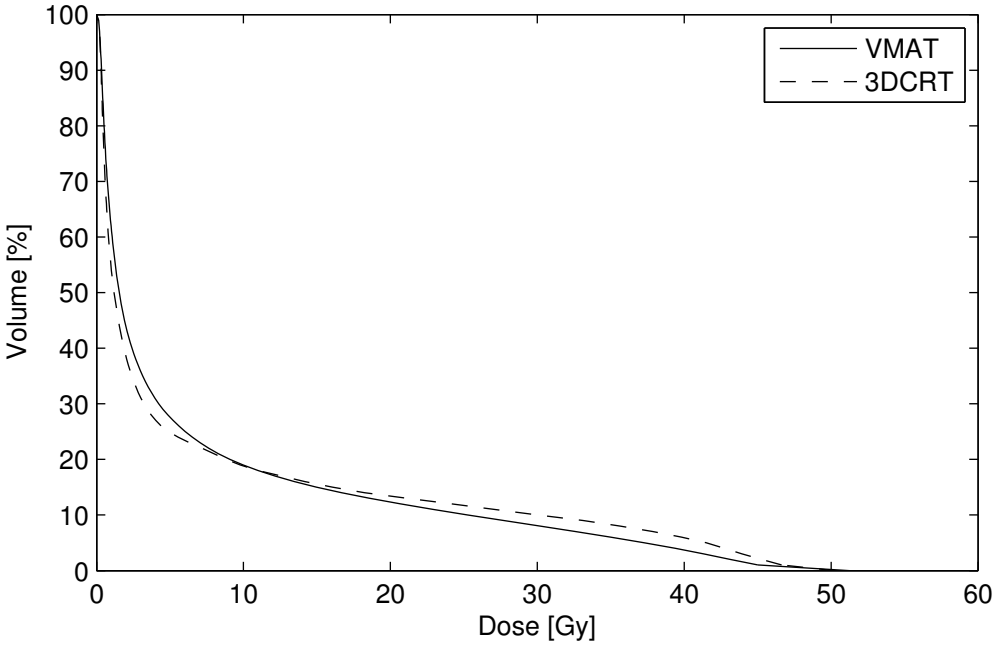

Figure 4.3: Dose-volume histogram for the RVR averaged over all patients for the full-arc VMAT plans and the 3DCRT plans. The volume resolution used was 1%.

The prescribed doses in the escalated plans are listed in Tab. 4.2 and illustrated in Fig. 4.4. The mean prescribed dose was 59.0 Gy. The equivalent dose in 2 Gy fractions, EQD_2, was calculated for the prescribed doses using $\alpha/\beta = 10$ Gy, which is the standard value for tumors. Accelerated tumor repopulation was not taken into account. The highest prescribed was 83.7 Gy, which corresponds to an EQD_2 of 80.1 Gy. All OAR doses were well below the given limits for this patient, but it was decided to stop escalation at this level regardless. For the remaining patients, the limiting factor stopping further dose escalation was lung dose (mean lung dose, V_{20}, or V_5) for 10 patients, $D_{1\%}$ to the spinal canal for three patients (see comment regarding $D_{1\%}$ vs. $D_{0.1\mathrm{cm}^3}$ in Section 4.2.2), mean esophagus dose for two patients, and both lung V_{20} and mean esophagus dose for one patient.

When comparing with the 45 Gy plans, only the values of the 17 patients for whom dose escalation was possible were included. The mean values listed here will therefore differ from the values listed in Tab. 4.1, as the latter were calculated for all 20 patients.

Table 4.2: Number n of fractions, resulting prescribed dose (mean dose to the CTV) = PD, and equivalent dose in 2 Gy fractions (EQD_2) for the escalated plans. $\alpha/\beta = 10$ Gy was used, tumor repopulation was not taken into account. Dose escalation above 45 Gy was not possible for patient no. 51, 82, and 161.

Patient	n	PD (EQD_2) (Gy)	Patient	n	PD (EQD_2) (Gy)
19	42	62.5 (59.8)	82	-	-
30	41	61.2 (58.6)	83	34	50.9 (48.8)
36	47	70.3 (67.3)	86	33	49.5 (47.4)
43	50	74.9 (71.7)	93	39	58.2 (55.7)
45	32	48.3 (46.3)	100	31	46.1 (44.1)
51	-	-	109	39	58.5 (56.1)
52	49	73.1 (70.0)	120	33	49.5 (47.5)
59	37	54.9 (52.5)	149	56	83.7 (80.1)
70	36	53.2 (50.9)	151	31	46.3 (44.4)
71	41	61.1 (58.5)	161	-	-

4.2.1 Target coverage

$V_{90\%,\mathrm{PTV}}$ was higher than 95% for all patients, with a mean value of 99.1%. This was significantly higher than for the full-arc VMAT plans (mean value 98.3%, $p < 0.05$) and the 3DCRT plans (mean value 95.7%, $p < 10^{-4}$).

The mean values for the near-minimum and near-maximum doses, $D_{98\%,\mathrm{PTV}}$ and $D_{2\%,\mathrm{PTV}}$, were 92.5% and 105.5% of the prescribed dose, respectively. $D_{98\%,\mathrm{PTV}}$ was significantly higher than for the full-arc VMAT plans (mean value 90.9%, $p < 0.05$) and the 3DCRT plans (mean value 87.6%, $p < 10^{-5}$).

$D_{98\%,\mathrm{CTV}}$ was higher than 95% of the prescribed dose for all patients (mean value 97.3%), and was significantly higher than for 3DCRT (mean value 94.1%, $p < 10^{-3}$). The mean homogeneity index was 0.057, which was better than for the 3DCRT plans (mean value 0.12, $p < 10^{-4}$). The mean conformity between the CTV volume and the 95% isodose was 0.39. This was a significant improvement compared to 3DCRT (mean value 0.28, $p < 10^{-4}$), but not VMAT (mean value 0.38, $p = 0.51$).

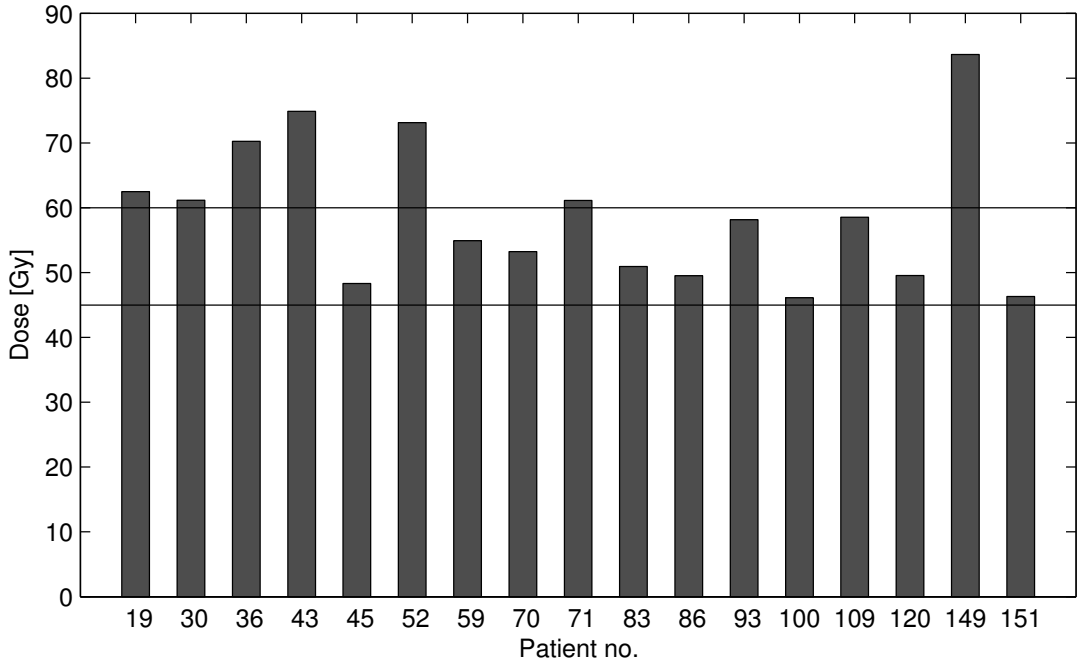

Figure 4.4: Prescribed dose (mean CTV dose) in the escalated plans for the 17 patients where dose escalation was possible. The horizontal lines are drawn at 45 Gy and 60 Gy.

4.2.2 Organs at risk

The plans were designed to give the highest possible dose to the target volumes while keeping the risk organ doses below the limits mentioned below. The dose-volume parameters for the lungs, spinal canal, and esophagus for the escalated plans were not compared with those of the 45 Gy plans.

Lungs

V_{20} to the residual lung volume was below 35% for 14 of the 17 patients. Small deviations from this limit were allowed, and the highest value was 35.7%. V_5 was below 65% and the mean lung dose was 20 Gy or lower for all patients.

The average values for V_{20}, V_5, and mean lung dose for all patients were 34.3%, 63.2%, and 18.8 Gy, respectively. The mean NTCP for radiation pneumonitis was 12.0%.

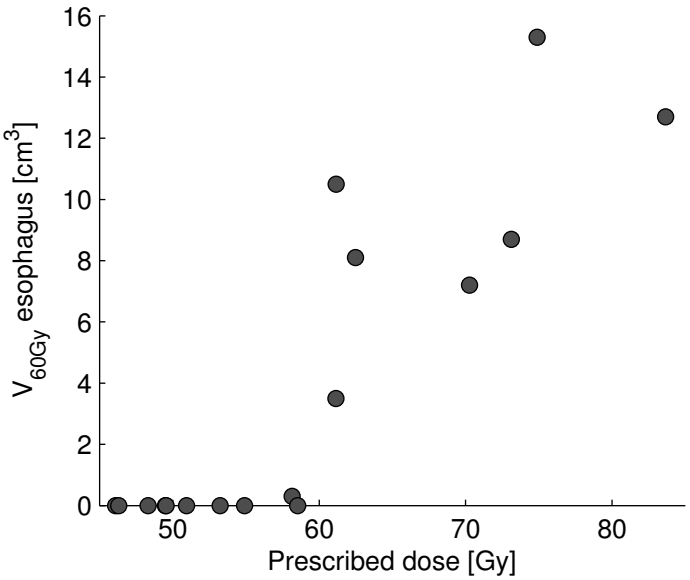

Figure 4.5: Prescribed dose vs. the esophageal volume receiving 60 Gy or higher for the escalated plans.

Spinal canal

During the escalation and de-escalation process, the dose to 1% of the spinal canal was evaluated. It was later decided to instead use the dose to 0.1 cm^3 of the volume for the final evaluation of all plans. While $D_{1\%}$ was below 45 Gy for all patients, this was not the case for $D_{0.1\text{cm}^3}$, which was higher than 45 Gy for four patients. The highest $D_{0.1\text{cm}^3}$ observed was 46.2 Gy.

Esophagus

The mean esophagus dose was lower than 34 Gy for all patients.

V_{60} was larger than zero for eight patients. These were the seven patients with prescribed dose 60 Gy or higher, plus one patient with prescribed dose 58.2 Gy. The highest observed value was 15.3 cm^3. It should be noted that this was in a patient with prescribed dose 74.9 Gy, i.e. not the patient with the highest prescribed dose. Images showing the anatomy of the esophagus relative to the target volumes for the patients with the highest V_{60} and the highest prescribed dose are showed in Fig. 4.6 and 4.7. The relationship between prescribed dose and V_{60} for all patients is shown in Fig. 4.5.

The mean NTCP for radiation esophagitis was 24.3%, with a range from 14.5%

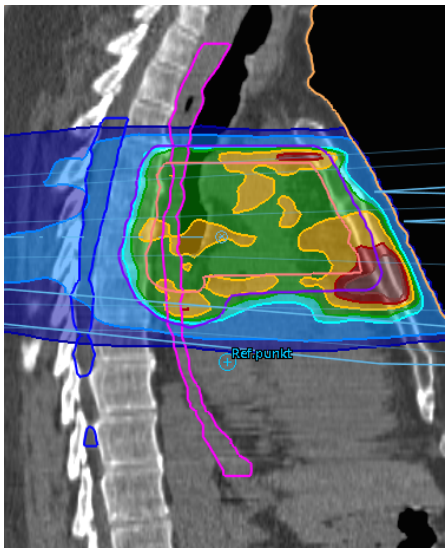

Figure 4.6: Sagittal cross section showing the anatomy of the patient with the highest esophagus V_{60}. The esophagus is contoured in hot pink, the PTV union in purple, and the CTV union in light pink.

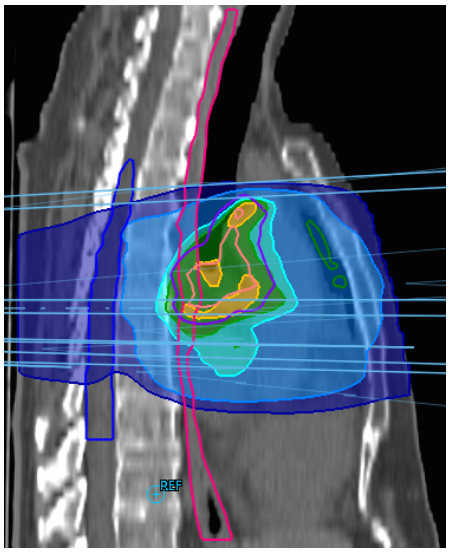

Figure 4.7: Sagittal cross section showing the anatomy of the patient with the highest prescribed dose. The esophagus is contoured in hot pink, the PTV union in purple, and the CTV union in light pink.

to 39.8%.

External/RVR

The volume receiving 90% of the prescribed dose, $V_{90\%}$, were lower for the escalated plans than the 3DCRT plans both for the total volume within the external contour and the remaining volume at risk. For external it was lowered from on average 1831 cm^3 to 1316 cm^3 ($p < 0.05$), and for the RVR it was lowered from 944 cm^3 to 520 cm^3 ($p < 0.005$). $V_{90\%}$ was not significantly different from the full-arc VMAT plans, neither for RVR ($p = 0.11$) or the volume within the external contour ($p = 0.88$).

4.3 Dose calculated in RayStation vs. Oncentra

Six radiation fields were used; two main fields and two segments in the anterior-posterior direction, and two fields of lower intensity in the left-right direction. This is illustrated in Fig. 4.10.

4.3.1 Without normalization

For the patient case, RayStation calculated higher doses than Oncentra inside the field, while Oncentra calculated higher doses in the penumbra region. Dose difference plots are shown in Fig. 4.12 and 4.13. The largest in-field differences were found in the build-up region of the beams, followed by air cavities, lung tissue, and bone (e.g. the vertebra). In soft tissue, the difference was between 1 and 3% of 45 Gy. In lungs, it was 2-6%. The difference was up to 12% in one of the bronchi. The DVHs for lungs and PTV are shown in Fig. 4.8. The dose difference in the lungs is apparent for the highest doses (above ∼35 Gy) in the DVH.

The largest deviations observed outside of the build-up regions was in an air cavity in the patient's right bronchus, as shown in Fig. 4.14. It was noted that the difference exceeded 5% where the CT numbers were below approximately HU = -990. The CT numbers, and thus density, were lower in the right bronchus than in the left, which may explain why the extreme deviations were only present in the right bronchus and not in the left.

Dose parameters for the two plans are summarized in Tab. 4.3. NTCP for radiation pneumonitis was calculated using the parameters listed in Section 3.4.2. Mean lung dose, NTCP, and V_5 were higher for the RayStation plan, while V_{20} was higher for the Oncentra plan. RayStation calculated ∼2% higher doses to the target volumes.

For the virtual water phantom, differences were mainly apparent in the build-up region and in the penumbra region (between 1% and 5%), see Fig. 4.16.

4.3.2 Normalized plans

Copies of both the plan made in RayStation and the plan made in Oncentra were normalized so D_{mean} to the CTV was 45 Gy. This resulted in smaller differences between the plans, as shown in the DVH for lungs and PTV in Fig 4.9 and the

Table 4.3: Dose-volume parameters for the plan calculated in RayStation (RS) and the plan calculated in Oncentra External Beam (OEB), and the ratio between the values. RP = radiation pneumonitis.

Parameter	RayStation	Oncentra	OEB/RS
Mean lung dose (Gy)	17.0	16.8	99%
NTCP for RP (%)	10.5	10.0	95%
V_{20} lungs (%)	34.3	34.9	102%
V_5 lungs (%)	61.5	61.2	100%
Mean dose external (Gy)	9.6	9.5	99%
Mean dose PTV (Gy)	45.4	44.3	98%
Mean dose CTV (Gy)	46.0	44.9	98%
$D_{98\%}$ CTV (Gy)	43.7	42.4	97%

Table 4.4: Dose-volume parameters for the plan calculated in RayStation (RS) and the plan calculated in Oncentra External Beam (OEB) after the plans were normalized to give $D_{\text{mean,CTV}} = 45$ Gy. OEB/RS is the ratio between the values. RP = radiation pneumonitis.

Parameter	RayStation	Oncentra	OEB/RS
Mean lung dose (Gy)	16.6	16.9	102%
NTCP for RP (%)	9.8	10.0	102%
V_{20} lungs (%)	34.1	34.9	102%
V_5 lungs (%)	60.5	61.3	101%
Mean dose external (Gy)	9.4	9.5	101%
Mean dose PTV (Gy)	44.4	44.3	100%
Mean dose CTV (Gy)	45.0	45.0	100%
$D_{98\%}$ CTV (Gy)	42.7	42.5	100%

dose difference plot in Fig. 4.15. The plan from RayStation no longer showed exclusively higher doses in the mediastinum; the difference was now between -2 and +2% (of 45 Gy). The differences were reduced to 2-4% in lungs, up to 9% in the bronchus, and below 3% in the vertebra.

Dose parameters were also calculated for the normalized plans. These are listed in Tab. 4.4. The differences in target dose parameters were reduced. All lung dose parameters were higher for the Oncentra plan than the RayStation plan after normalization.

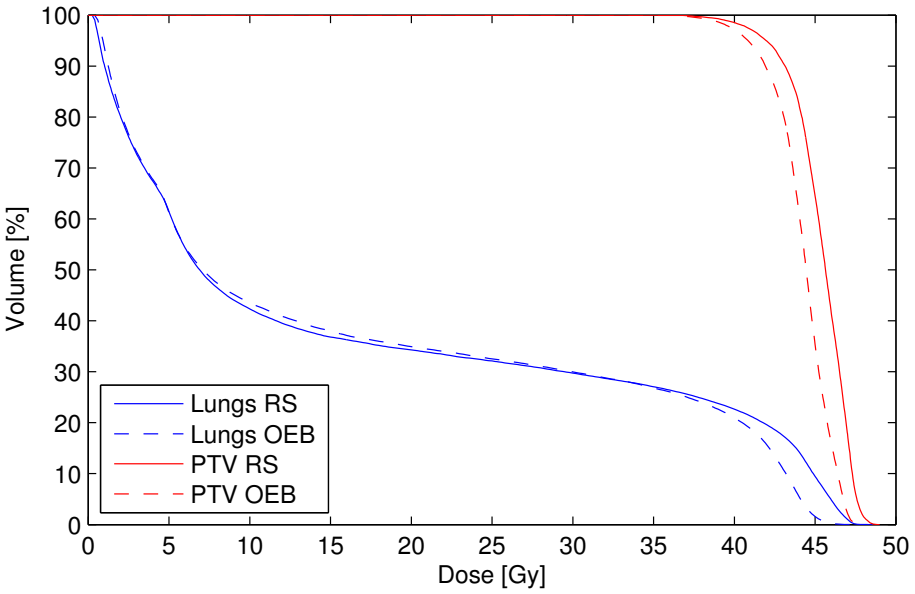

Figure 4.8: Dose to lungs and PTV calculated in RayStation (RS) and Oncentra External Beam (OEB).

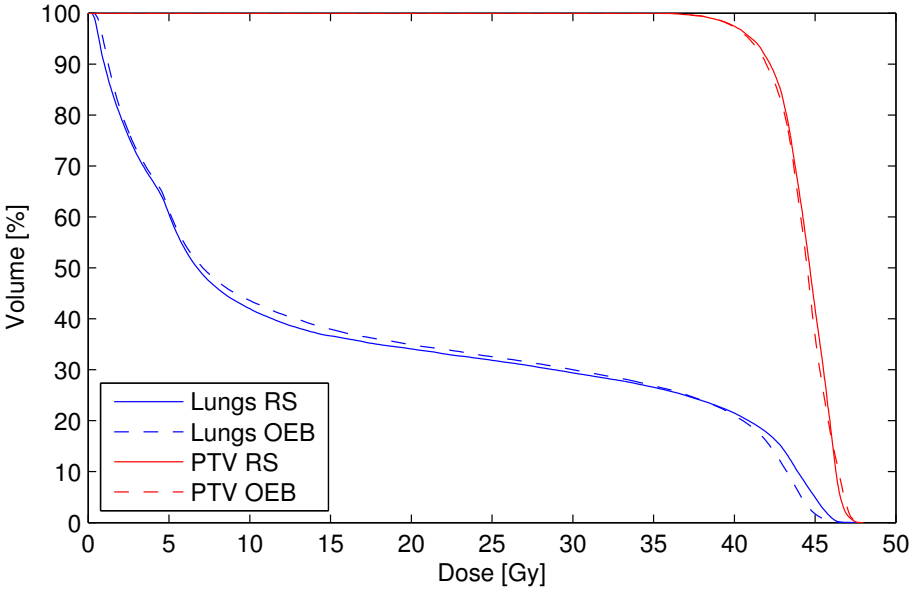

Figure 4.9: Dose to lungs and PTV calculated in RayStation (RS) and Oncentra External Beam (OEB) after the plans were normalized to give $D_{\text{mean,CTV}} = 45$ Gy.

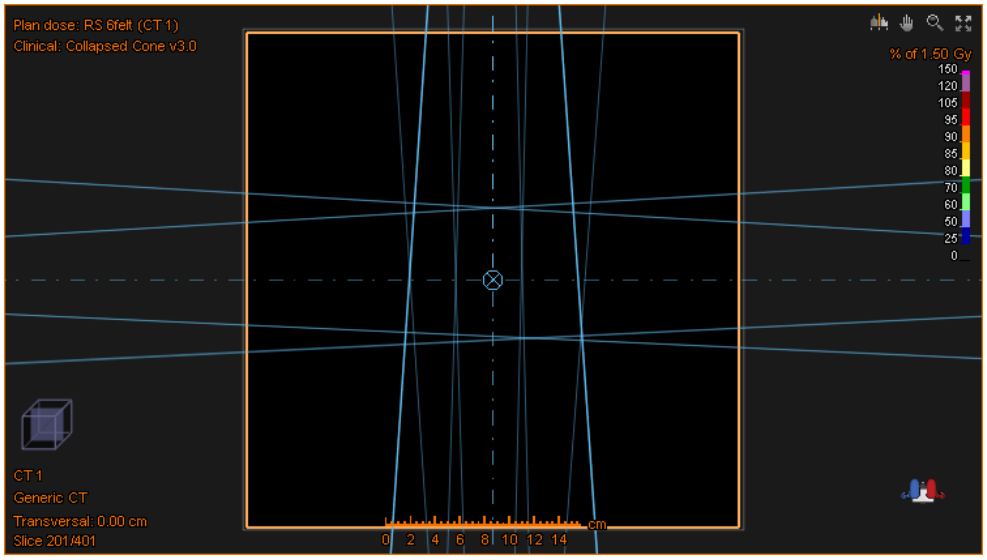

Figure 4.10: The radiation fields used in the RayStation vs. Oncentra comparison, here shown in the virtual phantom. Up/down in the picture corresponds to anterior/posterior in the patient. Left/right in the picture corresponds to the patient's right/left (seen from the patient's feet).

Figure 4.11: The isodose lines shown in the difference plots to follow. Dark blue indicates differences below -5%, purple between -3% and -5%, orange between 1% and 3%, red 3% - 4%, pink 4% - 5%, indigo 5% - 8%, light blue 8% - 10% and green above 10%.

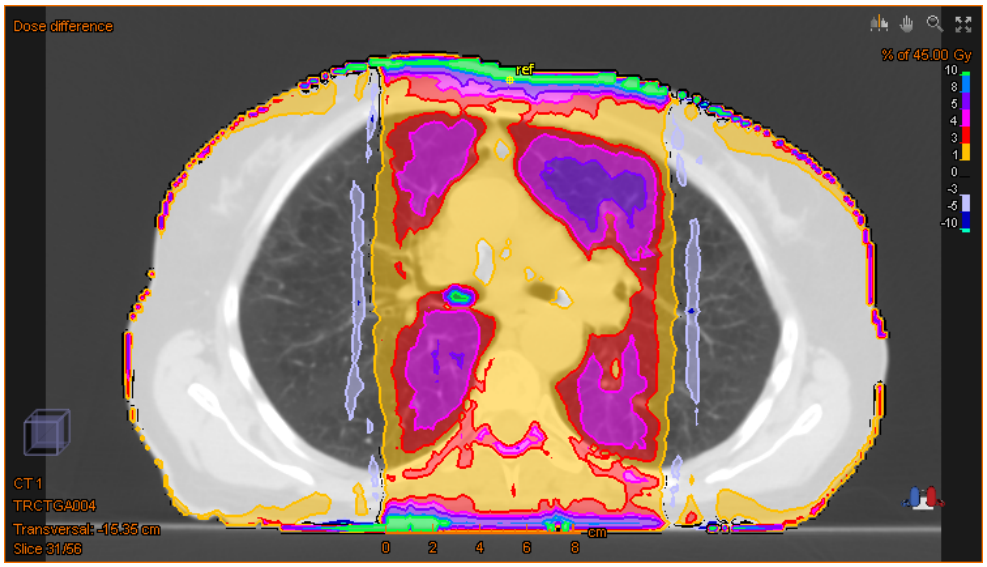

Figure 4.12: Difference plot showing the dose calculated in RayStation vs. Oncentra in an axial plane through the isocenter. The isodose lines are as explained in Fig 4.11, with reference value 45 Gy, and positive values indicating higher dose calculated in RayStation.

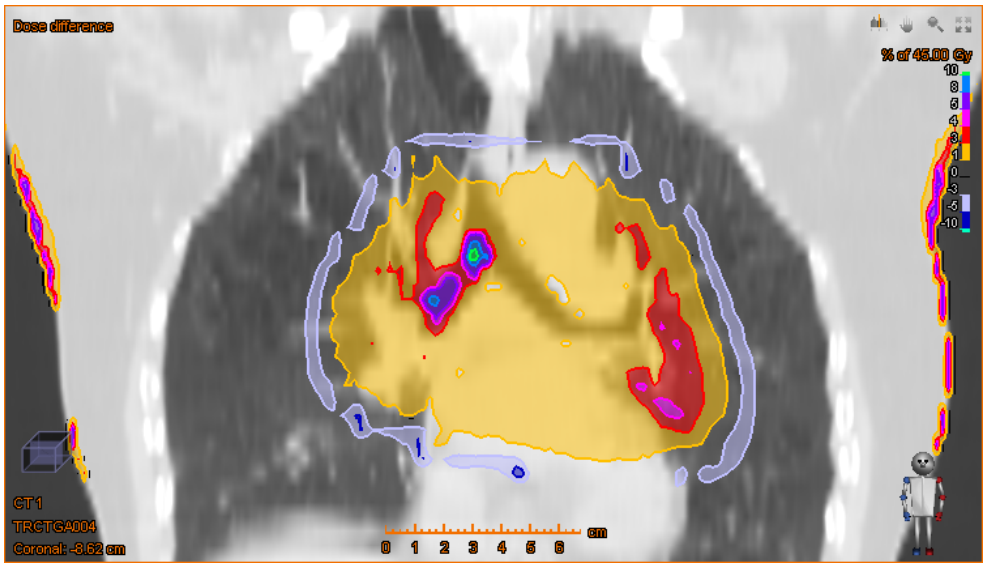

Figure 4.13: Difference plot RayStation vs. Oncentra in a coronal plane through the isocenter. The isodose lines are as explained in Fig 4.11, with reference value 45 Gy, and positive values indicating higher dose calculated in RayStation.

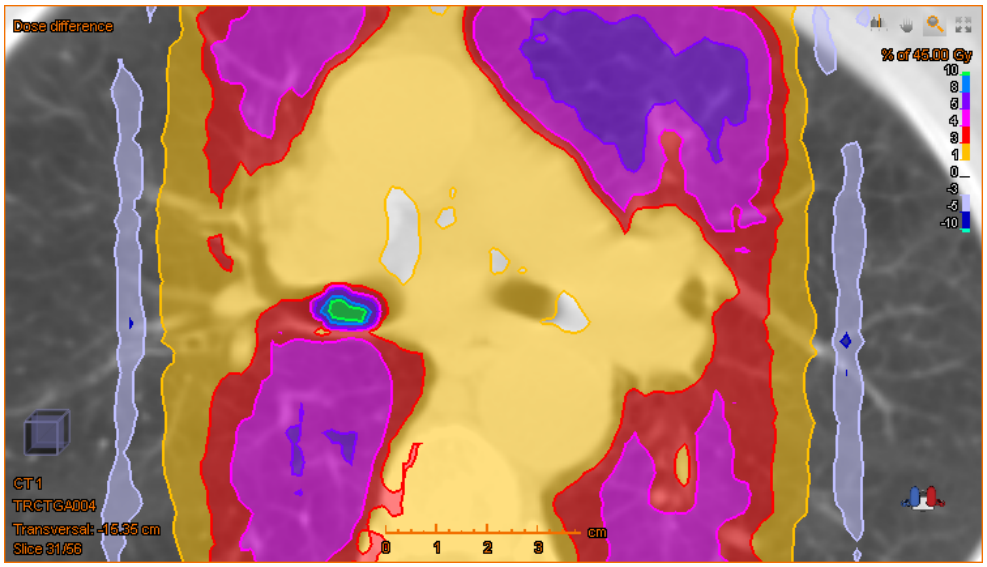

Figure 4.14: Difference plot in an axial plane zoomed in on an air cavity (the patient's right bronchus). The isodose lines are as explained in Fig 4.11, with reference value 45 Gy, and positive values indicating higher dose calculated in RayStation.

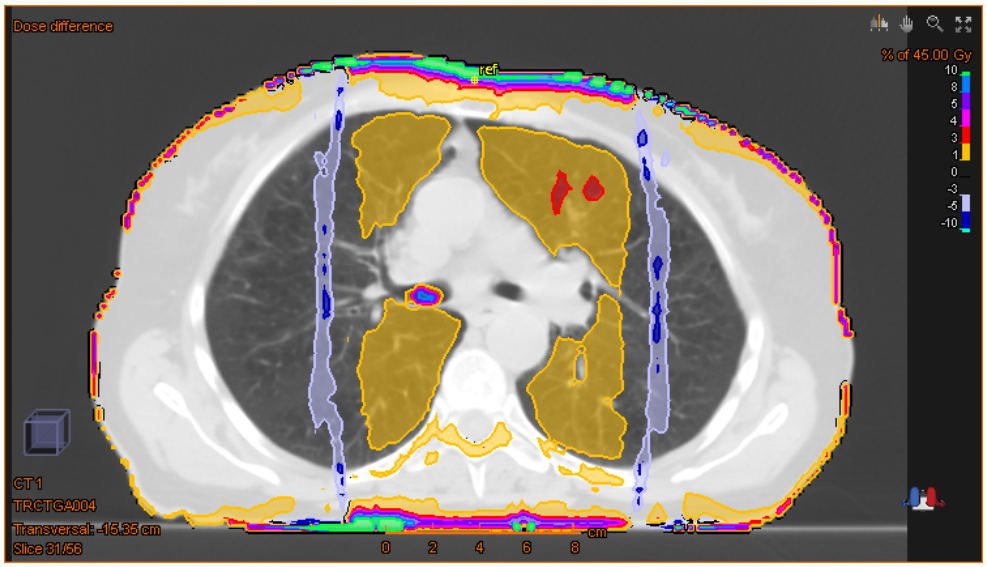

Figure 4.15: Difference plot showing the dose calculated in RayStation vs. Oncentra after the plans were normalized to give $D_{\text{mean,CTV}} = 45$ Gy in both plans. The isodose lines are as explained in Fig 4.11, with reference value 45 Gy, and positive values indicating higher dose calculated in RayStation.

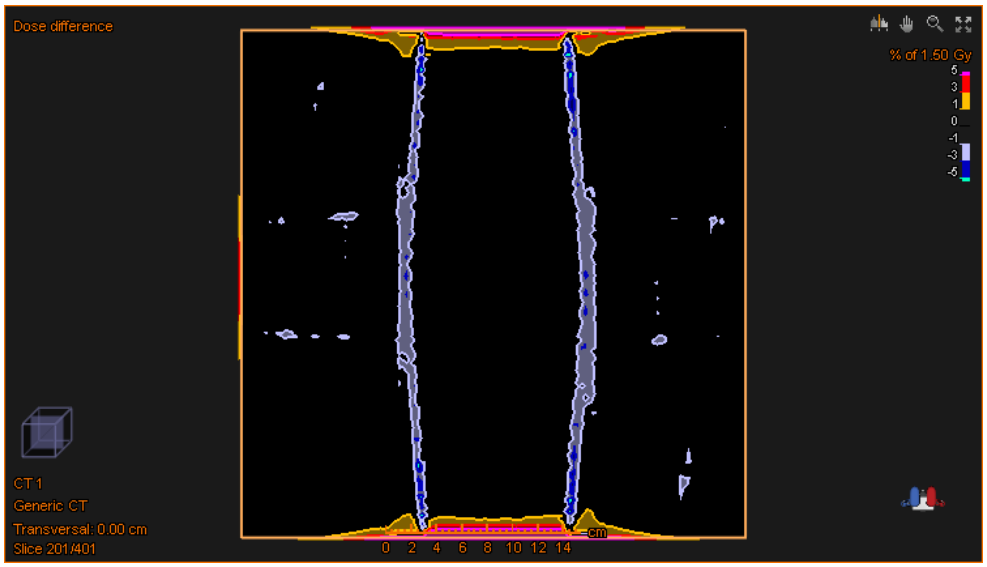

Figure 4.16: Difference plot showing the dose calculated in RayStation vs. Oncentra in the virtual phantom. The isodose lines shown are -5%, -3%, -1%, 1%, 3% and 5% of the maximum dose (1.5 Gy).

5 Discussion

Part of the scope of this thesis was to explore the possibilities of VMAT as a technique. In the first part of the study, the aim was to "push" the dose to healthy lung tissue as low as possible while keeping acceptable target dose levels and other organ at risk dose levels. In the second part, this was reversed: the dose to the target volumes was to be as high as possible, while keeping the dose to organs at risk below the given constraints. This was done to show how the deposition of dose can be "steared" using VMAT by changing the objectives used during the optimization. In radiotherapy, there is always a trade-off between high target doses/high conformity and low organ at risk doses, and VMAT may make it possible to control this trade-off to a larger degree.

The VMAT plans were made with the aim of equally good, or better, target dose coverage compared to the 3DCRT plans. This was achieved; $V_{90\%,\mathrm{PTV}}$, $V_{95\%,\mathrm{CTV}}$, $D_{98\%,\mathrm{PTV}}$, $D_{98\%,\mathrm{CTV}}$, conformity, and CTV homogeneity were all significantly improved for VMAT (both 45 Gy and the escalated plans) compared to 3DCRT. $V_{90\%}$ to the remaining volume at risk was reduced for VMAT compared to 3DCRT, which is also an indicator of improved target conformance.

In the 45 Gy plans, there was a significant reduction in all lung dose parameters for VMAT compared to 3DCRT. The mean reduction was 18% for V_{20}, 15% for mean lung dose, 10% for V_5, and 34% for NTCP. The other organ at risk dose parameters were below the desired limits for all patients.

Making plans with the aim of lowering the lung doses as much as possible would probably not be done in a clinical setting. More likely, a plan would be deemed acceptable as long as the organ at risk doses were below the given limits. It was observed that as the lung dose was reduced, high dose areas tended to appear outside the PTV for some patients. CTV conformity was improved for VMAT compared to 3DCRT, which can also be seen from the dose distributions in Appendix D, but it was still not ideal. It was also observed that the escalated plans had better PTV coverage (significantly higher $V_{90\%}$ and $D_{98\%}$) than the 45 Gy VMAT plans. Not reducing the lung doses more than necessary gives better target conformity.

The paired t-test was used for statistical analysis. The null hypothesis in this test is that the mean difference between paired observations is zero, and it is assumed that the differences between pairs are normally distributed. Deviations from the normal distribution affect the power of the test. The data in this study

were assumed to be normally distributed, or close enough to it to not affect the power of the test to a very large degree. Ideally, more patients should have been included in the study, both to get a more diverse selection of patients, and because the assumption of normal distribution is more likely to be valid for larger sample sizes. The number of suitable patients was however limited by the criteria set on the target volumes delineated and dose calculation algorithm used.

Locally advanced non-small cell lung cancer (NSCLC) is similar in anatomy to limited stage SCLC, and the same organ at risk dose constraints usually apply. The fractionation schemes used may differ due to biological differences of the tumor cells, e.g. in terms of radiosensitivity or proliferation. Regardless, the potential for reduced lung doses using VMAT may be applicable for NSCLC patients as well.

Little research has been done on using VMAT for SCLC patients. An abstract was published by Prokic et al., who did a comparison of 3DCRT and VMAT for patients with limited stage SCLC and found that VMAT enabled the delivery of higher tumor doses (between 45 and 54 Gy for 3DCRT, mean value 50.2 Gy; up to 60 Gy for VMAT) and resulted in higher target dose conformity [53]. This is in agreement with what was found here.

Multiple studies have been done on both VMAT and IMRT for patients with locally advanced NSCLC, and data on dose distributions and doses to organs at risk are likely to be transferrable between SCLC and NSCLC. Rousseau et al. compared VMAT and 3DCRT for NSCLC patients and found that VMAT greatly improved conformity, in addition to reducing mean dose and V_{20} to both lungs and body [54]. Mean dose and V_{20} to the whole body were not evaluated in the current study, but the other parameters mentioned showed similar improvements. Chan et al. also reported a small, but significant reduction in lung V_{20} and mean lung dose compared to 3DCRT, but the technique used in their study was a hybrid RapidArc[1] technique (two arcs with two additional static fields) [55].

Chang and Price argued for and against IMRT being the preferred technique for treating locally advanced NSCLC with high dose radiotherapy [56, 57]. Chang refers to three retrospective clinical reviews indicating that IMRT can reduce the incidence and severity of pneumonitis and esophagitis compared to 3DCRT in NSCLC patients receiving concomitant chemotherapy [58–60], in addition to a review which showed that IMRT lead to increased local control and higher survival rates without increasing toxicity, even when used for large tumors and

[1] Varian's VMAT implementation

tumors close to critical organs [61]. These benefits may also be the case for VMAT. Bertelsen et al. compared VMAT and IMRT in a planning study of NSCLC patients, and found the differences in dose distributions and NTCP values to be small and likely of limited clinical relevance, however slightly in favor of VMAT [62].

5.1 Concerns about VMAT

Price raised concerns about the increased volume receiving low doses when IMRT is used, referring to a study by Stathakis et al. suggesting that these increased low-dose volumes lead to an increased risk of secondary cancers [57, 63]. Another factor mentioned was the potential for interplay between collimator motion and target motion, often due to respiration in the case of lung tumors, which may lead to a degradation of the tumor coverage. These concerns are also relevant for VMAT.

The effects of tumor motion on IMRT dose delivery have been shown to be of little importance when the entire treatment course is considered, due to averaging effects [64]. The same should apply for VMAT. Accurate target volume margins and proper accounting for tumor motion should still be stressed, especially with increasing target conformity. 4D-CT, which will be discussed further in Section 5.2.2, can be helpful in achieving this. Frequent imaging during the treatment course (image-guided radiation therapy, IGRT) is also useful.

Fig. 4.3 shows the DVHs for the remaining volume at risk for VMAT and 3DCRT averaged over all patients. Larger volumes receive doses below approximately 10 Gy for VMAT, while the mean dose is higher for 3DCRT. Similar results were observed for the whole volume within the external contour. This, along with the reduction in lung V_{20} and V_5, indicate that VMAT leads to higher low-dose volumes than 3DCRT. Higher low-dose volumes are associated with an increased risk of inducing second cancers. The risk of second cancers increases with dose at low doses (up to a few Gy), but the dose-response relationship is uncertain at higher doses [65]. Some data suggest that the increasing relationship continues, other suggest that it levels off, or that the risk may decrease at higher doses.

In addition to the increased low-dose volumes, the number of monitor units used is generally increased using IMRT/VMAT. This will increase leakage radiation and thus total body exposure. Both factors may increase the risk of second cancers [65, 66]. The number of MUs was not evaluated in this study.

Currently, the primary concern for SCLC patients is to improve life expectancy and lower the rates of complications. The risk of second cancers is of limited importance due to the low survival rate. However, the life expectancy of SCLC patients will hopefully increase with improving treatment techniques, and the potential risk of second malignancies will be of increasing importance.

5.2 Plan design

The partial-arc plans were created to see if removing angles not optimal for dose delivery could lead to better plans, e.g. with respect to lung doses. The remaining segments were mainly in the patients' anterior-posterior direction. There were fewer segments with beam entrance through the lungs. There was no obvious advantage of using shorter arcs instead of full arcs for all patients as a whole; however, an individual assessment should be done for each patient.

The same objectives were used for the partial-arc plans as for the full-arc plans, and altering these (e.g. changing the objective weights) might have lead to better plans. If partial arcs with angles similar to those used in this study are to be used, the dose to the spinal cord may be a greater limitation than if full arcs are used due to the limited angles of incident radiation.

5.2.1 Dose calculation algorithms

The reasons for choosing Collapsed Cone instead of Pencil Beam are summarized in Section 2.6.2. Pencil Beam is less accurate than Collapsed Cone in lung tissue.

The 3DCRT and VMAT plans were calculated using Oncentra and RayStation's CC algorithms, respectively. These algorithms are not identical, and dose distributions calculated in Oncentra and RayStation differ slightly, as shown in Section 4.3. Ideally, the same algorithm should have been used. This could have been done by recalculating the 3DCRT plans using RayStation's CC, or by making the VMAT plans in Oncentra's treatment planning system. Recalculation was not possible, as the models for the different treatment machines were not available. The VMAT plans were made in RayStation because its optimization program is much faster than the one in Oncentra. Making the VMAT plans in Oncentra would have taken much longer, and there might not have been time to include as many patients as was done here. However, the differences between RayStation and Oncentra were most likely of limited clinical relevance, as will be further explained in Section 5.6.

5.2.2 Volume definition and delineation

The volume definitions used in the HAST study were based on the tools available at the time. Today, new imaging techniques are available to help delineate target volumes. One example is PET/CT, which can be used to locate tumor activity in the body. When PET is used for lung cancers, only the lymph nodes where there is confirmed cancer activity (PET-positive lymph nodes) are defined as target volumes, and the irradiation of the whole mediastinum is unnecessary [67, 68]. PET may help limit the size of the target volumes [69]. Parts of the esophagus were inside the target volume in many of the patients, and reducing the overlap between the esophageal volume and the target volume may have a positive effect on esophageal dose and toxicity. In addition, delineating each affected lymph node separately and not as part of a mediastinum target volume will lead to multiple smaller target volumes instead of one large target volume, and it may be easier to conform the treatment fields to multiple target volumes with VMAT than 3DCRT. This is illustrated for a patient with a satellite tumor in Fig. D.4.

In the HAST study, the ITV was generated from the CTV using one margin in the transverse plane and another in the cranio-caudal direction. This may not be an accurate representation of the tumor motion. The movement may vary in different directions, and how much the tumor moves may depend on its location in the lung. In later years, 4D-CT has been increasingly used to account for tumor motion. While a regular CT scan only captures the tumor at a random point of the patient's respiratory cycle, a 4D-CT scan provides information about the tumor's location during the breathing cycle. KVIST currently recommends defining the ITV based on 4D-CT scans if available [4].

Breath hold techniques and gating (irradiation during a shorter period of the breathing cycle) may also help reduce the tumor motion margins. The total lung volume is increased when using deep inspiration breath hold techniques, which may contribute to reducing lung dose parameters such as V_{20} [70–72].

5.2.3 Photon energy

For the VMAT plans, photon energy 6 MV was used, while both 6 and 15 MV were used in the 3DCRT plans. The choice to use 6 MV was made based on recommendations from the KVIST group: 6 MV or lower should be used as the effect of the lack of electron equilibrium is less pronounced for lower energies [4]. Wang et al. did Monte Carlo calculations for 6 MV and 15 MV photons for treatment of lung cancer. Target coverage parameters, especially $V_{95\%,\mathrm{PTV}}$, were

significantly worse for 15 MV than for 6 MV. This was believed to be due to the broadening of the beam penumbra at higher energies [73].

However, the KVIST recommendations also state that higher energies can be considered when suitable dose calculation algorithms are used [4]. This is supported by a study done by Weiss et al., who compared 6 MV and 18 MV plans for IMRT of lung cancer. No clinically or statistically significant differences were found, and it was concluded that high photon energies can be considered when dose calculation algorithms are used that accurately account for heterogeneities [74].

As mentioned earlier, there were problems with hot spots outside the PTV for some patients, often in parts of the mediastinum anterior to the target volume. This was due to the focus on sparing the lungs as much as possible, which resulted in higher intensity of incoming radiation in the anterior-posterior direction. An example is shown in Fig. 5.1. This was a more pronounced problem for patients with a large anteroposterior distance. These patients may benefit from the increased penetration depth of higher energy photon beams. The linear accelerators at St. Olavs Hospital can deliver 10 MV and 15 MV photon beams as well as 6 MV, and the consequences of using these energies for SCLC patients should be investigated further.

5.3 Organs at risk

5.3.1 Choice of dose-volume constraints

The OAR dose-volume constraints used here were mostly taken from QUANTEC recommendations, which are based on 2 Gy fractions once daily, while 1.5 Gy per fraction twice daily was used here. Ideally, the dose limits should have been recalculated using the α/β ratio for each organ. However, correcting only for fractionation may not be sufficient, as there are multiple other factors affecting the difference between QUANTEC numbers and the plans made in this study. Different treatment techniques and dose calculation algorithms may have been used, and most dose-volume constraints in use today are typically based on data calculated without tissue heterogeneity correction, or using very simple methods for correction [75].

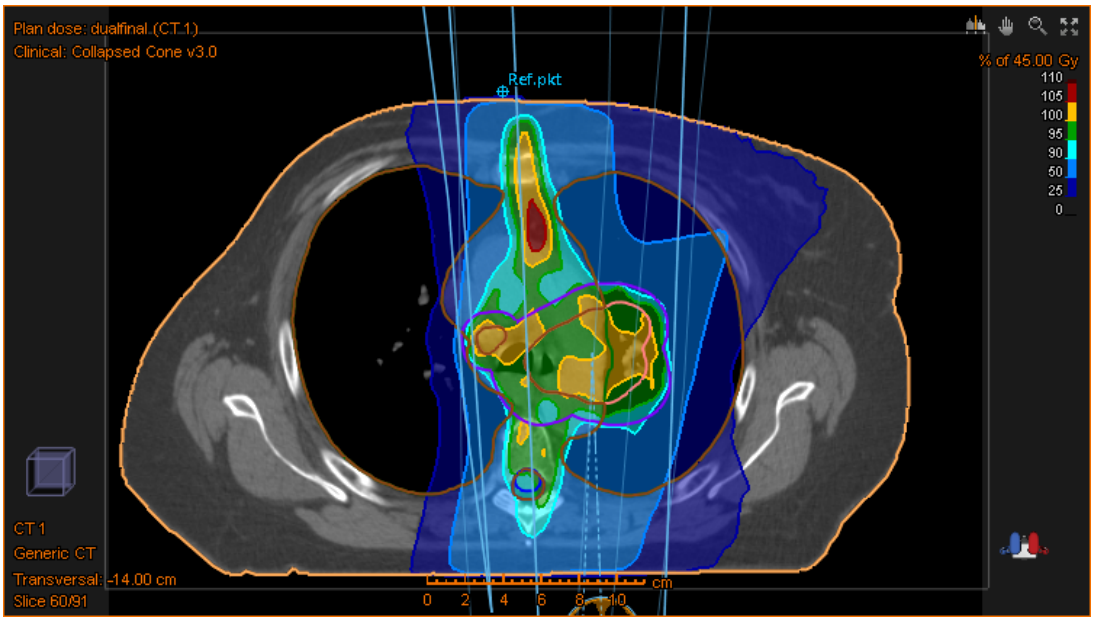

Figure 5.1: The dose distribution in an axial plane for a patient with hot spots outside the PTV (contoured in purple) in the VMAT plan.

5.3.2 Lungs

The dose-volume constraints used here were $V_{20} < 35\%$, $V_5 < 65\%$, and mean lung dose < 20 Gy. These parameters are based on data from conventionally fractionated treatments, i.e. with fraction doses 1.8-2.0 Gy. However, the same constraints are used in a study for which St. Olavs Hospital is responsible (THORA[2]), where 1.5 Gy fractions are used. It was therefore decided that these constraints were acceptable for the patients in this study as well.

Mean lung dose, V_{20}, and NTCP have been identified as some of the most important predictors for radiation pneumonitis in lung patients [76–78], but other dosimetric parameters may also be relevant. Tsujino et al. looked specifically at patients with limited stage SCLC receiving 1.5 Gy x 30 twice daily and concomitant chemotherapy, and found that lung V_{15}, V_{20}, V_{30}, and NTCP were significant predictors for radiation pneumonitis, while mean lung dose was marginally significant [79].

$\alpha/\beta = 3$ Gy was used as the fractionation sensitivity for radiation pneumonitis.

[2] A randomized phase II study comparing 1.5 Gy x 30 (twice daily) and 1.5 Gy x 40 (twice daily) for limited disease SCLC patients.

This is the value most commonly used in literature, e.g. when finding NTCP parameters. However, Bentzen et al. estimated $\alpha/\beta = 4.0 \pm 0.9$ Gy [80]. The possible errors that may result from using the wrong α/β value are not that important here, as the focus is not on the absolute NTCP values, but rather on whether there is a relative difference in NTCP between VMAT and 3DCRT.

The repair half time values for radiation pneumonitis used to calculate EQD_2 for the NTCP calculations were taken from the biological evaluation module in RayStation 4.4.100. The model in RayStation used a biexponential repair model with $T_{(1/2),s} = 0.3$ h and $T_{(1/2),l} = 4$ h, with equal weight of the two components. These values are uncertain. $T_{1/2}$ values in literature are usually based on animal data. References for the values used in the RayStation model were not found, but they might be based on a two-component repair model for irradiation of the mouse lung found by van Rongen et al., where $T_{(1/2),s} = 0.4$ h, $T_{(1/2),l} = 4$ h, and the weight of the fast component is approximately 4 times that of the slow component [81].

In the 45 Gy plans, mean lung dose, V_{20}, and NTCP were reduced for all patients for VMAT compared to 3DCRT. V_5 was higher for VMAT for three patients, likely due to the dose smearing effect of VMAT. The recommendation for the original HAST plans was that V_{20} was not to exceed 50% [48], against $V_{20} < 35\%$ here, and a reduction in V_{20} was therefore to be expected.

5.3.3 Spinal canal

The spinal canal was used as a PRV for the spinal cord, and the dose to the hottest 0.1 cm^3 ($D_{0.1cm^3}$) was chosen to represent the maximum dose. An absolute volume was chosen instead of a relative volume to account for possible differences in delineation.

The dose to the spinal cord was not taken into consideration when the original HAST plans were made, as the maximum dose was not likely to exceed the prescription doses (42 Gy in 2.8 Gy fractions once daily, or 45 Gy in 1.5 Gy fractions twice daily). The 42 Gy plans were rescaled to 45 Gy for comparison with the VMAT plans, and for these patients the maximum spinal cord dose values mentioned here are slightly higher. The recalculation from Pencil Beam to Collapsed Cone done for some patients might also have affected the dose levels. In addition, spinal cord effects have a low α/β and thus a high sensitivity to fractionation changes. Whether a patient received 2.8 Gy x 15 or 1.5 Gy x 30 also affected the "real" received dose.

The aim of the VMAT plans was not to reduce the spinal cord dose compared to the 3DCRT plans, but to keep $D_{0.1\text{cm}^3}$ to the spinal canal below 45 Gy. This was achieved in all full-arc VMAT plans, and in 13 of the 17 escalated plans.

Radiation induced spinal cord damage (myelopathy) can be severe and irreparable, and can result in pain, sensory deficits, and paralysis. According to a QUANTEC review, EQD_2 should be kept below 54 Gy to keep the risk of myelopathy below 1% [29]. The same review found $\text{EQD}_2 = 50$ Gy to correspond to a myelopathy rate of 0.2%. Concomitant chemotherapy might decrease the radiation tolerance of the spinal cord, but this is not accounted for in these limits.

EQD_2 for doses to the spinal cord for different fractionation schemes (30, 40 and 56 fractions, delivered twice daily) was calculated using Eq. 2.19, with $\alpha/\beta = 0.87$ Gy [30], monoexponential repair ($l = 1$) with repair half time $T_{(1/2),l} = 5$ hours [42, 82], and time between fractions q and $q + 1$

$$\Delta t_q = \begin{cases} 6 \text{ hours} & \text{for } q = 1, 3, 5, ... \\ 66 \text{ hours} & \text{for } q = 10, 20, 30, ... \\ 18 \text{ hours} & \text{otherwise.} \end{cases} \tag{5.1}$$

The results are shown in Tab. 5.1. Factors that may affect the EQD_2 values

Table 5.1: EQD_2 for doses to the spinal cord for fractionation schemes with 30, 40, and 56 fractions twice daily. Calculated using $\alpha/\beta = 0.87$ Gy, monoexponential repair with $T_{1/2} = 5$ hours.

n	D (Gy)	EQD_2 (Gy)
30	45	50.7
30	44.7	50
40	54	56.4
40	52.7	54
40	50.3	50
40	45	41.4
56	60.4	54
56	57.7	50
56	45	33.5

include the uncertainty of the repair half time and α/β ratio.

The limit in this study was set to 45 Gy, which is equivalent to 50.7 in 2 Gy fractions when 30 fractions are given. If the total EQD_2 is to be kept below 50 Gy, 44.7 Gy can be given in 30 fractions. The same limit (maximum physical dose 45 Gy) was used for the escalated plans, regardless of the number of fractions. If 40 fractions are given (as in the THORA study), a dose of 52.7 Gy to the spinal cord is equivalent to 54 Gy in 2 Gy fractions, and 50.3 Gy is equivalent to 50 Gy in 2 Gy fractions. The dose limit that was used here, 45 Gy in 40 fractions, results in $EQD_2 = 41.4$ Gy. The protocol for the THORA study allows a maximum dose of 54 Gy to the spinal cord, but it is not clear whether this is in 2 Gy fractions once daily or 1.5 Gy fractions twice daily [4, 83]. 54 Gy in 1.5 Gy fractions twice daily corresponds to $EQD_2 = 56.4$ Gy.

The maximum number of fractions in the escalated plans was 56. $EQD_2 = 50$ Gy would correspond to a physical dose of 57.7 Gy in 56 fractions, and $EQD_2 = 54$ Gy would correspond to 60.4 Gy in 56 fractions.

$D_{0.1\text{cm}^3}$ to the spinal canal in the escalated plans was recalculated as EQD_2. The results are shown in Fig. 5.2, and illustrate that the dose limit could have been set higher. The spinal canal was the limiting factor preventing further dose escalation in three of the patients, and it is likely that a higher prescribed dose could be achieved for these patients if the dose constraint to the spinal cord had been set higher or adjusted according to the prescribed dose level. In addition, setting a higher dose level could allow the beam segments entering through the spinal canal to have higher intensity, which could possibly reduce the intensity of segments entering through the lung, which could help reduce lung dose and again allow further dose escalation.

5.3.4 Esophagus

Radiation esophagitis is a very common side effect in SCLC patients, and lowering the esophagus dose is important for reducing the incidence. No change in mean esophagus dose or NTCP for esophagitis was observed when comparing VMAT and 3DCRT.

During dose escalation, constraints were set on the mean esophageal dose and the volume receiving the prescribed dose or higher. V_{60} was evaluated, but not used for plan selection. The relationship between V_{60} and esophagitis incidence found in a study by Bradley et al. is shown in Fig. 5.3. The data comes from

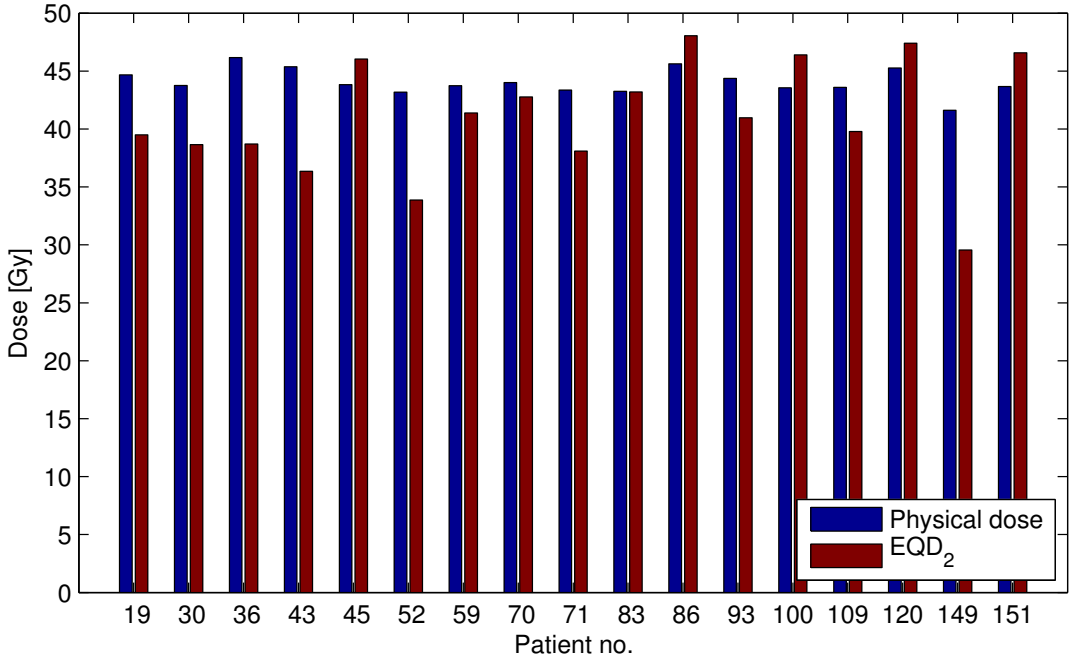

Figure 5.2: $D_{0.1\text{cm}^3}$ to the spinal canal for the escalated plans, as physical dose and EQD_2.

patients with stage I-III NSCLC treated with 3DCRT.

The highest V_{60} observed in the escalated plans was 15.3 cm^3. If the relationship in Fig. 5.3 is assumed to be accurate for the patients in the current study as well, this would correspond to a probability of esophagitis of approximately 60% if concurrent chemotherapy is given, and around 30% otherwise. If dose escalation above 60 Gy is to be considered, dose-volume constraints corresponding with an acceptable risk of esophagitis need to be determined.

The 45 Gy plans and the escalated plans used the same limit for mean esophageal dose (below 34 Gy). This value is based on data from treatments giving 2 Gy per fraction [28]. EQD_2 calculations were done for fractionation schemes of 30, 40 and 56 fractions (twice daily) using Eq. 2.18 with $\alpha/\beta = 10$ Gy. The results are listed in Tab. 5.2. 34 Gy in 30 fractions is equivalent to 31.5 Gy in 2 Gy fractions. The allowed mean dose could have been increased to 36.4 Gy for the 45 Gy plans to get $\text{EQD}_2 = 34$ Gy, and higher for the escalated plans (up to 38.2 Gy for the plan with 56 fractions). The change in fractionation has a smaller effect on EQD_2 for the esophagus than the spinal cord due to the much higher α/β.

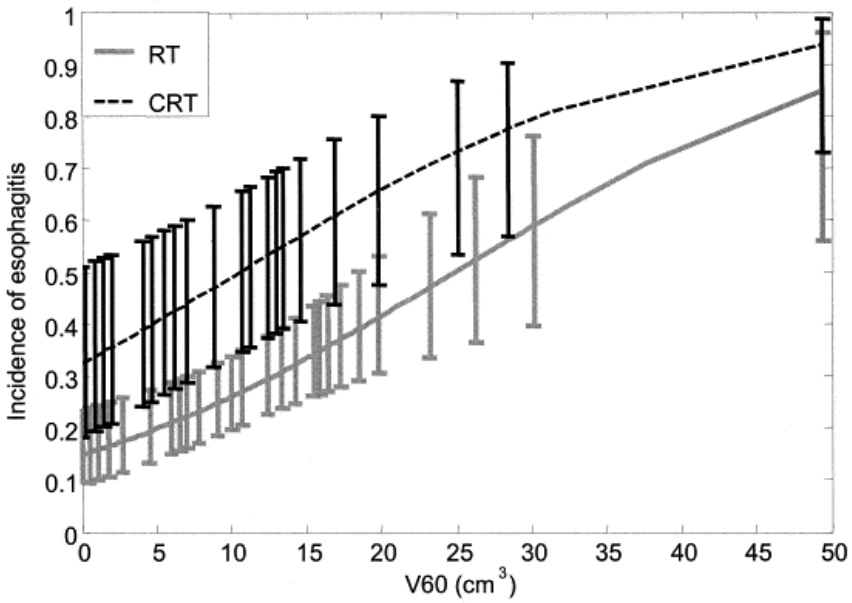

Figure 5.3: Rate of Grade $\geq$2 esophagitis vs. esophageal volume receiving 60 Gy or higher, in a study done by Bradley et al. [27]. The error bars represent 95% confidence intervals (p=0.0004). RT = radiotherapy alone or chemotherapy followed by radiotherapy; CRT = concurrent chemotherapy and radiotherapy. Used with permission.

Table 5.2: EQD_2 for doses to the esophagus for fractionation schemes with 30, 40, and 56 fractions twice daily. Calculated using α/β = 10 Gy, not corrected for incomplete repair between fractions.

n	D (Gy)	EQD_2 (Gy)
30	34	31.5
30	36.4	34
40	34	30.7
40	37.3	34
56	38.2	34

The NTCP values for esophagitis were calculated based on the DVH for the full treatment course. However, as esophagitis can appear before the end of treatment, it has been suggested to instead analyze the DVH per fraction, and to consider the number of fractions separately as an additional risk factor [84].

The same repair model as used for pneumonitis, see Section 5.3.2, was used for esophagitis in RayStation. However, no data was found to back up these values, and correction for incomplete repair was not done when calculating EQD_2 for the esophagus.

5.3.5 Heart

The heart was only delineated in 10 of the selected patients, and it appeared to be only partly delineated in some patients. Therefore, no limits were set on heart dose during the optimization, and no parameters were assessed in the evaluation.

Radiation induced heart toxicity is not commonly reported as a side effect of radiotherapy of lung tumors. This is partly due to the patients' short life expectancy, i.e. they do not live long enough to develop late cardiac toxicities. If they do survive long enough to experience changes in heart function, these will often be attributed to existing heart conditions or to local progression of the tumor [85]. However, as treatment techniques improve, more patients survive and the possibility of heart side effects must be considered to a larger degree. In addition to conditions directly affecting the heart, there have also been found indications that heart dose is correlated with the risk of radiation pneumonitis [86]. Recommended dose-volume constraints for the heart are listed in the KVIST recommendations [4].

5.4 The use of NTCP for plan evaluation

Many factors affect the accuracy of NTCP models and parameters. Two of these are the dose calculation algorithm used, and the choice of patient group. The NTCP parameters for pneumonitis found by Seppenwoolde et al. were derived for a correction-based Pencil Beam algorithm, and the data came from patients with multiple types of cancer [50]. Hedin and Bäck adjusted these parameters to be valid for four different dose calculation algorithms and three types of cancer treatments [49]. The parameters used here were the parameters found by Hedin and Bäck when Seppenwoolde's parameters were adjusted to be valid for lung cancer treatments using Oncentra's Collapsed Cone algorithm. As mentioned in Section 2.6, the CC algorithms used in Oncentra and RayStation are not

identical, and one might be concerned that the parameters might not be optimal for the plans calculated in RayStation. However, the comparison of RayStation and Oncentra done here showed a small difference in NTCP values (Tab. 4.4) and that the differences found between 3DCRT and VMAT were not affected by this difference (Tab. 5.3 in Section 5.6).

The choice of treatment technique might affect the NTCP parameters, in addition to the choice of clinical end points, size of the patient group, and toxicity scoring systems. The patient's age, lung function at baseline, smoking, possible comorbidities, and use of chemotherapy may also affect the risk of pneumonitis and thus also the NTCP parameters.

The NTCP parameters for esophagitis used here were based on data where Grade $\geq$2 esophagitis (according to the RTOG toxicity criteria) counted as events, but only Grade 2-3 events occurred. The parameters might not be good enough to predict Grade 4 esophagitis.

It should therefore be stressed that due to all these uncertainties, the NTCP values calculated here must not be used directly as probabilities for complication. The relative differences between NTCP values, or rather whether there is a difference or not, are what should be considered.

Another uncertainty of NTCP models based on DVH reduction is that DVHs do not give spatial information, and treat all parts of the organ as having the same importance. This may not always be the case. For instance, Schultheiss found indications that the thoracic part of the spinal cord is less radiation sensitive than the cervical part [30], and there have been found indications that certain parts of the lung are more radiosensitive than others [87]. In addition, it may not be appropriate to analyze the entire DVH when calculating the NTCP for acute toxicities that may occur during the treatment course, as mentioned in Section 5.3.4.

NTCP-based planning and evaluation tools are available in some newer treatment planning systems. Accurate models and parameters are essential if NTCP alone is to be used for clinical decisions, and caution should be exercised [45]. Using NTCP values to compare alternate treatment plans is a "safer" approach, although some advise against this as well [88].

Changing from 3DCRT to VMAT leads to a dose smearing effect, or a change from "a lot to a little" to "a little to a lot". The resulting DVHs will have different

shapes, and only evaluating parameters such as V_{20} or the mean dose may not be sufficient. NTCP models take the whole DVH into account and may thus be relevant to use here.

Further work could include collecting patient data (treatment plans and toxicity outcomes) and finding corresponding NTCP parameters according to QUANTEC recommendations [89]. End points and scoring systems should be clearly defined, and it should be explored how the parameters are changed when using different combinations of 3DCRT/VMAT, Pencil Beam/Collapsed Cone, dose to water/medium, etc.

5.5 Dose escalation

Results from dose escalation trials involving patients with locally advanced NSCLC and other cancer types indicate that increased tumor dose may improve local control and survival. Machtay et al. analyzed data from seven clinical trials in which dose escalation for patients with locally advanced NSCLC receiving chemoradiotherapy (fraction doses 1.2-2.0 Gy, once or twice daily) was investigated, and found that a 1 Gy increase in biologically effective dose (BED) was associated with a 4% relative improvement in survival [8]. Kong et al. reported that much higher doses than traditionally administered could be safely delivered to most patients with locally advanced NSCLC. Doses between 63 and 103 Gy were delivered in 2.1 Gy fractions. The 5-year control rates were 12%, 35%, and 49% for patients receiving 63-69 Gy, 74-84 Gy, and 92-103 Gy, respectively. The incidences of pneumonitis and fibrosis were found to not be associated with tumor dose, but significantly associated with lung dose parameters such as mean lung dose, V_{20}, and NTCP [9, 10]. The patients in the analysis by Kong et al. did not receive concomitant chemotherapy.

Dose escalation was possible for 17 of the 20 patients. When the escalated plans were compared with the 45 Gy plans, the plans of the three remaining patients were excluded to get a fair comparison. The three excluded patients (no. 51, 82, and 161) had the highest lung V_{20} in the VMAT plans and the highest mean lung dose in the 3DCRT plans (as shown in Fig. C.1 and C.2) and may be considered "difficult" patients. Not excluding these from the comparison would have lead to an unfair advantage for the escalated plans.

Whether dose escalation is possible for a patient is determined by the size of the target volumes, location within the lung, and location relative to other organs at risk. For the patients here, lung dose parameters were the most common limiting

factor for further dose escalation (10 of 17 patients). The maximum dose to the spinal canal was the limiting factor for three patients, the mean esophagus dose for two patients, and a combination of lung dose parameters and mean esophagus dose for one. As mentioned in Section 5.3.3, the dose to the spinal canal could have restricted the escalation less if the dose constraint were adjusted.

Parts of the esophagus volume were included in the PTV for many of the patients here. However, mean dose was the only criterion used for the esophagus in the plan selection, and the location of the esophagus did not limit the escalation as much as it would have if the maximum esophageal dose, or volume receiving dose above a given level, were to be used as a constraint. Challenges related to the esophageal tolerance were demonstrated by Lievens et al., who evaluated the potential for dose escalation with IMRT for patients with locally advanced NSCLC. The patients' target volumes were defined with the help of PET. Escalation was done until lung, spinal cord, and heart constraints were reached, followed by de-escalation to get below the esophageal dose limits. IMRT allowed delivery of higher tumor doses and increased sparing of organs at risk when the esophageal dose was not considered, but these advantages were lost after de-escalation [90].

Dose escalation above 60 Gy was done for seven patients, and the highest dose was 83.7 Gy. Accurate volume delineation and sufficient conformity becomes more important with increasing dose. In addition, additional fractions means a prolonged treatment time, and the possibility of accelerated repopulation of tumor cells must be taken into consideration. De Ruysscher et al. found that the time from the start of any treatment (chemo- or radiotherapy) to the end of radiotherapy was the most important predictor of survival in limited stage SCLC patients [91, 92].

An alternative to escalating the whole tumor volume is to escalate only central parts of the tumor, or parts of the tumor where there is high tumor activity confirmed by PET. Aerts et al. found an overlap between PET active volumes before and after radiotherapy, indicating that these areas might be more radioresistant and require higher doses [93, 94]. Limiting the volume receiving the highest doses might reduce the risk of normal tissue complications compared to giving the same dose to the whole tumor volume. Møller et al. found that PET active areas of lung tumors could be escalated to doses above 82 Gy without compromising normal tissue constraints [95].

5.6 Dose calculated in RayStation vs. Oncentra

Both RayStation 4.5 and Oncentra External Beam v4.3 are in use in the radiotherapy department at St. Olavs Hospital today, and it is important to be aware of any differences that may exist if plans made in the two programs are to be compared.

5.6.1 Without normalization

When the plans were calculated for a phantom of density 1 g/cm^3, differences were apparent in the build-up region and penumbra areas, with RayStation calculating higher doses in the build-up region and Oncentra calculating higher doses in the penumbra regions. These differences were also present when the plans were calculated on the images of a patient. However, the plan calculated in RayStation showed higher doses inside the field as well for the patient, with differences of about 1-3% (of 45 Gy) in soft tissue, up to 5-6% in lung tissue, and up to 12% in air cavities.

This may indicate that the deviations observed in the build-up- and penumbral region are due to different linac model parameters, while the differences in the patient tissues may be due to differences in the Collapsed Cone algorithms used, because RayStation calculates dose-to-water while Oncentra calculates dose-to-medium, or the difference may lie in how the two systems assign materials to different mass densities. More research is needed to clarify this.

The dose difference in lung tissue was between 2 and 6% in areas of the lung inside the main fields. This mainly affected the high dose levels in the DVH, and had little effect on the mean lung dose, V_5, and V_{20}. In fact, V_{20} was higher for the plan calculated in Oncentra. The relative difference was larger for the NTCP values than the other mentioned parameters, the NTCP calculated for the Oncentra plan was 95% of the NTCP calculated for the RayStation. This is an indication of the effect of the higher dose levels on the NTCP value.

The most extreme deviations outside of the build-up regions were observed in the patient's right bronchus, especially in areas where the CT numbers were below approximately HU = -990. The left bronchus did not have CT numbers this low. This could be due to tumor infiltration, as the GTV encompassed the left bronchus in some image slices, or due to organ movements during the CT scan. The bronchi with lumen are delineated as organs at risk for some patients (e.g.

patients receiving stereotactic lung treatments), and it is important to be aware of the differences between the two dose planning systems if dose parameters are to be reported for these patients.

RayStation calculated higher doses to the vertebra, as shown in Fig. 4.12. The vertebra is adjacent to the spinal cord, and this deviation may be of importance e.g. if large margins are used to generate the PRV for the spinal cord, so that the PRV contains bone.

5.6.2 Normalized plans

The RayStation plan and Oncentra plan were then normalized to give $D_{\text{mean}} = 45$ Gy to the CTV. This reduced the difference in target dose parameters between RayStation and Oncentra compared to when the plans were not normalized. While there were still areas of the lung where RayStation calculated higher doses, all lung dose parameters evaluated were now lower for RayStation (listed in Tab. 4.4) This indicates that areas where RayStation calculates higher doses are of limited importance, or balanced out by the areas where Oncentra calculates higher doses in the penumbra region.

If the 3DCRT plans in this study were to be recalculated in RayStation and then normalized, this would result in smaller differences between the lung doses in the VMAT and 3DCRT plans than without recalculation (the 3DCRT "boxes" in the boxplots in Fig. 4.2 would move closer to the VMAT "boxes").

To investigate how the differences found between RayStation and Oncentra would affect the significance of the reduction in lung dose parameters, the 3DCRT values were corrected according to the results from Tab. 4.4, and new t-tests were performed between the resulting values and the parameters for the VMAT plans. The results of the correction are listed in Tab. 5.3, along with the mean values of V_{20}, V_5, mean lung dose, and NTCP for radiation pneumonitis in the VMAT and 3DCRT plans (from Tab. 4.1), and the p-values found when comparing them.

The factors of 1.02 and 1.01 are not necessarily valid for all patients, and it is not known how they may vary between patients. However, the low p-values of V_{20}, mean lung dose, and NTCP listed in Tab. 5.3 indicate that the reduction in these parameters would still be significant if the 3DCRT plans were to be recalculated, while the reduction in V_5 may be more uncertain.

Mean lung dose, V_5, and V_{20} are the parameters typically used for evaluation of

Table 5.3: Mean values for selected lung dose parameters in the VMAT and 3DCRT plans. The values in the "not corrected" column are the values used for comparison earlier in the study, and are the actual values retrieved from the 3DCRT plans after import to RayStation and normalization. The values in the "corrected" column are the values in the "not corrected" column divided by 1.02 (V_{20}, mean dose, NTCP) or 1.01 (V_5), and serve as indicators of how the values would change if the 3DCRT plans were to be recalculated in RayStation and normalized. The p-values indicate the significance of the difference between the VMAT plans and the 3DCRT plans in the respective column.

Parameter	VMAT	3DCRT	p	3DCRT	p
		Not corrected		Corrected	
V_{20} (%)	27.7	33.6	$< 10^{-7}$	33.0	$< 10^{-6}$
V_5 (%)	52.4	59.1	< 0.05	58.5	< 0.05
Mean dose (Gy)	13.8	16.3	$< 10^{-7}$	15.9	$< 10^{-6}$
NTCP for RP (%)	6.3	10.1	$< 10^{-4}$	9.9	$< 10^{-4}$

lung toxicity when making lung plans in the clinic today. The differences in these parameters were small, both for the scaled and unscaled plans, and not likely to affect clinical decisions.

A difference in dose delivered per MU was observed between RayStation and Oncentra for the one patient selected. Further work should include comparing with measurements, using a larger selection of patients with varying lung densities, and investigating the cause of these differences. The clinical consequences of the differences found should also be discussed further.

6 Conclusion

VMAT plans were simulated using the CT images of 20 patients with SCLC-LS treated at different hospitals in Norway. The aim was to maintain or improve target coverage and conformity compared to the 3DCRT plans originally used to treat the patients, and to reduce dose to healthy lung tissue as much as possible. Dose escalation with VMAT was also attempted.

Target coverage, conformity, and homogeneity were kept unchanged or slightly improved for all VMAT plans compared to 3DCRT. All lung dose parameters were significantly reduced, and dose to the esophagus and spinal cord were kept below given constraints. Mean lung dose was significantly reduced from 16.3 Gy to 13.8 Gy, V_{20} from 33.6% to 27.7%, and V_5 from 59.1% to 52.4%. NTCP for radiation pneumonitis was reduced from an average of 10.1% for 3DCRT to 6.3% for VMAT. The NTCP values can not be used as absolute indicators of the probability of radiation pneumonitis, but the reduction in the values implies that VMAT could lead to a reduction in the number of patients developing severe pneumonitis.

For 17 of the 20 patients in the study, it was possible to deliver target doses above 45 Gy (up to 83.7 Gy, mean value 59.0 Gy) while keeping dose to organs at risk below given constraints. Adjusting the dose constraints for the spinal canal according to biological effect at the different prescribed dose levels might allow further escalation of target doses.

It was observed that RayStation 4.5 delivered higher dose per MU than Oncentra External Beam in large parts of the the treated volume in a test patient. The differences in dose-volume parameters between plans from the two treatment planning systems are not likely to be clinically relevant; however, more research is needed, both regarding potential consequences and the cause of these differences.

There will always be a compromise between high tumor doses and low organ at risk doses in radiotherapy. In this study, it has been shown that both low lung doses with acceptable tumor doses and high tumor doses with acceptable organ at risk doses are feasible with VMAT. Target dose conformity was not ideal in either of these cases, and may be improved if lung doses are not reduced more than necessary. The ideal trade-off between tumor coverage, conformity, and organ at risk doses must be determined individually for each patient case.

VMAT can be introduced either as a substitute for 3DCRT, or an alternative.

The potential for decreased lung doses may be especially beneficial in cases where lung dose objectives are not easily fulfilled using 3DCRT, and it may be natural to start with these cases if VMAT is to be gradually introduced. The planning process may also be faster with VMAT than 3DCRT for these cases, especially when using the optimization function in RayStation. Compensating for target volume motion is particularly important with the increased target conformity of VMAT and must be kept in mind. Additionally, as always when introducing new treatments or techniques, patients must be followed up closely to see if there are any changes in toxicity and recurrences.

Bibliography

[1] Kreftregisteret. *Cancer in Norway 2013: Cancer incidence, mortality, survival and prevalence in Norway*. Oslo, Norway, 2015.

[2] David M. Jackman and Bruce E. Johnson. "Small-cell lung cancer". *The Lancet* 366.9494 (2005), pp. 1385–1396.

[3] Helsedirektoratet. *Nasjonalt handlingsprogram med retningslinjer for diagnostikk, behandling og oppfølging av lungekreft*. Oslo, Norway, Dec. 2014.

[4] Norsk Lunge Cancer Gruppe og KVIST-gruppen. *Faglige anbefalinger for strålebehandling ved ikke-småcellet lungecancer*. July 2014.

[5] Odd Terje Brustugun. *Medikamentell behandling av småcellet lungekreft*. Oncolex: Onkologisk oppslagsverk. June 1, 2015. URL: http://www.oncolex.no/Lunge/Prosedyrekatalog/BEHANDLING/Medikamentell%20behandling/Medikamentell%20behandling%20av%20SCLC.aspx?lg=procedure.

[6] S.C.J. Yeung, C.P. Escalante, and R.F. Gagel. *Medical Care of Cancer Patients*. PMPH USA Ltd Series. People's Medical Publishing House, 2009.

[7] Bjørn Henning Grønberg et al. "Randomized phase II trial comparing two schedules of thoracic radiotherapy (TRT) in limited disease small-cell lung cancer (LD SCLC)". *Journal of Clinical Oncology, 2012 ASCO Annual Meeting Abstracts* 30.15 suppl. (2012), p. 7027.

[8] Mitchell Machtay et al. "Higher biologically effective dose of radiotherapy is associated with improved outcomes for locally advanced non–small cell lung carcinoma treated with chemoradiation: An analysis of the radiation therapy oncology group". *International Journal of Radiation Oncology* Biology* Physics* 82.1 (2012), pp. 425–434.

[9] Feng-Ming Kong et al. "High-dose radiation improved local tumor control and overall survival in patients with inoperable/unresectable non–small-cell lung cancer: Long-term results of a radiation dose escalation study". *International Journal of Radiation Oncology* Biology* Physics* 63.2 (2005), pp. 324–333.

[10] Feng-Ming Kong et al. "Final toxicity results of a radiation-dose escalation study in patients with non–small-cell lung cancer (NSCLC): Predictors for radiation pneumonitis and fibrosis". *International Journal of Radiation Oncology* Biology* Physics* 65.4 (2006), pp. 1075–1086.

[11] Philip Mayles, Alan E. Nahum, and Jean-Claude Rosenwald. *Handbook of Radiotherapy Physics: Theory and Practice*. Boca Raton, FL, USA: Taylor & Francis, 2007.

[12] Ervin B. Podgorsak. *Radiation Oncology Physics: A Handbook for Teachers and Students*. Vienna, Austria: International Atomic Energy Agency, 2005.

[13] Paul M. DesRosiers et al. "Lung cancer radiation therapy: Monte Carlo investigation of "under dose" by high energy photons". *Technology in cancer research & treatment* 3.3 (2004), pp. 289–294.

[14] Kenneth E. Ekstrand and Walter H. Barnes. "Pitfalls in the use of high energy X rays to treat tumors in the lung". *International Journal of Radiation Oncology* Biology* Physics* 18.1 (1990), pp. 249–252.

[15] R.O. Kornelsen and M.E.J. Young. "Changes in the dose-profile of a 10 MV x-ray beam within and beyond low density material". *Medical Physics* 9.1 (1982), pp. 114–116.

[16] M.E.J. Young and R.O. Kornelsen. "Dose corrections for low-density tissue inhomogeneities and air channels for 10-MV x rays". *Medical Physics* 10.4 (1983), pp. 450–455.

[17] Sverre Levernes. *Volum og doser i ekstern stråleterapi - Definisjoner og anbefalinger. StrålevernRapport 2012:9*. Østerås, Norway: Statens strålevern (NRPA), 2012.

[18] "ICRU Report 83: Prescribing, Recording, and Reporting Photon-Beam Intensity-Modulated Radiation Therapy (IMRT)". *Journal of the ICRU* 10.1 (2010).

[19] H. Rodney Withers, Jeremy M. G. Taylor, and Boguslaw Maciejewski. "Treatment volume and tissue tolerance". *International Journal of Radiation Oncology* Biology* Physics* 14.4 (1988), pp. 751–759.

[20] Cedric X. Yu. "Intensity-modulated arc therapy with dynamic multileaf collimation: an alternative to tomotherapy". *Physics in Medicine and Biology* 40.9 (1995), p. 1435.

[21] Karl Otto. "Volumetric modulated arc therapy: IMRT in a single gantry arc". *Medical Physics* 35.1 (2008), pp. 310–317.

[22] *RayStation 4.5: A guide to optimization in RayStation*. RaySearch Laboratories. July 2014.

[23] Andrzej Niemierko. "Reporting and analyzing dose distributions: a concept of equivalent uniform dose". *Medical Physics* 24.1 (1997), pp. 103–110.

[24] Andrzej Niemierko. "A generalized concept of equivalent uniform dose (EUD)". *Medical Physics* 26.6 (1999), p. 1100.

[25] Lawrence B. Marks et al. "Radiation dose–volume effects in the lung". *International Journal of Radiation Oncology* Biology* Physics* 76.3 (2010), S70–S76.

[26] Maria Werner-Wasik et al. "Radiation dose–volume effects in the esophagus". *International Journal of Radiation Oncology* Biology* Physics* 76.3 (2010), S86–S93.

[27] Jeffrey Bradley et al. "Dosimetric correlates for acute esophagitis in patients treated with radiotherapy for lung carcinoma". *International Journal of Radiation Oncology* Biology* Physics* 58.4 (2004), pp. 1106–1113.

[28] Anurag K. Singh, Mary Ann Lockett, and Jeffrey D. Bradley. "Predictors of radiation-induced esophageal toxicity in patients with non-small-cell lung cancer treated with three-dimensional conformal radiotherapy". *International Journal of Radiation Oncology* Biology* Physics* 55.2 (2003), pp. 337–341.

[29] John P. Kirkpatrick, Albert J. van der Kogel, and Timothy E. Schultheiss. "Radiation dose–volume effects in the spinal cord". *International Journal of Radiation Oncology* Biology* Physics* 76.3 (2010), S42–S49.

[30] Timothy E. Schultheiss. "The radiation dose–response of the human spinal cord". *International Journal of Radiation Oncology* Biology* Physics* 71.5 (2008), pp. 1455–1459.

[31] K.K. Ang et al. "Impact of spinal cord repair kinetics on the practice of altered fractionation schedules". *Radiotherapy and Oncology* 25.4 (1992), pp. 287–294.

[32] Anders Ahnesjö. "Collapsed cone convolution of radiant energy for photon dose calculation in heterogeneous media". *Medical Physics* 16.4 (1989), pp. 577–592.

[33] Nikos Papanikolaou et al. "Investigation of the convolution method for polyenergetic spectra". *Medical Physics* 20.5 (1993), pp. 1327–1336.

[34] *RayStation 4.5: Reference Manual*. RaySearch Laboratories. July 2014.

[35] Bongile Mzenda et al. "Modeling and dosimetric performance evaluation of the RayStation treatment planning system". *Journal of Applied Clinical Medical Physics* 15.5 (2014).

[36] Lasse Rye Aarup et al. "The effect of different lung densities on the accuracy of various radiotherapy dose calculation methods: implications for tumour coverage". *Radiotherapy and Oncology* 91.3 (2009), pp. 405–414.

[37] Anders Ahnesjö, Mikael Saxner, and Avo Trepp. "A pencil beam model for photon dose calculation". *Medical Physics* 19.2 (1992), pp. 263–273.

[38] Maria M. Aspradakis et al. "Experimental verification of convolution/superposition photon dose calculations for radiotherapy treatment planning". *Physics in Medicine and Biology* 48.17 (2003), p. 2873.

[39] Martin Polednik et al. "Evaluation of calculation algorithms implemented in different commercial planning systems on an anthropomorphic breast phantom using film dosimetry". *Strahlentherapie und Onkologie* 183.12 (2007), pp. 667–672.

[40] Pedro Andreo. "Dose to 'water-like' media or dose to tissue in MV photons radiotherapy treatment planning: still a matter of debate". *Physics in Medicine and Biology* 60.1 (2015), p. 309.

[41] C.M. Ma and Jinsheng Li. "Dose specification for radiation therapy: dose to water or dose to medium?" *Physics in Medicine and Biology* 56.10 (2011), p. 3073.

[42] Michael Joiner and Albert van der Kogel. *Basic Clinical Radiobiology*. 4th edition. London, United Kingdom: Hodder Arnold, 2009.

[43] Eric J. Hall and Amato J. Giaccia. *Radiobiology for the Radiologist*. 6th Edition. Philadelphia, PA, USA: Wolters Kluwer Health/Lippincott Williams & Wilkins, 2006.

[44] Daphne Levin-Plotnik et al. "A model for optimizing normal tissue complication probability in the spinal cord using a generalized incomplete repair scheme". *Radiation Research* 155.4 (2001), pp. 593–602.

[45] X. Allen Li et al. *The Use and QA of Biologically Related Models for Treatment Planning: Report of AAPM Task Group 166 of the Therapy Physics Committee*. College Park, MD, USA: American Association of Physicists in Medicine, Mar. 2012. URL: http://www.aapm.org/pubs/reports/RPT_166.pdf.

[46] Radhe Mohan et al. "Clinically relevant optimization of 3-D conformal treatments". *Medical Physics* 19.4 (1992), pp. 933–944.

[47] Eric W. Weisstein. *Normal Distribution Function*. MathWorld – A Wolfram Web Resource. May 29, 2015. URL: http://mathworld.wolfram.com/NormalDistributionFunction.html.

[48] Bjørn Henning Grønberg and Stein Sundstrøm. *Hyperfraksjonert akselerert strålebehandling ved småcellet lungekreft, begrenset sykdom: HAST-studien*. The Cancer Clinic, St. Olavs Hospital, Apr. 2005.

[49] Emma Hedin and Anna Bäck. "Influence of different dose calculation algorithms on the estimate of NTCP for lung complications". *Journal of Applied Clinical Medical Physics* 14.5 (2013).

[50] Yvette Seppenwoolde et al. "Comparing different NTCP models that predict the incidence of radiation pneumonitis". *International Journal of Radiation Oncology* Biology* Physics* 55.3 (2003), pp. 724–735.

[51] Olivier Chapet et al. "Normal tissue complication probability modeling for acute esophagitis in patients treated with conformal radiation therapy for non-small cell lung cancer". *Radiotherapy and Oncology* 77.2 (2005), pp. 176–181.

[52] MATLAB version 8.1.0 (R2013a). Natick, MA, USA, 2013.

[53] V. Prokic et al. "EP-1562 VMAT versus 3D conformal planning in patients with limited disease small-cell lung cancer". *Radiotherapy and Oncology* 103 (2012), S599.

[54] D. Rousseau et al. "Are there any dosimetric advantages in using VMAT for treatment of locally advanced non-small cell lung cancer?" *Cancer Radiothérapie: Journal de la Société Française de Radiotherapie Oncologique* 16.7 (2012), pp. 619–626.

[55] Oscar S.H. Chan et al. "The superiority of hybrid-volumetric arc therapy (VMAT) technique over double arcs VMAT and 3D-conformal technique in the treatment of locally advanced non-small cell lung cancer–A planning study". *Radiotherapy and Oncology* 101.2 (2011), pp. 298–302.

[56] Joe Y. Chang. "Intensity-Modulated Radiotherapy, Not 3 Dimensional Conformal, Is the Preferred Technique for Treating Locally Advanced Disease With High-Dose Radiotherapy". In: *Seminars in Radiation Oncology*. Vol. 25. 2. WB Saunders. 2015, pp. 110–116.

[57] Allan Price. "Intensity-Modulated Radiotherapy, Not 3 Dimensional Conformal, Is the Preferred Technique for Treating Locally Advanced Disease With High-Dose Radiotherapy: The Argument Against". In: *Seminars in Radiation Oncology*. Vol. 25. 2. WB Saunders. 2015, pp. 117–121.

[58] Sue S. Yom et al. "Initial evaluation of treatment-related pneumonitis in advanced-stage non–small-cell lung cancer patients treated with concurrent chemotherapy and intensity-modulated radiotherapy". *International Journal of Radiation Oncology* Biology* Physics* 68.1 (2007), pp. 94–102.

[59] Shervin M. Shirvani et al. "Comparison of 2 common radiation therapy techniques for definitive treatment of small cell lung cancer". *International Journal of Radiation Oncology* Biology* Physics* 87.1 (2013), pp. 139–147.

[60] Zhongxing X. Liao et al. "Influence of technologic advances on outcomes in patients with unresectable, locally advanced non–small-cell lung cancer receiving concomitant chemoradiotherapy". *International Journal of Radiation Oncology* Biology* Physics* 76.3 (2010), pp. 775–781.

[61] Sonal Sura et al. “Intensity-modulated radiation therapy (IMRT) for inoperable non-small cell lung cancer: the Memorial Sloan-Kettering Cancer Center (MSKCC) experience”. *Radiotherapy and Oncology* 87.1 (2008), pp. 17–23.

[62] Anders Bertelsen, Olfred Hansen, and Carsten Brink. “Does VMAT for treatment of NSCLC patients increase the risk of pneumonitis compared to IMRT? A planning study”. *Acta Oncologica* 51.6 (2012), pp. 752–758.

[63] Sotirios Stathakis et al. “A prediction study on radiation-induced second malignancies for IMRT treatment delivery”. *Technology in cancer research & treatment* 8.2 (2009), pp. 141–147.

[64] Thomas Bortfeld et al. “Effects of intra-fraction motion on IMRT dose delivery: statistical analysis and simulation”. *Physics in Medicine and Biology* 47.13 (2002), p. 2203.

[65] Eric J. Hall and Cheng-Shie Wuu. “Radiation-induced second cancers: the impact of 3D-CRT and IMRT”. *International Journal of Radiation Oncology* Biology* Physics* 56.1 (2003), pp. 83–88.

[66] Eric J. Hall. “Intensity-modulated radiation therapy, protons, and the risk of second cancers”. *International Journal of Radiation Oncology* Biology* Physics* 65.1 (2006), pp. 1–7.

[67] Judith van Loon et al. “Selective nodal irradiation on basis of 18 FDG-PET scans in limited-disease small-cell lung cancer: a prospective study”. *International Journal of Radiation Oncology* Biology* Physics* 77.2 (2010), pp. 329–336.

[68] Jong-Ryool Oh et al. “Whole-body metabolic tumour volume of 18F-FDG PET/CT improves the prediction of prognosis in small cell lung cancer”. *European Journal of Nuclear Medicine and Molecular Imaging* 39.6 (2012), pp. 925–935.

[69] Luc J. Vanuytsel et al. “The impact of ^{18}F-fluoro-2-deoxy-D-glucose positron emission tomography (FDG-PET) lymph node staging on the radiation treatment volumes in patients with non-small cell lung cancer”. *Radiotherapy and Oncology* 55.3 (2000), pp. 317–324.

[70] Kenneth E. Rosenzweig et al. "The deep inspiration breath-hold technique in the treatment of inoperable non–small-cell lung cancer". *International Journal of Radiation Oncology* Biology* Physics* 48.1 (2000), pp. 81–87.

[71] Joseph Hanley et al. "Deep inspiration breath-hold technique for lung tumors: the potential value of target immobilization and reduced lung density in dose escalation". *International Journal of Radiation Oncology* Biology* Physics* 45.3 (1999), pp. 603–611.

[72] Elizabeth A. Barnes et al. "Dosimetric evaluation of lung tumor immobilization using breath hold at deep inspiration". *International Journal of Radiation Oncology* Biology* Physics* 50.4 (2001), pp. 1091–1098.

[73] Lu Wang et al. "Dosimetric advantage of using 6 MV over 15 MV photons in conformal therapy of lung cancer: Monte Carlo studies in patient geometries". *Journal of Applied Clinical Medical Physics* 3.1 (2002), pp. 51–59.

[74] Elisabeth Weiss, Jeffrey V. Siebers, and Paul J. Keall. "An analysis of 6-MV versus 18-MV photon energy plans for intensity-modulated radiation therapy (IMRT) of lung cancer". *Radiotherapy and Oncology* 82.1 (2007), pp. 55–62.

[75] David A. Jaffray et al. "Accurate accumulation of dose for improved understanding of radiation effects in normal tissue". *International Journal of Radiation Oncology* Biology* Physics* 76.3 (2010), S135–S139.

[76] Mary V. Graham et al. "Clinical dose–volume histogram analysis for pneumonitis after 3D treatment for non-small cell lung cancer (NSCLC)". *International Journal of Radiation Oncology* Biology* Physics* 45.2 (1999), pp. 323–329.

[77] Stefan L.S. Kwa et al. "Radiation pneumonitis as a function of mean lung dose: an analysis of pooled data of 540 patients". *International Journal of Radiation Oncology* Biology* Physics* 42.1 (1998), pp. 1–9.

[78] George Rodrigues et al. "Prediction of radiation pneumonitis by dose–volume histogram parameters in lung cancer—a systematic review". *Radiotherapy and oncology* 71.2 (2004), pp. 127–138.

[79] Kayoko Tsujino et al. "Radiation pneumonitis following concurrent accelerated hyperfractionated radiotherapy and chemotherapy for limited-stage small-cell lung cancer: dose–volume histogram analysis and comparison with conventional chemoradiation". *International Journal of Radiation Oncology* Biology* Physics* 64.4 (2006), pp. 1100–1105.

[80] S. M. Bentzen, J. Z. Skoczylas, and J. Bernier. "Quantitative clinical radiobiology of early and late lung reactions". *International Journal of Radiation Biology* 76.4 (2000), pp. 453–462.

[81] Eric van Rongen, Howard D. Thames Jr., and Elizabeth L. Travis. "Recovery from radiation damage in mouse lung: interpretation in terms of two rates of repair". *Radiation Research* 133.2 (1993), pp. 225–233.

[82] Stanley Dische and Michele I. Saunders. "Continuous, hyperfractionated, accelerated radiotherapy (CHART): an interim report upon late morbidity". *Radiotherapy and Oncology* 16.1 (1989), pp. 65–72.

[83] Bjørn Henning Grønberg. *A Randomized Phase II Study Comparing Two Schedules of Hyperfractionated Thoracic Radiotherapy in Limited Disease Small-Cell Lung Cancer*. The Cancer Clinic, St. Olavs Hospital, Oct. 2014.

[84] Daniel R. Gomez et al. "Predictors of high-grade esophagitis after definitive three-dimensional conformal therapy, intensity-modulated radiation therapy, or proton beam therapy for non-small cell lung cancer". *International Journal of Radiation Oncology* Biology* Physics* 84.4 (2012), pp. 1010–1016.

[85] Robert G. Prosnitz, Yu Husuan Chen, and Lawrence B. Marks. "Cardiac toxicity following thoracic radiation". In: *Seminars in Oncology*. Vol. 32. Elsevier. 2005, pp. 71–80.

[86] Ellen X. Huang et al. "Heart irradiation as a risk factor for radiation pneumonitis". *Acta Oncologica* 50.1 (2011), pp. 51–60.

[87] Yvette Seppenwoolde et al. "Regional differences in lung radiosensitivity after radiotherapy for non–small-cell lung cancer". *International Journal of Radiation Oncology* Biology* Physics* 60.3 (2004), pp. 748–758.

[88] Mark Langer, Steven S. Morrill, and Richard Lane. "A test of the claim that plan rankings are determined by relative complication and tumor-

control probabilities". *International Journal of Radiation Oncology* Biology* Physics* 41.2 (1998), pp. 451–457.

[89] Andrew Jackson et al. "The lessons of QUANTEC: recommendations for reporting and gathering data on dose–volume dependencies of treatment outcome". *International Journal of Radiation Oncology* Biology* Physics* 76.3 (2010), S155–S160.

[90] Yolande Lievens et al. "Intensity-Modulated Radiotherapy for Locally Advanced Non–Small-Cell Lung Cancer: A Dose-Escalation Planning Study". *International Journal of Radiation Oncology* Biology* Physics* 80.1 (2011), pp. 306–313.

[91] Dirk De Ruysscher et al. "Time between the first day of chemotherapy and the last day of chest radiation is the most important predictor of survival in limited-disease small-cell lung cancer". *Journal of Clinical Oncology* 24.7 (2006), pp. 1057–1063.

[92] Anthony M. Brade and Ian F. Tannock. "Scheduling of radiation and chemotherapy for limited-stage small-cell lung cancer: repopulation as a cause of treatment failure?" *Journal of Clinical Oncology* 24.7 (2006), pp. 1020–1022.

[93] Hugo J.W.L. Aerts et al. "Identification of residual metabolic-active areas within individual NSCLC tumours using a pre-radiotherapy 18 Fluorodeoxyglucose-PET-CT scan". *Radiotherapy and Oncology* 91.3 (2009), pp. 386–392.

[94] Michael P. Mac Manus et al. "Metabolic (FDG–PET) response after radical radiotherapy/chemoradiotherapy for non-small cell lung cancer correlates with patterns of failure". *Lung cancer* 49.1 (2005), pp. 95–108.

[95] Ditte Sloth Møller et al. "A planning study of radiotherapy dose escalation of PET-active tumour volumes in non-small cell lung cancer patients". *Acta Oncologica* 50.6 (2011), pp. 883–888.

A MATLAB scripts

Scripts and code snippets used for plotting of data are not included.

readDVH.m

```
%% Reads cumulative dose-volume histograms from RayStation 4.5
% Header containing PatientName, PatientId, Dosename, RoiName
% Requires that the DVH contains dose data in cGy, volume data in %

function data = readDVH(filename)

data = {};
plans = {};
rois = {};
dvhSize = {};
numberOfRois = 0;

[file, message] = fopen(filename, 'r');
if file == -1
    error('Failed to read DVH file "%s": %s', filename, message);
end

while ~feof(file)
    line = fgetl(file);
    if ~isempty(strfind(line,':'))
        c = textscan(line,'%s%s','delimiter',':');
        if strcmp(c{1}{1},'#PatientName')
            data(1).roi(1).patientName = c{2}{1};
        end
        if strcmp(c{1}{1},'#PatientId')
            data(1).roi(1).patientId = c{2}{1};
        end
        if strcmp(c{1}{1},'#Dosename')      % nb: c is now {2x1 cell} {1x1
            cell}
            plans{length(plans)+1} = c{1}{2};
        end
        if strcmp(c{1}{1},'#RoiName')
            rois{length(rois)+1} = c{2}{1};
            if length(plans) == 1
                numberOfRois = numberOfRois+1;
            end
            dvhSize{length(rois)-(length(plans)-1)*numberOfRois,length(
                plans)} = 0;
        end
    elseif ~isempty(strfind(line,'.'));
        b = textscan(line,'%f%f');
        dvhSize{length(rois)-(length(plans)-1)*numberOfRois,length(plans)}
            = dvhSize{length(rois)-(length(plans)-1)*numberOfRois,length(
            plans)}+1;
        currentDvhSize = dvhSize{length(rois)-(length(plans)-1)*
            numberOfRois,length(plans)};
        data(length(plans)).roi(length(rois)-(length(plans)-1)*numberOfRois
            ).dvh(currentDvhSize,1)=b{1};
        data(length(plans)).roi(length(rois)-(length(plans)-1)*numberOfRois
            ).dvh(currentDvhSize,2)=b{2};
    end
```

```
end

for i=1:length(data)
    for j=1:length(data(1).roi)
        data(i).roi(j).patientName = data(1).roi(1).patientName;
        data(i).roi(j).patientId = data(1).roi(1).patientId;
        data(i).roi(j).planName = plans{i};
        data(i).roi(j).roiName = rois{j};
        % change from cGy to Gy:
        data(i).roi(j).dvh(:,1) = data(i).roi(j).dvh(:,1)/100;
    end
end

fclose(file);
return;
```

dv.m

```
%% d_v: minimum dose to relative volume v
% Parameters:
% - cumulative DVH (absolute dose, relative volume)
% - volume (must be between 0 and 100)
function d_v = dv(dvh,volume)
if volume < 0 || volume > 100
    disp('Error: volume must be between 0 and 100');
end
ind = find(dvh(:,2)<=volume,1);
d_v = dvh(ind,1);
end
```

vd.m

```
%% v_d: relative volume (0-100) receiving dose d or higher
% Parameters:
% - cumulative DVH (absolute dose, relative volume)
% - dose (in Gy)
function v_d = vd(dvh,dose)
ind = find(dvh(:,1)>=dose,1);
v_d = dvh(ind,2);
end
```

meandose.m

```
%% Calculate mean dose
% Parameters:
% - cumulative dvh (absolute dose, relative volume)
function md = meandose(dvh)
[nb,N]=size(dvh);
for i=2:nb
    dvh(i-1,1)=dvh(i-1,1)+(dvh(i,1)-dvh(i-1,1))/2;
    dvh(i-1,2)=(dvh(i-1,2)-dvh(i,2));
end
md=sum(dvh(:,1).*dvh(:,2))/sum(dvh(:,2));
end
```

ntcp_lkb.m

```
%% NTCP: LKB model
% Parameters:
% - cumulative DVH (absolute dose in Gy, relative volume)
% - number of fractions
% - ab: alpha/beta ratio
% - n: volume describing parameter
% - d50: dose corresponding to a 50% complication rate
% - m: steepness parameter

function [ntcp, ntcp_rep] = ntcp_lkb(dvh,numberOfFractions,ab,n,d50,m)

[nb,N]=size(dvh);
nf=numberOfFractions;

% Converting cumulative DVH to differential DVH
for i=2:nb
    dvh(i-1,1)=dvh(i-1,1)+(dvh(i,1)-dvh(i-1,1))/2;
    dvh(i-1,2)=(dvh(i-1,2)-dvh(i,2));
end

dvh(nb,:)=[];
[nb,N]=size(dvh);

% Calculate EQD2 without repair
eqd=zeros(1,nb);
for i = 1:nb
   eqd(i) = dvh(i,1)*(dvh(i,1)/nf+ab)/(2+ab);
end

% EQD2 with incomplete repair:
Tlong = 4;
Tshort = 0.3;
t6 = 6;
t18 = 18;
t66 = 66;
ts6=exp(-log(2)*t6/Tshort);
ts18=exp(-log(2)*t18/Tshort);
ts66=exp(-log(2)*t66/Tshort);
tl6=exp(-log(2)*t6/Tlong);
tl18=exp(-log(2)*t18/Tlong);
tl66=exp(-log(2)*t66/Tlong);

ts=zeros(nf-1,1);
tl=zeros(nf-1,1);

for i=1:nf-1
    if mod(i,2)     % i=1,3,5,...
        ts(i)=ts6;
        tl(i)=tl6;
    elseif mod(i,10) == 0 % i=10,20,30,...
        ts(i)=ts66;
        tl(i)=tl66;
    else
        ts(i)=ts18;
        tl(i)=tl18;
    end
end
```

```
eqd_rep=zeros(nb,1);
eqd_corr=zeros(nf,nb);
for i=1:nb
    for k=1:nf
        for p=1:k-1
            eqd_corr(k,i)=eqd_corr(k,i)+(dvh(i,1)/nf)*(prod(ts(p:k-1))+prod
                (tl(p:k-1)));
        end
        eqd_rep(i)=eqd_rep(i)+(dvh(i,1)/nf)*(1+dvh(i,1)/(nf*ab)+(1/ab)*
            eqd_corr(k,i));
    end
end
eqd_rep=eqd_rep./(1+(2/ab));

% Calculate effective dose D_eff (EUD)
d_eff=0;
d_eff_rep=0;
for i=1:nb
    d_eff = d_eff + (dvh(i,2)/100).*(eqd(i)).^(1/n);    % dvh(:,2) sums to
        100
    d_eff_rep = d_eff_rep + (dvh(i,2)/100).*(eqd_rep(i)).^(1/n);
end
d_eff=d_eff^n;
d_eff_rep=d_eff_rep^n;

% Calculate t and NTCP:
t = (d_eff-d50)/(m*d50);
t_rep = (d_eff_rep-d50)/(m*d50);
ntcp=0.5+0.5*erf(t/sqrt(2));
ntcp_rep=0.5+0.5*erf(t_rep/sqrt(2));

end
```

eqd2.m

```
function d = eqd2(totalDose,numberOfFractions,ab)
d = totalDose*((totalDose/numberOfFractions)+ab)/(2+ab);
end
```

eqd2_rep.m

```
%% EQD2 w/ incomplete repair
% monoexponential repair with repair half time Thalf (in hours)
function eqd_rep = eqd2_rep(fractionDose,numberOfFractions,ab,Thalf)
nf=numberOfFractions;
totalDose=nf*fractionDose;
t6 = 6; t18 = 18; t66 = 66;
th6=exp(-log(2)*t6/Thalf);
th18=exp(-log(2)*t18/Thalf);
th66=exp(-log(2)*t66/Thalf);
th=zeros(nf-1,1);

for i=1:nf-1
    if mod(i,2)     % i=1,3,5,...
        th(i)=th6;
```

```
    elseif mod(i,10) == 0 % i=10,20,30,...
        th(i)=th66;
    else
        th(i)=th18;
    end
end

eqd_rep=0;
eqd_corr=zeros(nf,1);
for k=1:nf
    for p=1:k-1
        eqd_corr(k)=eqd_corr(k)+(totalDose/nf)*2*prod(th(p:k-1));
    end
    eqd_rep=eqd_rep+(totalDose/nf)*(1+totalDose/(nf*ab)+(1/ab)*eqd_corr(k))
        ;
end
eqd_rep=eqd_rep./(1+(2/ab));

end
```

readAllData.m

```
%% Reads all DVHs, calculates dosimetric parameters, plots data

%% read all DVHs + other data
patientNumbers=[19 30 36 43 45 51 52 59 70 71 82 83 86 93 100 109 120 149
    151 161];

allPas(20,3).roi = 0;
% allPas(1,3).roi(2).dvh => gir dvh for roi nr 2, plan nr 3, pas nr 1
% 1.dual, 2.partial, 3.konv
for i = patientNumbers
    pasfile = sprintf('/Users/veragjervan/Dropbox/Masteroppgave/DVH/pas%d.
        dvh',i);
    ind = find(patientNumbers==i);
    allPas(ind,:) = readDVH(pasfile);
end

allPas60(20,1).roi = 0;
for i = patientNumbers
    pasfile = sprintf('/Users/veragjervan/Dropbox/Masteroppgave/DVH60/pas%
        d_60gy.dvh',i);
    ind = find(patientNumbers==i);
    allPas60(ind,:) = readDVH(pasfile);
end

allPasEsc(17,1).roi = 0;        % eskalert for 17 av 20 pas (ikke: 51, 82,
    161)
patientNumbersEsc=[19 30 36 43 45 52 59 70 71 83 86 93 100 109 120 149
    151];
escDose=[63 61.5 70.5 75 48 73.5 55.5 54 61.5 51 49.5 58.5 46.5 58.5 49.5
    84 46.5];

for i = patientNumbersEsc
    ind = find(patientNumbersEsc==i);
    pasfile = sprintf('/Users/veragjervan/Dropbox/Masteroppgave/DVHeskalert
        /pas%d_%d.dvh',i,10*escDose(ind));
```

```
    allPasEsc(ind,:) = readDVH(pasfile);
end

ptvVolum = xlsread('volumer medulladose.xlsx',1,'B3:B22');
extVolum = xlsread('volumer medulladose.xlsx',1,'C3:C22');
maxMedulla = xlsread('volumer medulladose.xlsx',1,'D3:H22'); % dual-partial
    -3dcrt-60gy-optimal
rvrVolum = xlsread('volumer medulladose.xlsx',1,'I3:I22');
v60esophagusEsc = xlsread('doseeskalering.xlsx',1,'H2:H20');
maxMedullaEsc=maxMedulla(all(~isnan(maxMedulla),2),5);  % remove NaN's
v60esophagusEsc=v60esophagusEsc(all(~isnan(v60esophagusEsc),2),:);

%% Parameters: 45 Gy
% 3 planer: dual - partial - 3dcrt
d90ptv=zeros(20,3);
v90ptv=zeros(20,3); % nb: vd(dvh,dose) tar dose i Gy, ikke prosent
d2ptv=zeros(20,3);
d98ptv=zeros(20,3);
d90ctv=zeros(20,3);
d95ctv=zeros(20,3);
d98ctv=zeros(20,3);
d2ctv=zeros(20,3);
v95ctv=zeros(20,3);
v20lunge=zeros(20,3);
v5lunge=zeros(20,3);
meandoselunge=zeros(20,3);
meanesophagus=zeros(20,3);
d2ext=zeros(20,3);
v90ext=zeros(20,3); % nb: in ccm
v90rvr=zeros(20,3);

for i=1:20
    for j=1:3
        for k=1:length(allPas(i,j).roi)
            if strcmp(allPas(i,j).roi(k).roiName,'PTV union')
                d90ptv(i,j) = dv(allPas(i,j).roi(k).dvh,90);
                d98ptv(i,j) = dv(allPas(i,j).roi(k).dvh,98);
                d2ptv(i,j) = dv(allPas(i,j).roi(k).dvh,2);
                v90ptv(i,j) = vd(allPas(i,j).roi(k).dvh,40.5);
            elseif strcmp(allPas(i,j).roi(k).roiName,'CTV union')
                d90ctv(i,j) = dv(allPas(i,j).roi(k).dvh,90);
                d95ctv(i,j) = dv(allPas(i,j).roi(k).dvh,95);
                d98ctv(i,j) = dv(allPas(i,j).roi(k).dvh,98);
                d2ctv(i,j) = dv(allPas(i,j).roi(k).dvh,2);
                v95ctv(i,j) = vd(allPas(i,j).roi(k).dvh,42.75);
            elseif strcmp(allPas(i,j).roi(k).roiName,'OR TOTAL LUNG_min_GTV
                 TAHA')
                v20lunge(i,j) = vd(allPas(i,j).roi(k).dvh,20);
                v5lunge(i,j) = vd(allPas(i,j).roi(k).dvh,5);
                meandoselunge(i,j) = meandose(allPas(i,j).roi(k).dvh);
            elseif strcmp(allPas(i,j).roi(k).roiName,'OR ESOPHAGUS TAHA')
                meanesophagus(i,j) = meandose(allPas(i,j).roi(k).dvh);
            elseif strcmp(allPas(i,j).roi(k).roiName,'External')
                d2ext(i,j) = dv(allPas(i,j).roi(k).dvh,2);
                v90ext(i,j) = vd(allPas(i,j).roi(k).dvh,40.5)*extVolum(i)
                    /100;
            elseif strcmp(allPas(i,j).roi(k).roiName,'RVR')
                v90rvr(i,j) = vd(allPas(i,j).roi(k).dvh,40.5)*rvrVolum(i)
                    /100;
```

```
            end
        end
    end
end

ctvhomogeneity=(d2ctv-d98ctv)./d50ctv;

%% Parameters optimal escalated plan
d90ptvEsc=zeros(17,1);
d98ptvEsc=zeros(17,1);
d2ptvEsc=zeros(17,1);
v90ptvEsc=zeros(17,1);
d95ctvEsc=zeros(17,1);
d98ctvEsc=zeros(17,1);
d2ctvEsc=zeros(17,1);
v95ctvEsc=zeros(17,1);
PD=zeros(17,1); % prescribed dose
v20lungeEsc=zeros(17,1);
v5lungeEsc=zeros(17,1);
meandoselungeEsc=zeros(17,1);
meanesophagusEsc=zeros(17,1);
d2extEsc=zeros(17,1);
v90extEsc=zeros(17,1);
v90rvrEsc=zeros(17,1);

for i=1:17
    for k=1:length(allPasEsc(i,1).roi)
        if strcmp(allPasEsc(i,1).roi(k).roiName,'CTV union')
            PD(i) = meandose(allPasEsc(i,1).roi(k).dvh);
        end
    end
end

for i=1:17
    for k=1:length(allPasEsc(i,1).roi)
        if strcmp(allPasEsc(i,1).roi(k).roiName,'PTV union')
            d90ptvEsc(i) = dv(allPasEsc(i,1).roi(k).dvh,90)/PD(i);
            d98ptvEsc(i) = dv(allPasEsc(i,1).roi(k).dvh,98)/PD(i);
            d2ptvEsc(i) = dv(allPasEsc(i,1).roi(k).dvh,2)/PD(i);
            v90ptvEsc(i) = vd(allPasEsc(i,1).roi(k).dvh,0.9*PD(i));
        elseif strcmp(allPasEsc(i,1).roi(k).roiName,'CTV union')
            d95ctvEsc(i) = dv(allPasEsc(i,1).roi(k).dvh,95)/PD(i);
            d98ctvEsc(i) = dv(allPasEsc(i,1).roi(k).dvh,98)/PD(i);
            d2ctvEsc(i) = dv(allPasEsc(i,1).roi(k).dvh,2)/PD(i);
            v95ctvEsc(i) = vd(allPasEsc(i,1).roi(k).dvh,0.95*PD(i));
        elseif strcmp(allPasEsc(i,1).roi(k).roiName,'OR TOTAL LUNG_min_GTV
            TAHA')
            v20lungeEsc(i) = vd(allPasEsc(i,1).roi(k).dvh,20);
            v5lungeEsc(i) = vd(allPasEsc(i,1).roi(k).dvh,5);
            meandoselungeEsc(i) = meandose(allPasEsc(i,1).roi(k).dvh);
        elseif strcmp(allPasEsc(i,1).roi(k).roiName,'OR ESOPHAGUS TAHA')
            meanesophagusEsc(i) = meandose(allPasEsc(i,1).roi(k).dvh);
        elseif strcmp(allPasEsc(i,1).roi(k).roiName,'External')
            d2extEsc(i) = dv(allPasEsc(i,1).roi(k).dvh,2)/PD(i);
            v90extEsc(i) = vd(allPasEsc(i,1).roi(k).dvh,PD(i)*0.9)*extVolum
                (i)/100;
        elseif strcmp(allPasEsc(i,1).roi(k).roiName,'RVR')
            v90rvrEsc(i) = vd(allPasEsc(i,1).roi(k).dvh,PD(i)*0.9)*rvrVolum
                (i)/100;
```

```
        end
    end
end

ctvhomogeneity_esc = (d2ctvEsc-d98ctvEsc)./d50ctvEsc;

%% NTCP pneumonitis
ntcp_lunge = zeros(20,3); % brukes ikke
ntcp_lungerep = zeros(20,3);
ntcp_lungeesc = zeros(17,1); % brukes ikke
ntcp_lungerepesc = zeros(17,1);

abl=3;
nl=0.99;
d50l=28.4;
ml=0.374;

for i=1:20
    for j=1:3
        for k=1:length(allPas(i,j).roi)
            if strcmp(allPas(i,j).roi(k).roiName,'OR TOTAL LUNG_min_GTV
                TAHA')
                [ntcp_lunge(i,j), ntcp_lungerep(i,j)] = ntcp_lkb(allPas(i,j
                    ).roi(k).dvh,30,abl,nl,d50l,ml);
            end
        end
    end
end

for i=1:17
    for k=1:length(allPasEsc(i,1).roi)
        if strcmp(allPasEsc(i,1).roi(k).roiName,'OR TOTAL LUNG_min_GTV TAHA
            ')
            [ntcp_lungeesc(i,1), ntcp_lungerepesc(i,1)] = ntcp_lkb(
                allPasEsc(i,1).roi(k).dvh,escDose(i)/1.5,abl,nl,d50l,ml);
        end
    end
end

%% NTCP esophagitis
ntcp_eso = zeros(20,3);
ntcp_esorep = zeros(20,3); % brukes ikke
ntcp_esoesc = zeros(17,1);
ntcp_esorepesc = zeros(17,1); % brukes ikke

abe=10;
ne=0.44;
d50e=51;
me=0.32;

for i=1:20
    for j=1:3
        for k=1:length(allPas(i,j).roi)
            if strcmp(allPas(i,j).roi(k).roiName,'OR ESOPHAGUS TAHA')
                [ntcp_eso(i,j), ntcp_esorep(i,j)] = ntcp_lkb(allPas(i,j).
                    roi(k).dvh,30,abe,ne,d50e,me);
            end
        end
    end
```

```
end

for i=1:17
    for k=1:length(allPasEsc(i,1).roi)
        if strcmp(allPasEsc(i,1).roi(k).roiName,'OR ESOPHAGUS TAHA')
            [ntcp_esoesc(i,1), ntcp_esorepesc(i,1)] = ntcp_lkb(allPasEsc(i
                ,1).roi(k).dvh,escDose(i)/1.5,abe,ne,d50e,me);
        end
    end
end


%% Jaccard values (45 Gy)
jaccard = zeros(20,3);
jaccardEsc = zeros(17,1);

% fila med union/intersect-volumer har rekkefolgen dual-konv-partial
for i = patientNumbers
    filename = sprintf('/Users/veragjervan/Dropbox/Masteroppgave/Jaccard/
        conf%d.txt',i);
    ind = find(patientNumbers==i);  % index of value i
    file = fopen(filename,'r');
    patId = textscan(file,'%n',1,'delimiter','\n');
    numbers = textscan(file,'%f');
    tall = numbers{1};
    jaccard(ind,1) = tall(2)/tall(1);   % dual
    jaccard(ind,3) = tall(4)/tall(3);   % konv
    jaccard(ind,2) = tall(6)/tall(5);   % partial
    fclose(file);
end

for i = patientNumbersEsc
    ind = find(patientNumbersEsc==i);
    filenameEsc = sprintf('/Users/veragjervan/Dropbox/Masteroppgave/
        JaccardEscNew/confEsc%d.txt',i);
    fileEsc = fopen(filenameEsc,'r');
    patIdEsc = textscan(fileEsc,'%n',1,'delimiter','\n');
    numbersEsc = textscan(fileEsc,'%f');
    tallEsc = numbersEsc{1};
    jaccardEsc(ind) = tallEsc(2)/tallEsc(1);
    fclose(fileEsc);
end

%% Comparison optimal escalated with other plans
v90ptvComp=zeros(17,3);
d98ptvComp=zeros(17,3);
d2ptvComp=zeros(17,3);
v95ctvComp=zeros(17,3);
d98ctvComp=zeros(17,3);
jaccardComp=zeros(17,3);
ctvhomogeneityComp=zeros(17,3);
ntcp_esorepComp=zeros(17,3);
ntcp_esoComp=zeros(17,3);
v90rvrComp=zeros(17,3);
v90extComp=zeros(17,3);

for i=patientNumbersEsc
    indEsc=find(patientNumbersEsc==i);
    indComp=find(patientNumbers==i);
```

```
    v90ptvComp(indEsc,:)=v90ptv(indComp,:);
    d98ptvComp(indEsc,:)=d98ptv(indComp,:);
    d2ptvComp(indEsc,:)=d2ptv(indComp,:);
    v95ctvComp(indEsc,:)=v95ctv(indComp,:);
    d98ctvComp(indEsc,:)=d98ctv(indComp,:);
    jaccardComp(indEsc,:)=jaccard(indComp,:);
    ntcp_esorepComp(indEsc,:)=ntcp_esorep(indComp,:);
    ntcp_esoComp(indEsc,:)=ntcp_eso(indComp,:);
    ctvhomogeneityComp(indEsc,:)=ctvhomogeneity(indComp,:);
    v90rvrComp(indEsc,:)=v90rvr(indComp,:);
    v90extComp(indEsc,:)=v90ext(indComp,:);
end

d98ptvComp=d98ptvComp/45;
d2ptvComp=d2ptvComp/45;
d98ctvComp=d98ctvComp/45;

%% Calculate EQD2 for prescribed doses
% use a/b=10 Gy

PD_EQD=zeros(1,17);
maxMedullaEscEQD=zeros(17,1);
numberOfFractionsEsc=escDose/1.5;

for i=1:17
    PD_EQD(i)=eqd2(PD(i),numberOfFractionsEsc(i),10);
    maxMedullaEscEQD(i)=eqd2_rep(maxMedullaEsc(i)/numberOfFractionsEsc(i),
        numberOfFractionsEsc(i),0.87,5);
end

%% Average DVH external and RVR
volumematrix = 0:100;
extVMATdose = zeros(1,101);
ext3Ddose = zeros(1,101);
rvrVMATdose = zeros(1,101);
rvr3Ddose = zeros(1,101);

for a=1:length(volumematrix)
    for i=1:20
        for k=1:length(allPas(i,1).roi)
            if strcmp(allPas(i,1).roi(k).roiName,'External')
                extVMATdose(a)=extVMATdose(a)+allPas(i,1).roi(k).dvh(find(
                    allPas(i,1).roi(k).dvh(:,2)==volumematrix(a),1),1);
                ext3Ddose(a)=ext3Ddose(a)+allPas(i,3).roi(k).dvh(find(
                    allPas(i,3).roi(k).dvh(:,2)==volumematrix(a),1),1);
            elseif strcmp(allPas(i,1).roi(k).roiName,'RVR')
                rvrVMATdose(a)=rvrVMATdose(a)+allPas(i,1).roi(k).dvh(find(
                    allPas(i,1).roi(k).dvh(:,2)==volumematrix(a),1),1);
                rvr3Ddose(a)=rvr3Ddose(a)+allPas(i,3).roi(k).dvh(find(
                    allPas(i,3).roi(k).dvh(:,2)==volumematrix(a),1),1);
            end
        end
    end
end
extVMATdose=extVMATdose/20;
ext3Ddose=ext3Ddose/20;
rvrVMATdose=rvrVMATdose/20;
rvr3Ddose=rvr3Ddose/20;
```

B Partial arcs

Table B.1: The arc segments (in degrees) used in the partial arc plans. The gantry is in its top position at 0 degrees, and the gantry angle increases as the gantry moves clockwise. The gantry cannot pass between the angles 178° and 182°.

Patient	Arc 1	Arc 2	Arc 3	Arc 4	Total arc length (degrees)
19	178-134	10-318			96
30	178-154	14-306			92
36	146-122	74-318	206-182		164
43	178-146	34-314	206-182		136
45	178-150	46-310	206-182		148
51	178-150	50-322	206-182		140
52	178-126	34-314	266-182		216
59	178-130	46-282	206-182		196
70	178-126	6-314	282-246	218-182	176
71	178-314	222-182			264
82	178-142	58-302	206-182		176
83	178-114	14-294	206-182		168
86	178-150	18-326	206-182		104
93	178-110	26-306	206-182		172
100	178-122	54-326	210-182		172
109	178-142	34-322	238-182		164
120	178-154	22-322	206-182		108
149	178-146	46-346	242-182		152
151	178-138	46-310	270-182		224
161	178-146	30-306	262-182		196

C Illustration of selected OAR dose parameters

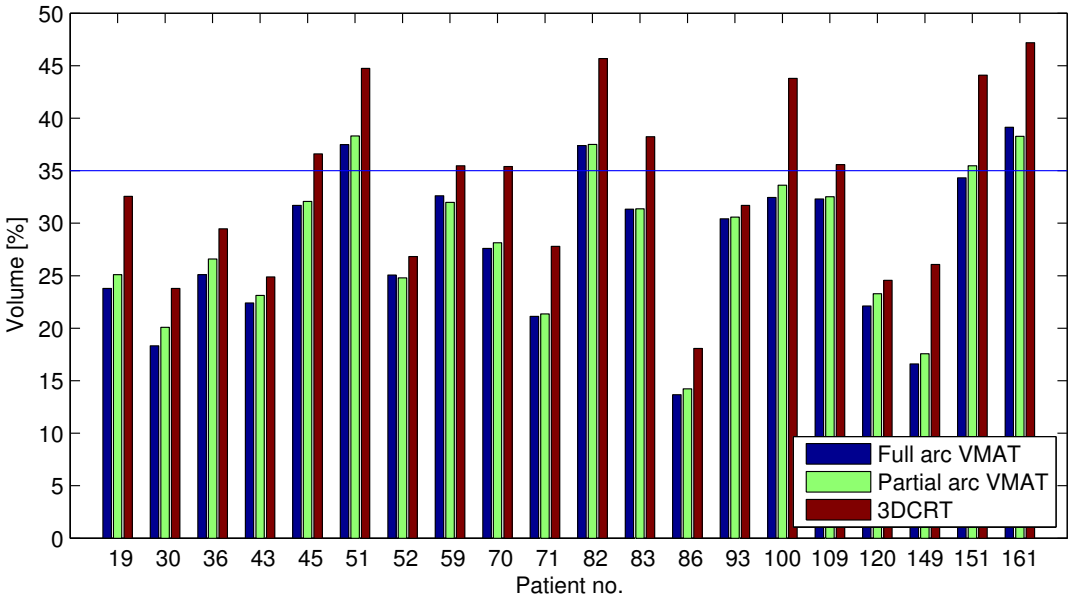

Figure C.1: V_{20} to the union of both lungs with the GTV subtracted in the full arc VMAT, partial arc VMAT and 3DCRT plans for all patients. The blue line marks $V_{20} = 35\%$.

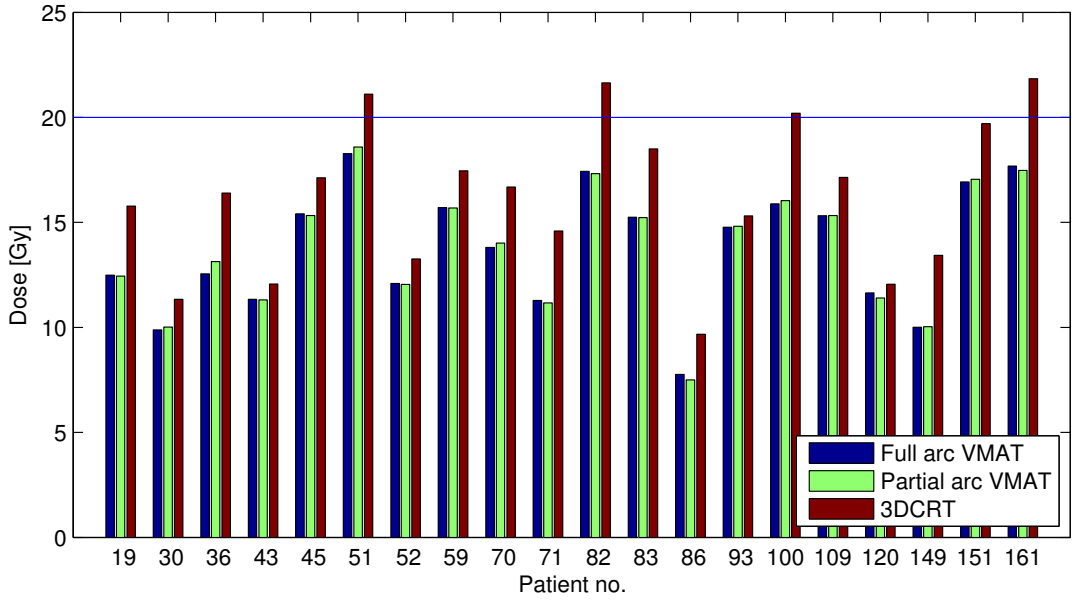

Figure C.2: Mean lung dose in the full arc VMAT, partial arc VMAT and 3DCRT plans for all patients. The blue line is drawn at 20 Gy.

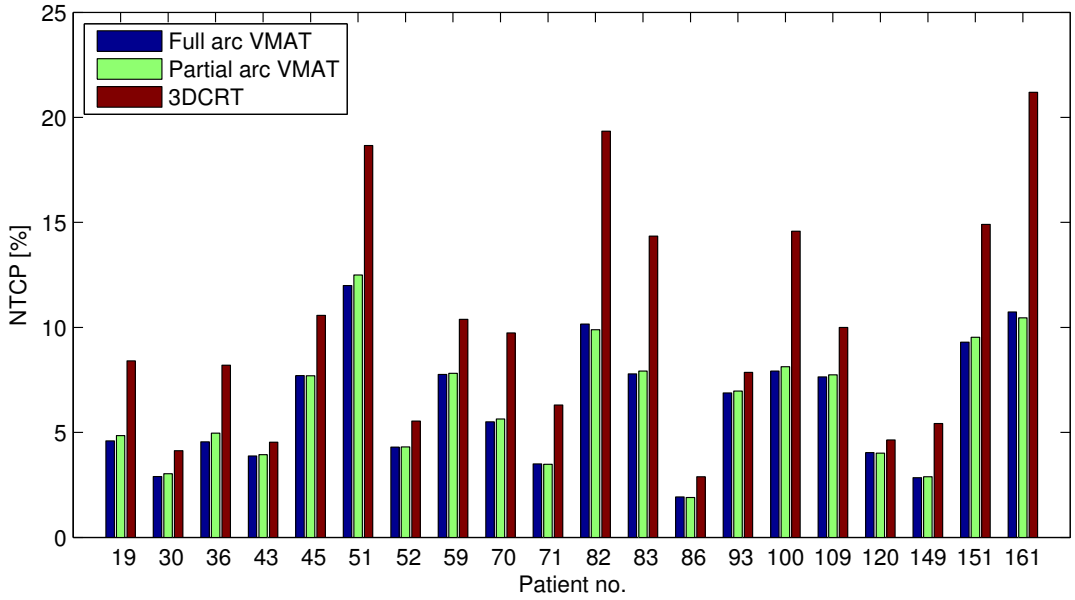

Figure C.3: NTCP for radiation pneumonitis calculated for the full arc VMAT, partial arc VMAT and 3DCRT plans for all patients.

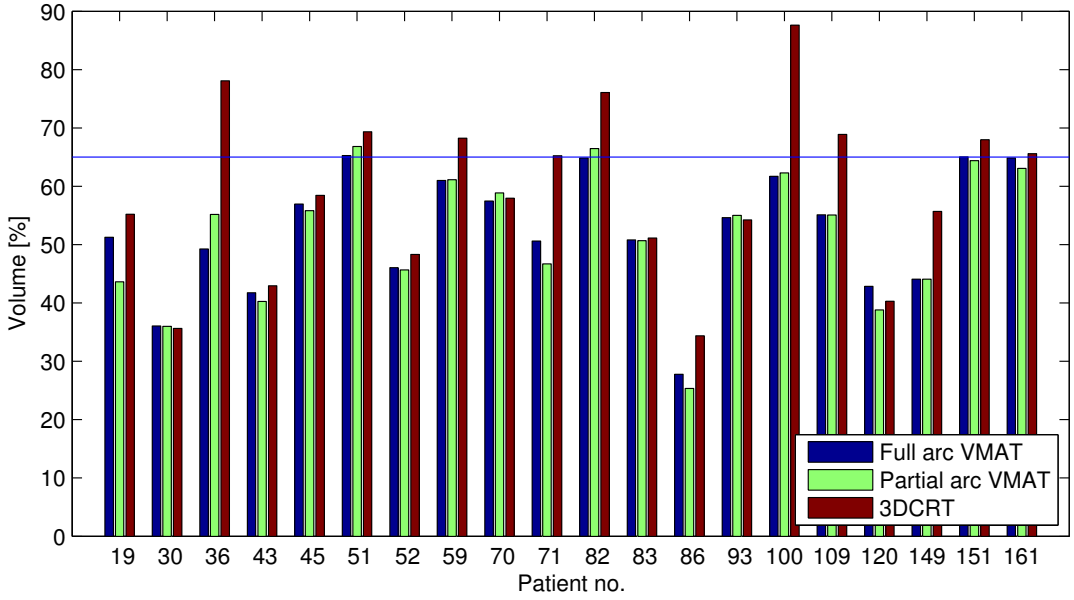

Figure C.4: V_5 to the union of both lungs with the GTV subtracted in the full arc VMAT, partial arc VMAT and 3DCRT plans for all patients. The blue line marks $V_5 = 65\%$.

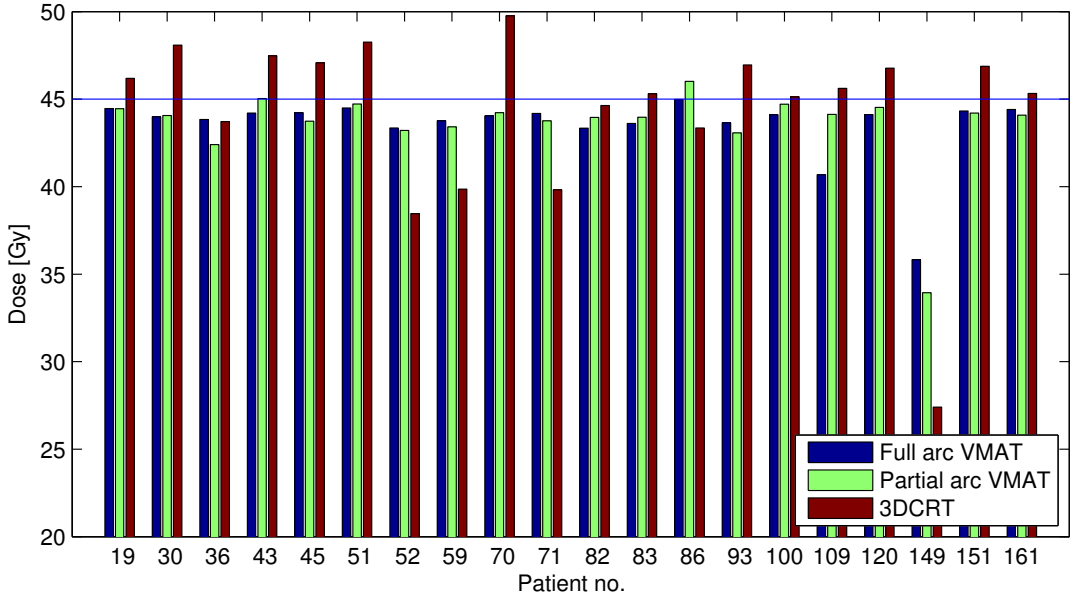

Figure C.5: $D_{0.1\text{cm}^3}$ to the spinal canal for the full arc VMAT, partial arc VMAT and 3DCRT plans for all patients. The blue line marks 45 Gy.

D Dose distributions/DVHs

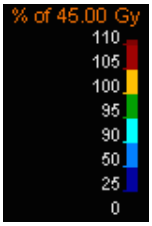

Figure D.1: The isodose lines used in the figures to follow.

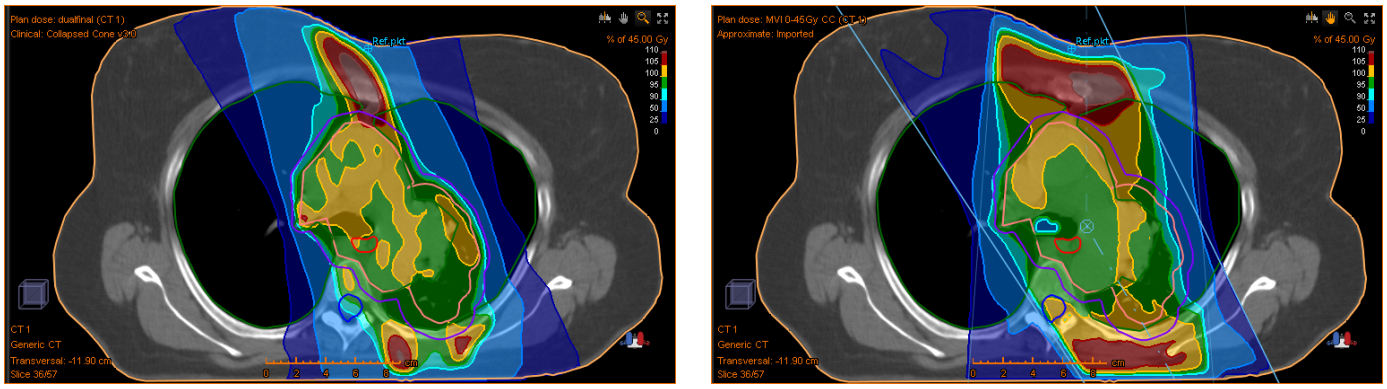

(a) Full arc VMAT **(b)** 3DCRT

Figure D.2: Dose distributions for patient no. 19.

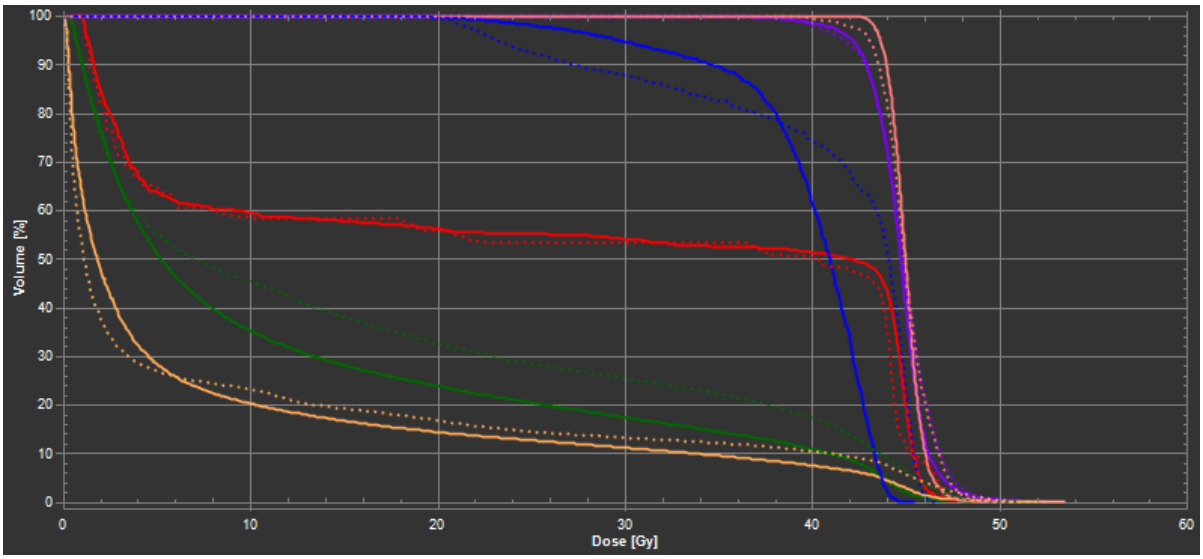

Figure D.3: DVH for patient no. 19. The full line is full arc VMAT, the dashed line is 3DCRT. The ROIs included are External (yellow), both lungs minus GTV (green), esophagus (red), spinal canal (blue), PTV (purple), CTV (pink).

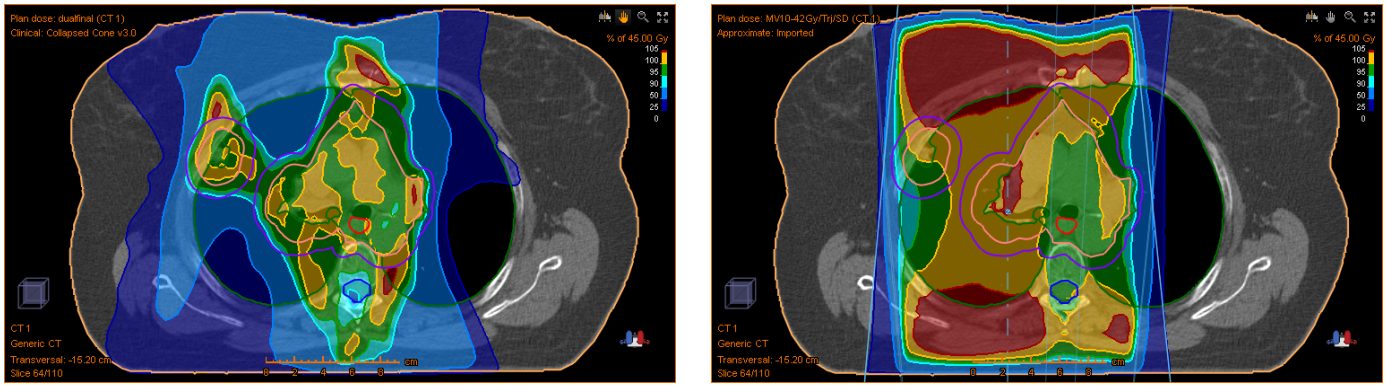

(a) Full arc VMAT **(b)** 3DCRT

Figure D.4: Dose distributions for patient no. 161, one of the patients where dose escalation was not possible.

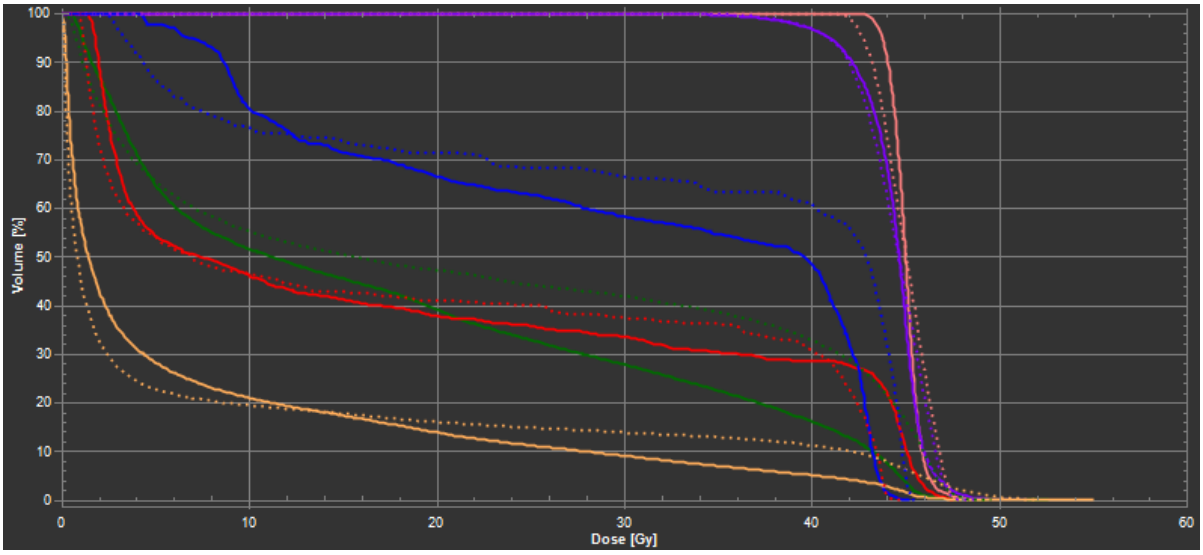

Figure D.5: Dose-volume histogram for patient no. 161. The full line is full arc VMAT, the dashed line is 3DCRT. The ROIs included are External (yellow), esophagus (red), both lungs minus GTV (green), spinal canal (blue), PTV (purple), CTV (pink).

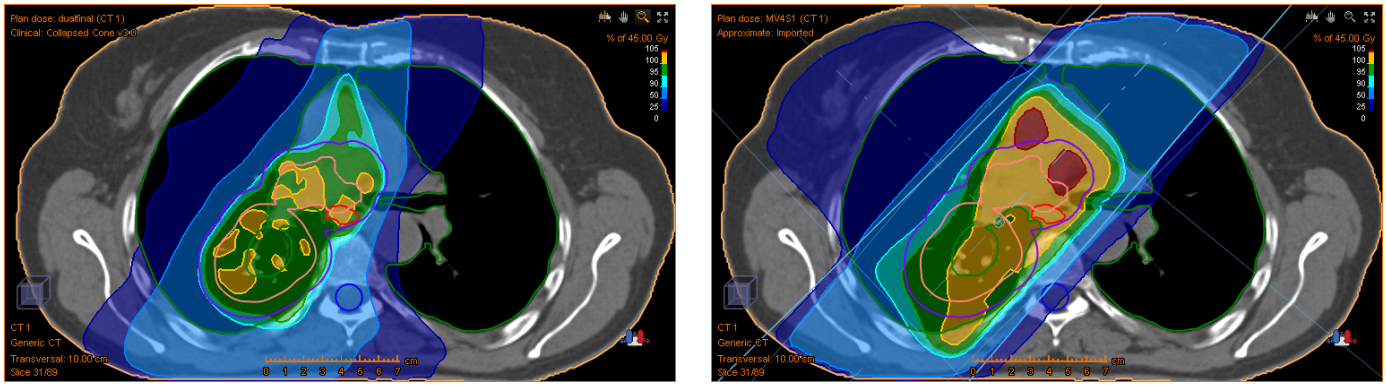

(a) Full arc VMAT **(b)** 3DCRT

Figure D.6: Dose distributions for patient no. 149, the patient with the largest reduction in V_{20} and mean lung dose from VMAT to 3DCRT. This was also the patient with the highest prescribed dose in the escalated plans.

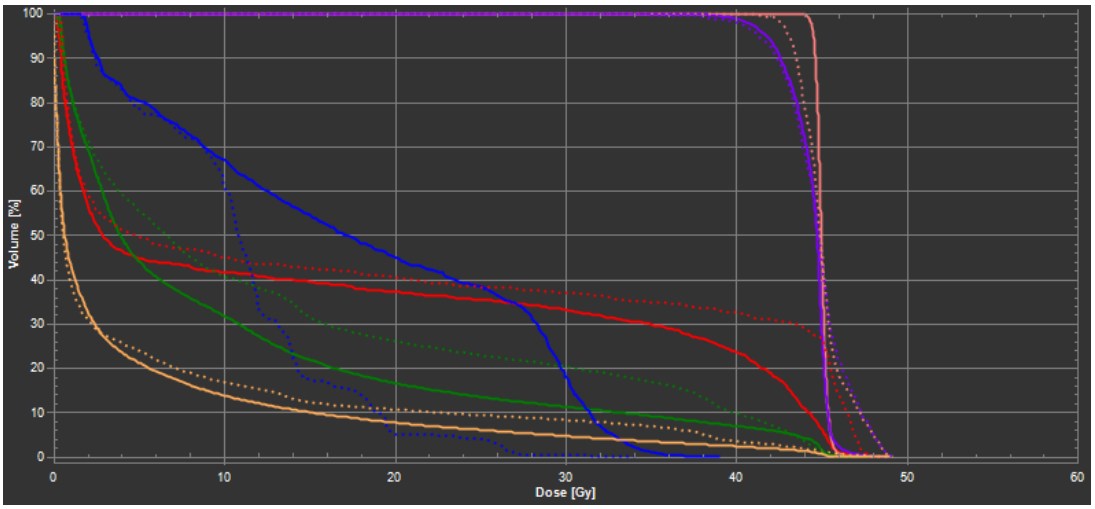

Figure D.7: Dose-volume histogram for patient no. 149. The full line is full arc VMAT, the dashed line is 3DCRT. The ROIs included are External (yellow), both lungs minus GTV (green), spinal canal (blue), esophagus (red), PTV (purple), CTV (pink).

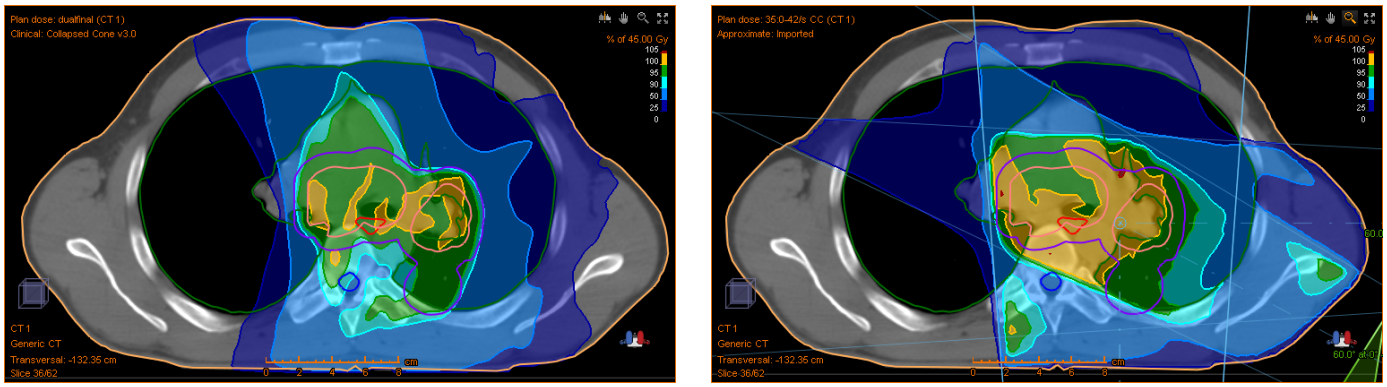

(a) Full arc VMAT **(b)** 3DCRT

Figure D.8: Dose distributions for patient no. 36, the patient with the largest reduction in V_5 from VMAT to 3DCRT.

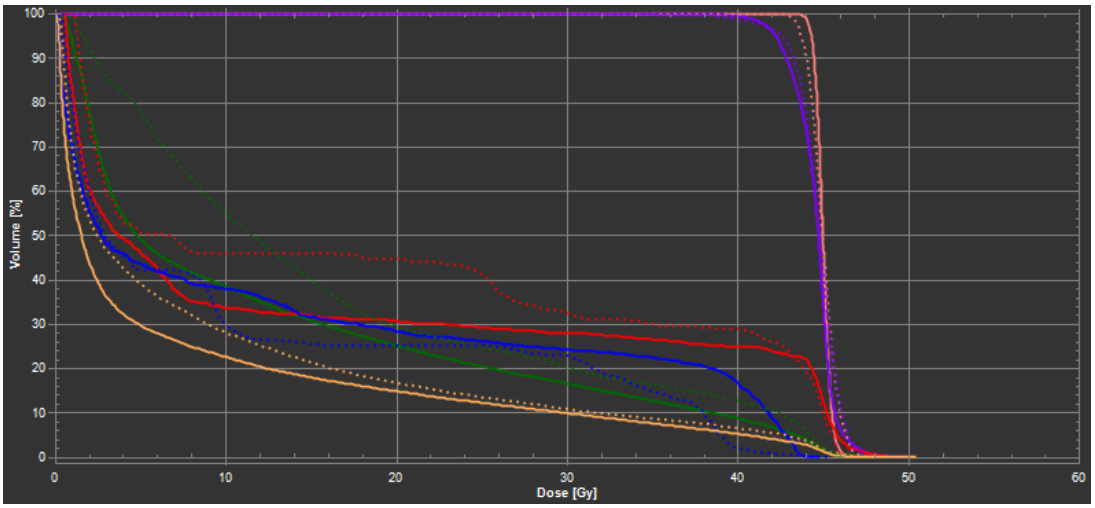

Figure D.9: Dose-volume histogram for patient no. 36. The full line is full arc VMAT, the dashed line is 3DCRT. The ROIs included are External (yellow), spinal canal (blue), esophagus (red), both lungs minus GTV (green), PTV (purple), CTV (pink).